Surface texture enhancement of SLS processed turbine blades using a mix of flexible media and abrasives.

By Matthew Titus (TTSMAT002)

This dissertation is presented for the degree of

Master of Science

Specialising in

Mechanical Engineering

Supervisor: Associate Professor Ramesh Kuppuswamy

May 2022

Declaration

This dissertation is submitted to the Department of Mechanical Engineering, University of Cape Town, in complete fulfilment of the requirements for the degree of Master of Science. It has not been submitted before for any degree or examination at this or any other university. The author confirms that this thesis is based on his own work. Portions of this work have been published in peer-reviewed journals and at refereed international conferences.

"I know the meaning of plagiarism and declare that all the work in the document, save for that which is properly acknowledged, is my own. This thesis/dissertation has been submitted to the Turnitin module (or equivalent similarity and originality checking software) and I confirm that my supervisor has seen my report and any concerns revealed by such have been resolved with my supervisor."

Signed by candidate

Signature

17/05/2022

Date

Acknowledgments

I would like to take a moment to appreciate everyone that has been part of my incredible journey towards submitting this dissertation. Firstly, to the high power out there, I would never have been able to come to this point without all the blessings I have received as well as the strength to persevere and push through to completing this dissertation. During this time of COVID I have lost many loved ones and the strength you have given me is what has been able to keep me on this path.

To the CSIR for supporting me through this journey as well as all the colleagues I have interacted with that have motivated me and inspired me to this point, I appreciate it.

To all the undergraduate students I have worked with that have supported my thesis both directly and indirectly, I appreciate their commitment and hard work in the various work packages they have completed that has aided me in getting to this point. They have made an already difficult journey easier and for that I am grateful.

To my friends and family that I have had numerous conversations with throughout my journey, thank you. Keeping me in check and motivated when I was not able to do so for myself. I appreciate you keeping me focused and driven towards the goal of completing my thesis. It would be very interesting to see where I would be today if I never had the incredible support structure that you bring.

To my "co-Researcher" Quintin, thank you for your assistance and motivation to keep me from pushing this through to the end.

Finally, to my supervisor Ramesh Kuppuswamy, I wanted to save you for last as you have been the biggest contributor to my success in finishing this thesis. I remember the first time I walked into your office to discuss this thesis while I was in my final year. Little did I know what was coming for me in the consequent years. Thank you so much for supervising me the way you have. We have had our highs and lows, but you have always been consistent in wanting the best for me. I do not believe there has ever been a time when I have felt that you have your own interests at heart. I appreciate you pushing me the way you have and only demanding excellence. Your vast knowledge and passion in the engineering space is commendable and I always admired this about you. I have also had the opportunity to witness how incredibly hard you work and even though I have never mentioned this, it has always been inspiring to work closely with someone that works extremely hard and has influenced me to work towards getting to that level. Walking away from this journey, I have another role model I can look up to for my professional career. So Prof, Thank you for walking this journey with me, I appreciate you for this.

It is very possible that there are parties I may have missed. I would also like to take this opportunity to thank those I may have missed in their role they played in my life during this time whether big or small. To get to this point, it is an accumulation of many experiences throughout this journey and every moment has had its role to play whether big or small.

Abstract

Additive manufacturing technologies such as Selective Laser Sintering of Grade 5 Titanium has been used extensively within the aerospace industry as it allows for the fabrication of complex shapes with minimal material wastage. With the increased use of complex shapes, newer polishing technologies need to be developed to accommodate the fabrication technological advancements. This dissertation proposes a novel abrasive flow polishing technology that can lower polishing times as well as limiting damage that polishing may have on a component due to excessive forces. This is achieved by the addition of a flexible media to the abrasive particles to achieve more desirable properties of the polishing media. The technology has been partially developed with further design requirements being investigated by means of explicit dynamic simulations within the Ansys package. The simulations include an asperity made of Grade 5 titanium, a SiC abrasive particle and, an HDPE particle as the flexible media. These simulations have tested process parameters such as abrasive size, asperity size and impact velocity. These simulations have shown that addition of the flexible media can increase the material removal rate of process by up to 200% due to a vibratory motion that was observed of the abrasive particle. These results are promising in showing that the proposed abrasive flow polishing technology can improve the material removal rate of the current aero lapping technology due to the addition of the flexible media. Preliminary testing for this technology has shown that the developed system is within a 22% performance range of similar literature. However, the verification of these simulations and findings needs to be completed through thorough testing of the physical technology.

List of Publications

- Ramesh Kuppuswamy, Matthew Titus, Quintin de Jong, (2021), “Polishing of a Selective Electron Beam Melting Processed Tungsten Carbide Punch through High Velocity Impinging of Flexible Media”, Journal of the Brazilian Society of Mechanical Sciences and Engineering, Manuscript Number: BMSE-D-21-01253, (accepted for publication)

- Quintin de Jongh, Matthew Titus, Ramesh Kuppuswamy (2022), “A Force Controlled Polishing Process Design, Analysis and Simulation Targeted at Selective Laser Sintered Aero-Engine Components”, COMA 22, International conference on Manufacturing Advances Stellenbosch, South Africa, March 9-11, 2022

Table of Contents

List of Figures

List of Tables

List of Abbreviations

Abbreviation	Definition
SLS	Selective Laser Sintering
SLM	Selective laser Melting
AM	Additive Manufacturing
UTS	Ultimate Tensile Strength
MRR	Material Removal Rate
PIC	Peripheral Interface Controller
CMP	Chemical Mechanical Polishing
SiC	Silicon Carbide
FEA	Finite Element Analysis
DEM	Discrete Element Method
CFD	Computational Fluid Dynamics
MD	Molecular Dynamics
CPU	Central Processing Unit
GPU	Graphics Processing Unit
MJP	Magnetorheological Jet Polishing
CO_2	Carbon Dioxide
AJM	Abrasive Jet Machining
CNC	Computer Numerical Control
3D	3-Dimension
CAD	Computer-Aided Design
PET	Polyethylene Terephthalate
HDPE	High-Density Polyethylene
PCD	Poly Crystalline Diamond

List of Symbols

Symbol	Unit	Definition
m	Kg	Mass
v	m/s	Velocity
F	N	Force
t	μs	Time
δ	μm	Local Deformation
D	μm	Equivalent Diameter
υ	N/A	Poisson Ratio
E	GPa	Modulus of Elasticity
ρ	Kg/m^3	Density
a	μm	Radius of Local Deformation
Ra	μm	Surface Roughness
BHN	Kgf/mm^2	Brinell Hardness Number
P	Kgf	Applied Normal Load
d	μm	Indentation Diameter
R	μm	Radius of abrasive particle
σ	MPa	Applied Stress
ΔP	Kg.m/s	Change in Momentum
KE	J	Kinetic Energy
V	m^3	Volume
WD	Nm	Work Done
σ_w	MPa	Flow Strength
K	N/A	Energy Scale Factor
u^N	N/A	Degree of Freedom
α	m/s^2	Acceleration
x	m	Displacement
$E_{Distortion}$	J	Distortion Energy
E_{losses}	J	Energy Lost
η	N/A	Efficiency factor

1 Introduction

1.1 Background

With the increased uptake of Additive Manufacturing (AM) technologies, companies have been able to design and manufacture complex components at a significantly faster rate than using historical manufacturing methods. Additive technologies are also increasingly used due to its ability to optimise the amount of material it uses in during the fabrication of components without compromising the structure and strength properties of components. This reduces the amount of material used for components which not only saves costs for companies but also limits material wastage which is essential when considering the global efforts to shift to more sustainable engineering approaches to engineering problems [1]. Titanium is an example of such a material that requires sustainable efforts if used during engineering practice [2].

The Ti6Al4V titanium alloy (Grade 5) is the most used titanium alloy within the biomedical and aerospace industries [3]. This material has excellent strength properties, resistance to corrosion and has low density which are critical requirements for applications within these industries [4]. However, titanium is expensive to use for engineering activities due to the processes that are required to convert the natural and raw material into a form that can be used for engineering applications. It is also considered a relatively rare material. Considering this, it is understandable why titanium is often paired with additive manufacturing technologies during the fabrication of components. Selective Laser Sintering (SLS) is an example of an additive manufacturing technology that can be used to fabricate titanium components [5].

Selective Laser Sintering is a commercialized additive manufacturing process and during this process a heat source induces fusion between powder particles [6]. Most of the selective laser sintered components used for aerospace applications require a post processing treatment such as a polishing operation to improve its surface texture [7]. Polishing increases the surface strength of these components as well as reducing friction within dynamic environments which improves the overall life of the component. During the finishing processes of a selective laser sintered component, any uncontrolled fracture further damages the component and enhances the scrape rate which is an inherent risk of the polishing action. Excessive polishing forces that are applied to components are usually the cause of these surface defects whereas lower applied polishing forces increases the polishing time. As a result, managing the present polishing methods offer many challenges. With the increased complexity of shapes that can be fabricated by SLS, there is a need to develop polishing technologies that are able to finish modern Selective Laser Sintered fabricated components by reducing polishing time without increasing the risk of surface damage due to excessive polishing forces. Therefore, a novel polishing process that applies flexible abrasive media for finishing a selective laser sintered component is investigated. Through velocity control and by managing abrasive features, the polishing characteristics of the process can be decided [8].

The proposed polishing process is expected to reduce the unwanted elements which creep into polishing processes such as edge chipping, micro grooving, and micro-cracks due to excessive polishing forces [8]. This is achieved by introducing flexible abrasive media and abrasives into the polishing process. This is done by mixing unconventional natural materials such as seaweed and/or gelatine with conventional abrasives such as Silicon Carbide (SiC) and Diamond Powder [9]. Therefore, this project

is aimed at investigating and developing an ecological friendly polishing technology for aero-engine components. The project would be executed in the Advanced Manufacturing Laboratory located at the Department of Mechanical Engineering, University of Cape Town, South Africa.

1.2 Objective

The aim of this research is to use currently existing knowledge pertaining to polishing by severe plastic deformation of brittle materials to develop an appropriate polishing technology through design and simulation of a flexible abrasive based polishing machine. This technology can be used to finish the machining of Grade 5 titanium-based aerospace components.

1.3 Scope

The scope of this research project can be summarised as follows:

- Gather substantial knowledge on existing polishing concepts
- Characterise necessary parameters in the investigation of the proposed polishing concept
- Undertake a numerical analysis of the polishing action using different theoretical approaches
- Simulate the polishing action of the machine with Ansys using Explicit Dynamics
- Analyse and discuss the results from the simulations and report the findings
- Draw conclusions from the findings of the simulation results
- Make recommendations from the conclusions drawn out

The scope of this research has changed during its undertaking due to the prevailed COVID-19 pandemic. The scope mentioned above is the updated scope for this research project and what is reported on in this document.

1.4 Thesis Outline

A brief overview of this thesis report is shown below. This diagram can be used as reference to understand how all the various sections are related.

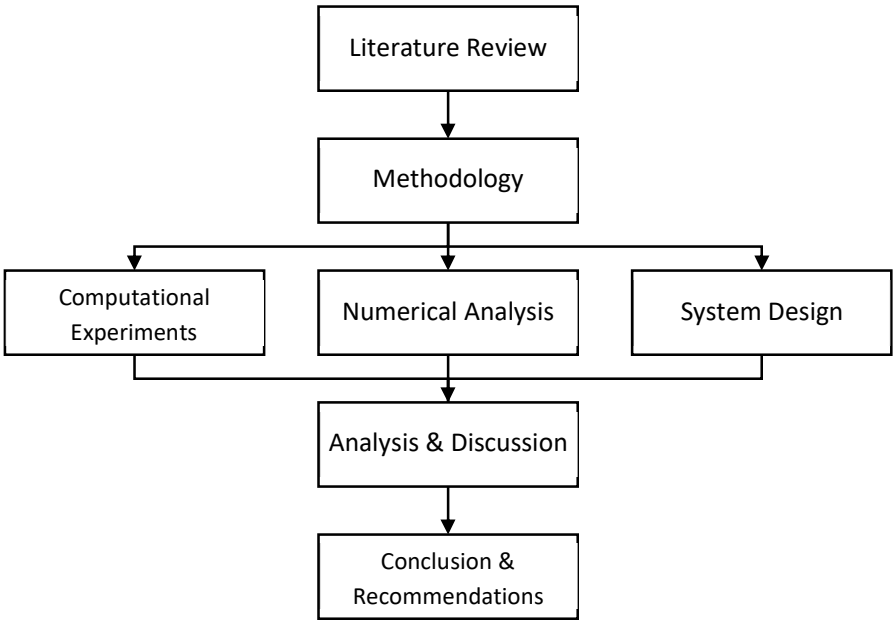

Figure 1: Thesis outline

2 Literature Review

The literature review is a comprehensive study of the current knowledge that exists that will inform the research completed within the report. The literature review will explore the modern developments regarding polishing technologies, current tools that are used to model polishing and, supplementary knowledge that assists with understanding the SLS process and how it may affect the polishing action.

2.1 Surface Roughness

Surface roughness is a metric that defines the condition of a surface regarding its texture. Specifically in relation to engineering, the surface texture is often analysed in relation to a machined component to understand its properties. Generally, the observed surface texture is due to fabrication processes of components and the material characteristics and its interaction with the environment [10]. The definitions and generally accepted standards in defining roughness is crucial for the undertaking of this polishing process.

2.1.1 Introduction

The surface profile typically has an arrangement of hills and valleys at the microscopic scale. The following diagram is a surface roughness profile of a helical gear that has been obtained using a stylus profilometer [11].

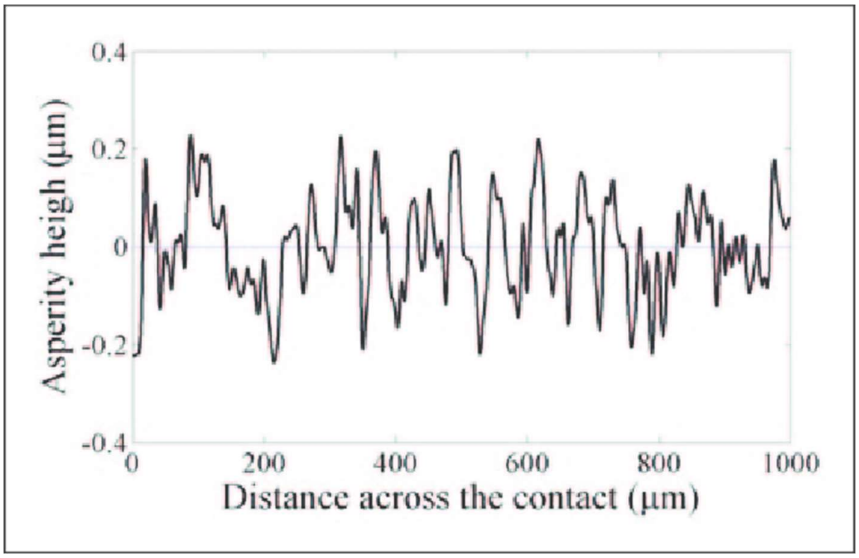

Figure 2: A diagram showing the surface profile of a helical gear across 1mm.

As shown in Figure 2, the surface profile has a shape that can be quantified by considering the maximum distance between a peak and valley and the distance between the peaks for example [10]. By quantifying these parameters, it becomes easier to understand the surface behaviour of the component specifically in operating conditions which is important for design decisions. A study on the static friction between two surfaces in contact with each other has found that surfaces with a lesser fractality (flatter surfaces) reduces static friction between two surfaces as well as increasing the surface wear which thus reduces component life [12]. This is one such example where the understanding of the surface texture can assist with component response in its environment and thus inform design decisions.

2.1.2 Surface Topography

Surface topography is the terminology used to reference the shape of the profile as well as quantifying the roughness by considering the waviness, frequency, and the magnitude of these surface profiles [13]. The comprehensive profile roughness parameters can be found in the ISO 4287 standard which includes both 2D and 3D surface roughness parameters [14]. The following table summarises a few of the parameters that can be calculated to quantify surface roughness [15].

Parameter	Description	Formula
Ra	Arithmetic mean deviation from the centre line	$Ra = \frac{1}{l}\int_0^l \lvert z(x)\rvert dx$
Rq	Root mean squared of Ra	$Rq = \sqrt{\frac{1}{l}\int_0^l z(x)^2 dx}$
Rv	Maximum depth below the centre line for a given profile length	$Rv = \lvert\min z(x)\rvert$
Rp	Maximum height of peak above the centre line for a given profile length	$Rp = \max z(x)$
Rz	Maximum length between the peak and valley for a given profile length	$Rz = Rp + Rv$

Table 1: A table summarising the surface parameters as well as the formulas to calculate each parameter [15].

For the above formulas, l is the total length of the sample that was taken, z(x) refers to the profile y value above or below the arithmetic mean line, x, which is used to as a reference along the sample length. The figure below visually illustrates how the defined parameters translate onto a sample surface profile.

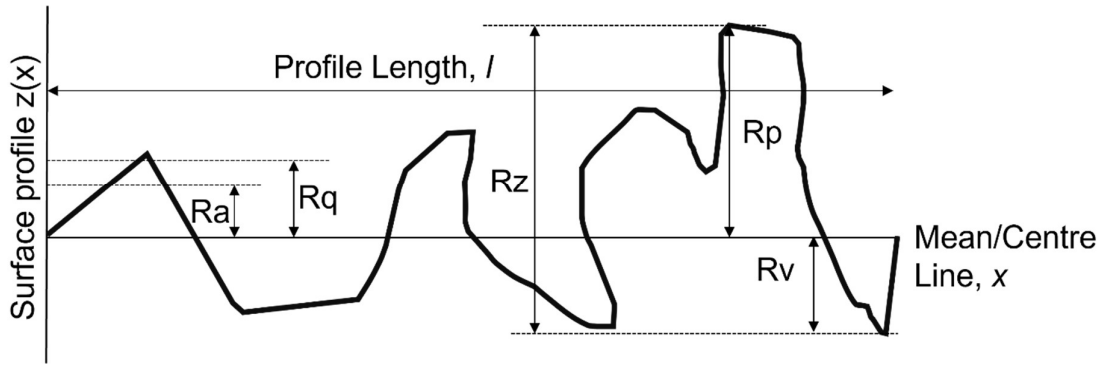

Figure 3: A sample surface profile to illustrate how a surface profile can be quantified.

Ra and Rq are closely related and are the most popular parameters used during analysis involving surface roughness. They are essentially a similar value usually about 10-25% difference between them [15]. The difference between the Ra and Rq values are that the Rq value is more sensitive and will increase quicker than Ra in situations where surface deviation is high in comparison to the mean which can also be understood by inspecting the equation [16]. For this research, Ra is the metric is used due to the simplification of the surface definitions/models that are defined during this study and therefore the difference between Ra and Rq will not be significant.

When defining these characteristics, the quantification process is only a surface sample significantly smaller than the entire workpiece that is assumed to be homogenous across the component. In most cases, this assumption is not feasible due to different sections of the component containing different

surface types due to the imperfect nature of manufacturing and thus a few samples are often taken and averaged when estimating the surface roughness parameters [17].

2.1.3 Surface Definitions

The nature of surface finishes is random and thus dependant on the samples taken on the workpiece surface. There can be slight differences that exist from component to component even on the same component. Therefore, the ISO standard has implemented a grading system where the surface finish for components can be defined and referred to by a standardised ISO grade. The table below shows the relevant roughness grade numbers that are correlated to the nominal surface Ra parameter as defined by ISO 1302 [18].

ISO Grade	Ra (µm)	Rq (µm)	Fabrication Technologies [19]
N12	50	55	Sand Blasting, Sawing, Hot Rolling, Flame Cutting
N11	25	27.5	Flame Cutting, Sawing, Hot Rolling
N10	12.5	13.75	Sawing, Rolling, Forging
N9	6.3	6.93	Forging, Sawing, Boring, Turning
N8	3.2	3.52	Planing, Shaping, Chemical Milling, Broaching
N7	1.6	1.76	Electron Beam Cutting, Laser Cutting, Drilling
N6	0.8	0.88	Grinding, Polishing, Electro-Polishing, Milling
N5	0.4	0.44	Grinding, Honing, Centrifugal Barrel Finishing
N4	0.2	0.22	Grinding, Electrolytic Grinding, Honing
N3	0.1	0.11	Grinding, Lapping, Centrifugal Barrel Finishing
N2	0.05	0.055	Lapping, Roller Burnishing, Super Finishing
N1	0.025	0.0275	Super Finishing, Centrifugal Barrel Finishing

Table 2: A table showing the ISO grade roughness with corresponding nominal Ra and Rq values with example fabrication technologies that have finishes at the respective grade.

There is a large overlap between fabrication technologies and their surface roughness they can achieve. The surface roughness of a component that a specific process achieves is dependent on its parameters at the time of fabrication [20]. The Aerolap polishing technology is expected to achieve surface finishing grades of N6-N3 dependant on its process parameters which will be explored at a later stage.

2.2 Polishing Overview

Understanding polishing as a field and understanding different approaches to polishing is paramount in investigating a polishing process. It provides the basis theory and approach which will best inform design decisions. The following section will discuss polishing as a field generally and then explores more specific polishing literature related to this project.

2.2.1 Introduction

Polishing is usually the final process when considering the manufacturing process of a part/component. This procedure involves the removal of microchips on the surface of a component which then improves the surface finish. This procedure has a range of benefits on component quality such as increased component longevity, decreased sound during dynamic operation and decreased friction which allows for increased torque (such the case of motor vehicle engines) [21]. A study was able to prove that polishing SLS Ti6Al4V samples improved the surface hardness of the samples which in turn resulted in higher rolling contact fatigue strength of the sample when compared to samples that are as built [22].

A critical aspect of an abrasive finishing procedure is the abrasive media that is used. The abrasive media removes microchips at the surface of the component. It has been found that as abrasive media is used, the wear on the abrasive media (due to an increase in abrasive particles in the medium) can cause the opposite effect and begin to damage the component which can lead to large scratches on the component [23]. At a nanometre scale, the abrasives essentially scratch the current surface of the workpiece to remove material from its current surface layer. This then creates a new surface layer that has finer scratches than that on the previous layer. This is done over a period to achieve a finer surface finish than before [24]. Scratching is a form of material failure due to crack propagation but not all polishing processes require this form of material behaviour. One study has been able to establish that additive manufactured Ti6Al4V can exhibit viscous behaviour during sliding contact polishing processes. This is due to the heat generated between the interaction which changes the material properties at the interaction point. Although these temperatures are not necessarily high enough to reach the melting zone of Ti6Al4V, the temperatures are enough to encourage recrystallisation of the surface which allows the surface layers to become more plastic and thus follow a different polishing mechanism [25]. Dependant on the polishing action required for the polishing process, abrasive material and size are two characteristics that are often altered to adjust the parameters of the process. All the above-mentioned considerations for polishing are critical in defining the polishing action for the polishing process being developed.

2.2.2 Abrasive Media

A critical aspect of an abrasive finishing procedure is the abrasive media that is used. The abrasive media removes microchips at the surface of the component and "absorbs" the chips. It has been found that as abrasive media is used, the wear on the media (due to an increase in abrasive particles in the medium) can cause the opposite effect and damage the component which can lead to large scratches on the component [23]. At a nanometre scale, the abrasives essentially scratch the current surface of the workpiece to remove material from its current surface layer. This then creates a new surface layer that has finer scratches than that on the previous layer. This is done over a period to achieve a finer surface finish than before [24].

Dependant on the properties required for the polishing processes, abrasive material and size are two characteristics that are altered to adjust the parameters of the process. This is mostly dependant on the mechanical properties of the workpiece to be polished whether it is a hard or soft material. The table below illustrates commonly used abrasives in industry [26]:

Table 3:Table illustrating commonly used abrasives, their strength and uses [26].

Abrasive	Mohs Hardness	Used For
Aluminium Oxide	9	Finishing steels that are hard or soft
Silicon Carbide	9.2	Finishing cast iron, nonferrous metals and non-metallic materials.
Diamond	10	Finishing tough materials such as hardened steel, glass and ceramics.
Cubic Boron Nitrate	9.5	Finishing superalloys and hardened steels [26]

As shown above, the hardness of the material is the characteristic that can scratch the workpiece surface and achieve a polishing action, therefore softer materials are finished with abrasives that have lower hardness. It is generally known that materials can only be scratched by materials that are harder than

itself [26]. Within the scope of this research, Silicon Carbide and Diamond powder are predominantly focused on as the abrasive material for polishing SLS manufactured Ti6Al4V samples.

2.2.3 Honing

Honing is an abrasive process used to polish the bores within an internal combustion engine. This technology is widely used across the industry with several other applications other than the internal combustion engine. This process typically involves making use of a bonded abrasive stick which is then rotated inside the cylinder to finish the inner walls of the internal combustion engine cylinder. This process also allows for a cross hatch finish on the surface of the cylinder which is useful for this specific application at it allows the cylinder to hold lubrication which will thus increase the lifetime of the component [27]. Another process that is like honing, known as rotational abrasive finishing, is a newer technology that introduces rotating both the workpiece and the abrasive stick which allowed for an increase in material removal rate. This process improved surface roughness during experiments by 70% from an initial surface roughness of 0.283µm to 0.88nm after 20 minutes [28].

2.2.4 Chemical Polishing

Chemical polishing is another polishing method whereby a workpiece is immersed into a polishing agent to remove minor deformation. This is usually performed after traditional mechanical polishing methods. Due to the nature of the method, it is usually used as a quick method to achieve a preliminary surface or the final preparation of the surface [29]. Chemical polishing is a glass manufacturing process that has been used for many years to attain desirable surface finish properties of glass [30]. Glass is widely applicable in a variety of industry such as high energy laser beams. An interesting study on chemical mechanical polishing investigated nano material removal on both silica glass and Bk7 glass. This study found that in the chemical mechanical polishing processes for the specific material, it was found that the chemical composition of the materials was a bigger indicator of material removal and the mechanical process can only assist until a certain threshold force [31]. It is also a process that is being incorporated into more modern fabrication methods such as SLS.

Chemical polishing is also effective in polishing SLS manufactured components since the chemical polishing solution is usually in a liquid form which allows it to cover the entire surface area of complex geometry as well as hard to reach areas that conventional polishing solutions may struggle to reach. A study on Ti6Al4V samples that are polished with a chemical solution of 5% hydrogen fluoride and 6% nitric acid was able to reduce the longitudinal and transverse surface roughness of a selective laser sintered sample by 1.5 and 11.34 times respectively [32]. Another study investigated the effect of heat treatment on selective laser melted Ti6Al4V samples before undergoing chemical polishing. The results from this study observed that heat treatment of these samples before chemical polishing can significantly differ the results of the chemical polishing process [33]. It should be noted that chemical etching is often used for SLS Ti6Al4V components due to the liquid nature of chemicals being able to surround complex geometry and uniformly lower surface roughness of a component. The effect of this is explored in a subsequent section.

2.2.5 Lapping

Lapping is one of the oldest finishing processes to decrease surface roughness and achieve good surface finish. This process involves making use of abrasives in a liquid carrier or as a paste that is placed between a plate and the workpiece and then rotated mechanically in numerous motions to achieve a fine

surface finish [34]. Dependant on the size of the abrasive in the slurry, different finishing characteristics can be achieved.

2.2.6 Modern Developments in Abrasive Jet Machining

The technology being developed is a variation of an Abrasive Jet Machining (AJM) method whereby the flow of abrasive media is used as part of the machining of a component. This section investigates more specifically the intricacies regarding the technology which informs of some of the decisions that will need to be made for this research. This section also discusses the current Aero Lapping technology which is the base technology for which this research improves on.

The benefits of AJM methods over conventional polishing methods are that abrasives in the form of a fluid can easily move around small intricate spaces and complex geometry to polish these surfaces [35]. With this being mentioned, these technologies require special machining devices which can be a limitation for some workshops dependant on accessibility. An attempt to overcome this issue is by attaching a tool bar made of cemented carbide to a rotational device (such as a CNC or drill) and placing a slurry of abrasive media compound between the tool and the workpiece. The tool bar can rotate at speeds between 4800-30000 rev/min which induces a fluid flow of the abrasive media which results in the polishing of the workpiece surface [36]. A study observed the various parameters of abrasive flow machining and observed that higher extrusion pressures resulted in better surface finishes and the number of cycles should be optimised between polishing and damaging [37]. Another technology, “Aero-lap polishing”, uses a mechanical process to fine-finish a component. This technology controls the amount of force applied to a component during the polishing process and found that surface damage could be significantly reduced by using this method of force control [8]. A study has considered the effect of hybrid abrasive media which contains various types of polymers. The outcome of this study has suggested that these hybrid abrasive materials can improve the surface finish of complex shapes. This study did however state that further development of the hybrid abrasive media is necessary to improve time and save on costs [38]. Another interesting development of fluid jet polishing system is the incorporation of magnetorheological fluid in the abrasive mixture. In doing so, changing the magnetic field’s intensity of the abrasive fluid can adjust the fluid flow properties and thus the polishing action [39].

Besides the advances in developing technologies that can be categorised as Abrasive Jet Machining, there has also been research conducted regarding the abrasive media that is used for these methods as mentioned above. Traditionally abrasives such as Aluminium Oxide, Silicon Carbide, Diamond powder and Cubic Boron Nitrate are used as the abrasive medium to polish surfaces [26]. As these modern techniques are developed, there has also been an increase in the study of composite abrasive media to optimise the properties of the abrasive media for the relevant technology which will be briefly discussed. During the abrasive flow machining process, a Silicon Gel has been added to abrasive particles to create a polishing media that flows as a liquid through a channel. A study has tested a variety of abrasive concentrations in two different Silicon gels and noted that the polishing action from the process can be varied according to requirements at hand such as surface finish, saving costs and improving efficiency [40]. Another study investigated the use of old and new abrasive slurry for an abrasive flow machine and concluded that these abrasive slurries begin to exhibit different properties such as viscosity and elasticity as they are used during the machining process due to an increase in debris from the process. The study also concluded that used abrasive slurries can result in a reduction of 30% in process efficiency and 20% lower surface quality [41]. Recent developments have attempted to improve jet micro-machining systems by adding a polymer (polyethylene oxide) to the traditional

water-only abrasive slurries that have been used. In doing so, the stability of the abrasive jet was improved [42].

2.3 Computational Methods

The research conducted for this investigation make use of numerical methods in its analysis. The simulations are also a form of numerical analysis with the modern computational power to analyse more mathematically intensive complexities within the system. This section examines the tools that researchers have used in similar studies to accurately mimic what is expected from a physical system.

2.3.1 Molecular Dynamics

Molecular Dynamics (MD) is a computational method that calculates the response of atoms by applying principles from Newton's equations of motion as well as the forces between these atomic particles due to their atomic energies [43]. Many studies have successfully been able to use this approach to replicate and develop polishing technologies. Such a paper investigated the surface changes that took place on a single Silicon crystal workpiece under three-body polishing conditions of diamond abrasives. The study was able to demonstrate a double abrasive polishing method and the relationship between the force, friction, potential energy, polishing depth, and thermal energy within the Newtonian layer of the interacting atoms [44]. Molecular dynamics has also been applied in the study of Chemical Mechanical Polishing (CMP) whereby a polyurethane pad was sandwiched between two silicon substrates. The output of this study was able to show the contact status between the pad and the silicon substrate under load and the conversion from elastic contact to plastic contact between the two elements [45].

A key aspect of the polishing process is the speed at which an abrasive particle impinges onto a surface. A paper investigating the polishing mechanism of sapphire using diamond abrasive was performed with the use of MD. In this paper, they were able to investigate the relationship between polishing speed and forces between the two materials by setting up experiments at different velocities. They were also able to alter the abrasive size and could determine the Material Removal Rate (MRR) from these simulations. The below image shows the MD simulation setup from this paper [46].

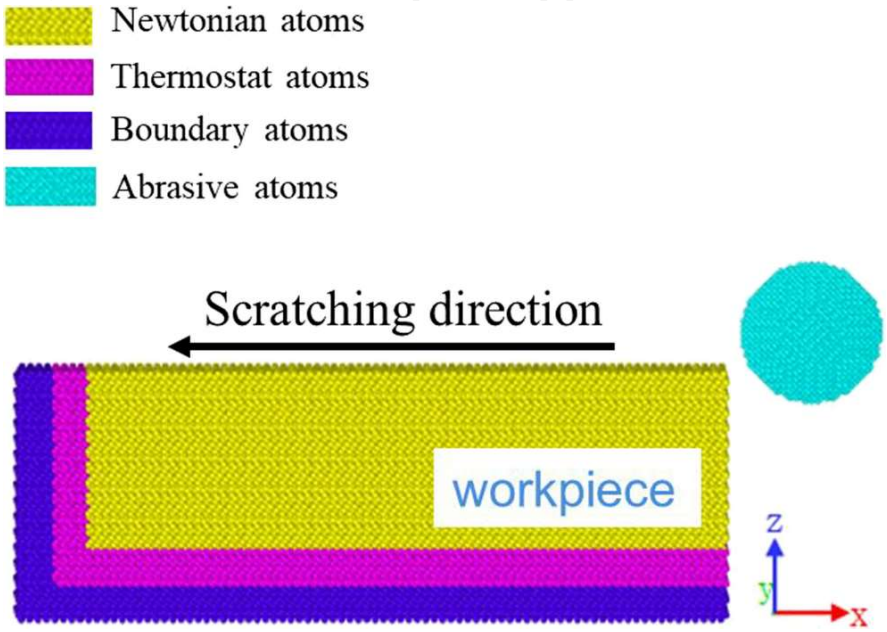

Figure 4: A molecular dynamics simulation setup for polishing sapphire with diamond abrasive.

The use of MD as a method to study polishing mechanisms has been used to successfully replicate an actual polishing action as well as computing the different process parameters that are important to understand when defining a polishing mechanism and furthermore designing the polishing technology to achieve said mechanism.

2.3.2 Finite Element Analysis

Finite Element Analysis (FEA) is a numerical approach to solve complex solid mechanics problems. The method is extremely popular and can be flexibly used in studying the response of structures and materials [47]. An investigation into nanoindentation of elastic-plastic micro spherical materials that used Finite element analysis was able to show that the loading curves for different materials can be retrieved from only one indentation [48]. The polishing system that is being developed is expected to undergo these nanoindentations onto an SLS Ti6Al4V workpiece using a flexible abrasive media 'indent'. One study investigated the nanoscale interactions between multiple surface roughness and specifically considering how these fractal interfaces are related to friction with the use of FEA. Although not directly related to polishing, it was able to show the elastic and plastic deformation response of the asperities on the surface and the interactions effect on friction. It discovered that the static coefficient of friction for a rough surface within specific parameters can have a lower friction coefficient than a smoother surface with the same material [49]. This is of course contradictory to what is generally initially assumed.

There is a subset of FEA that considers dynamic situations whereby conditions and material properties change over time that is known as Explicit Dynamics. Studying the proposed method of polishing would require this subset of analysis to accurately predict the polishing action. Although not directly related to polishing, a study investigating abrasive water jet machining considered the effect of a single particle impact into a Ti6Al4V alloy. The image below shows the setup of the simulation from this study.

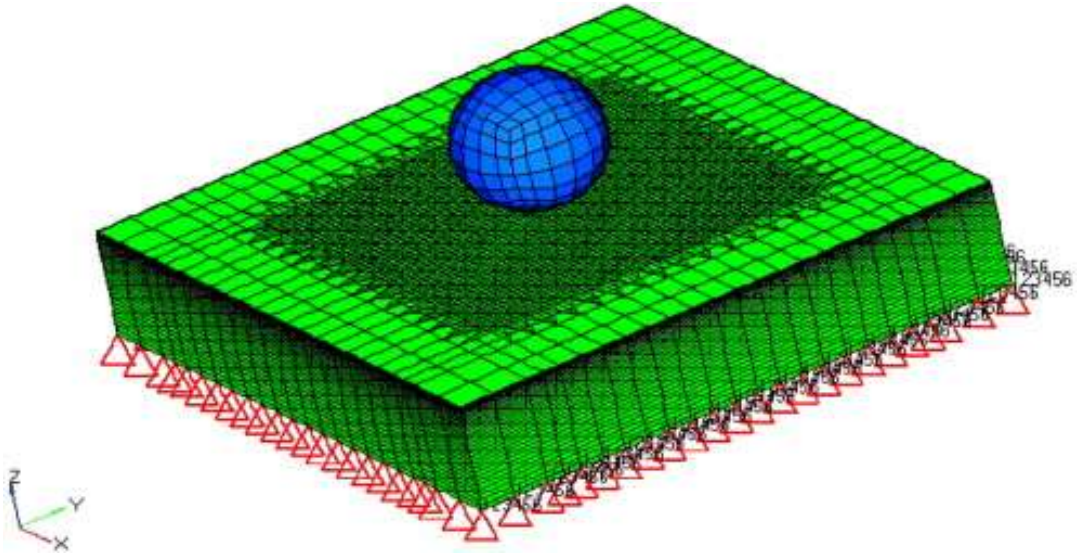

Figure 5: An FEA setup showing a single abrasive particle impacting a Ti6Al4V surface [50].

The researchers were able to use the results from these simulations to further develop their models and more accurately define the process mathematically. It was also mentioned that refining the model would require the simulation of an entire abrasive water jet to fully understand the material erosion which will be attempted in the future [50].The difference with this study and the Aerolap polishing process is that this study attempts to create material failure (cracking of the surface) in order to cut through the surface

rather than operate within the plastic and elastic limits of the Ti6Al4V surface and simulate deformation. Another study investigating drop tests of rigid bodies onto hybrid titanium composite laminates was able to indicate the impact response of the composite laminates and their layers to understand the different failure modes of the laminates. This was achieved with both a numerical and explicit FEA simulation [51]. Both the above studies use the same computational method as well as similar geometries, however, the computational inputs such as the simulation settings, material properties and initial conditions can achieve varying results that are applicable to the relevant application that produce completely different outputs. It can therefore be assumed that this method can work for the purposes of this research project.

2.3.3 Computational Fluid Dynamics

Combining fluid mechanics and mathematical models is a discipline known as fluid dynamics. Combining fluid dynamics with the computational power of modern computers is the computational method known as Computational Fluid Dynamics (CFD). It a well-developed and popular method used as a tool in research and engineering applications that involve fluid flow [52]. A study investigating the use of multiple jet polishing (and the advantages of this arrangement over single jet polishing) included a feasibility study that was achieved by means of a CFD Simulation. The results from this study verified that the multiple jet polishing method has a higher MRR than single jet polishing with similar parameters which makes this ideal for polishing larger areas of a shorter period. The simulations were able to inform design decisions such as the orientation of the jets due to an understanding of flow interference due to the multiple jets [53]. Magnetorheological Jet Polishing (MJP) is a superfinishing process specifically for optical elements such as glass that require an extremely low surface roughness due to its function [54].

A surface roughness model was developed with the use of CFD in researching the effect of a roughness distribution model on the material removal function of a MJP process. The theoretical model influenced by CFD simulations was able to define relationships within the process. However, these results were not perfect and there were some discrepancies that were noted when comparing the results from the model to the actual experimentation that was conducted. The discrepancies were mostly due to the difference in change of the distributed roughness model over polishing time as the CFD model is not able to accommodate some of the randomness and complexity that is found in the natural world [55].

The benefit of using CFD simulation is that it can study various types of flow and in these cases, create models that can define models between the flow and the MRR of the polishing method. The flow of a SiC abrasive slurry (of mesh size #4000) for a novel multi-jet polishing method was studied using CFD. The proposed polishing technology made use of multiple jets to fine finish the inner surfaces of rods and workpieces that are difficult to reach with conventional methods. Upon experimentation of the prototype, it was found that the proposed removal model developed by the CFD was effective and that it successfully predicted the erosion model of the physical technology [56].

2.3.4 Computational Method Review

Mathematical models that are applied with the computational power that exist because of modern computers have empowered researchers to perform studies and develop knowledge at a more rapid rate than before [57]. This literature survey has presented different computational methods and provided several examples of where similar polishing processes have been successfully replicated using simulations with each of these methods. The simulations have been able to accurately predict the

response of a physical system when the input parameters and boundary conditions have been setup correctly for each method. Each of these methods can simulate models using different mathematical equations to approach a problem.

Considering this understanding and referencing its applicability to the Aerolap polishing technology being developed, there are notes that can be made. The molecular dynamics method has been further investigated as a possible avenue for this research. It was found that due to the complex interactions of the workpiece, abrasive, and flexible media, defining the atomic arrangement of the system and the several interatomic potentials required a deep understanding into the chemistry of the system. After a consultation, it was realised that it would require vast experience in writing molecular dynamic programmes due to the increase complexity of the system and thus using molecular dynamics was an impractical method for this project.

The CFD approach has shown promising results with similar polishing methods and could potentially be used in simulating the proposed polishing with flexible abrasives technology that has been developed [8]. The benefit is that the abrasive material within a fluid, whether in the form of a slurry or air flow, the CFD approach was able to assign the fluid like nature to the solid abrasive as it could be represented as a fluid with the properties of an abrasive media. Due to the addition of the flexible media, the "fluid" begins to transition back into a semi-solid phase and thus assuming the homogenous properties of fluids during flow for the flexible abrasive media will create unreliable results. Another issue using this method is that the response by the workpiece surface upon impact of the flexible abrasive media will not be an accurate representation. This is because the CFD method does not consider the flexible abrasive media properties and internal interaction between the abrasive and flexible media but only the macro response of the fluid on the surface.

A recent development to overcome this issue is the CFD-DEM simulation packages which use principles from the Discrete Element Method (DEM) of solids within the fluid flow principles of CFD [58] . At face value, this new computational method is promising for the research community however, there are still significant challenges present with the biggest challenge being the computational power required to perform such a simulation specifically due to the DEM side of the method [59]. There have been developments in improving the computational efficiency of this method by making use of both Graphic Processing Unit and Central Processing Unit solvers but there is still more development that needs to be done [60]. On merit, a more mature version of this computational method incorporating aspects of FEA would be suitable for simulating the proposed polishing process but unfortunately it is not available as of writing.

The use of FEA is the most appropriate method in understanding the interface of the flexible abrasive media and the workpiece surface as it considers the material properties and the response for the interacting elements. Specifically, the use of the explicit dynamics subset of FEA will be essential to mimic the proposed polishing system due to the dynamic response of the materials during impact.

2.4 Selective Laser Sintering and Ti6Al4V Overview

This dissertation investigates the polishing process on a titanium alloy namely, Ti6Al4V (Grade 5) that is manufactured through the SLS process. Understanding the material and its properties after its fabrication process is important. This section covers the body of knowledge elaborating on these characteristics that influences the polishing process.

2.4.1 Selective Laser Sintering

Additive Manufacturing, and more specifically SLS, has many benefits over conventional manufacturing methods. To name a few of those benefits, SLS significantly reduces material waste as it only makes use of the material it needs. This therefore allows a significant saving in cost for components that are fabricated with expensive materials as well. When fabricating complex geometry, this process reduces machining costs and saves time during prototyping as parts with complex geometries can be produced much quicker than traditional methods [61].

SLS and Selective Laser Melting (SLM) are different words used to describe the same process. It is an Additive Manufacturing (AM) technology that makes use of CAD information to print a component layer by layer. This is achieved by spreading metallic powder into a thin layer and strategically focussing a laser that melts individual powders to each other as well as the previous layer to produce a 3D component-similar to the 3D printing process except with metals [62]. The surface roughness of a component produced using this method can be attributed to both process parameters and powder particle size [63]. The image below shows the schematic illustration of the process [64].

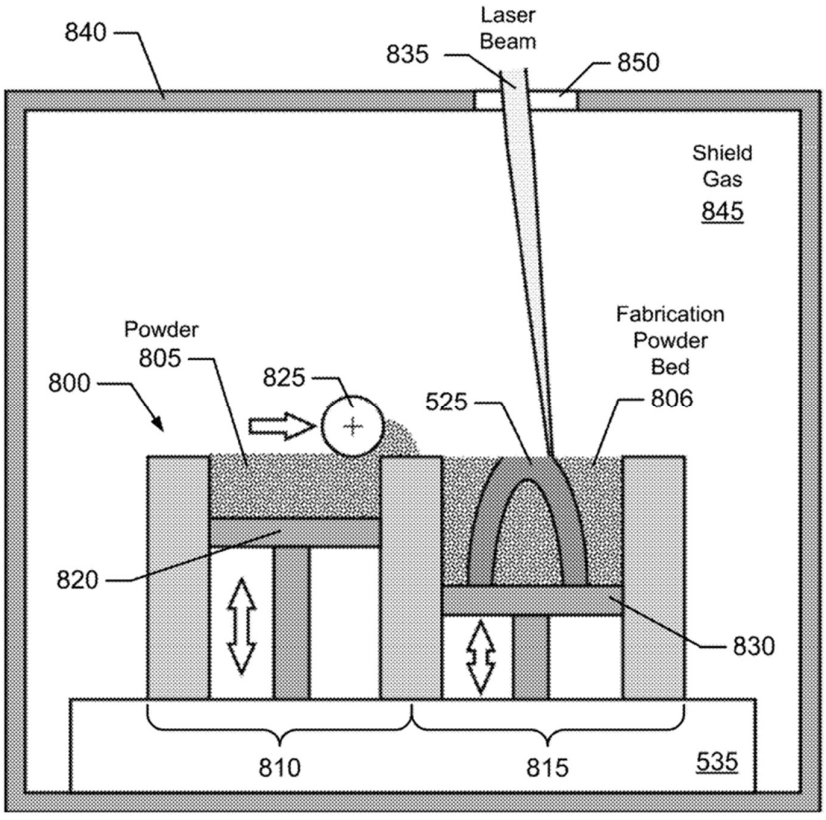

Figure 6: A schematic illustration of the Selective Laser Sintering Process [64].

2.4.2 Titanium Alloys

Many titanium alloys are being developed dependant on the specific requirements of its application, i.e., T-110 (Ti–5.5Al–1.2Mo–1.2V–4Nb–2Fe) is a high strength weldable alloy used to assist with air frames that are heavily loaded that require welding whereas the Ti–10V–2Fe–3V titanium alloy was not designed for welding and thus parts were fabricated as one large forging [65]. This further proves its versatility. This thesis will only investigate the Ti6Al4V titanium alloy as it is commonly used as the material of choice for SLS processes [66].

The Ti6Al4V titanium alloy (Grade 5) has low density, high specific strength, fracture toughness, resistance to crack propagation and good low-temperature toughness [67]. Thus, the titanium alloy has been used by the nuclear power, biomedical, aerospace and automotive industries [65]. Referring to the aerospace industry, titanium has a weight share of 25% in modern aeroengines. These parts include the; fan vane frame; fan disk; tail plug; manifold; compressor spool; booster spool as well as the booster case [4]. Due to the complex geometry of aerospace parts as well as the light weight of Ti6Al4V, aerospace components are often fabricated through SLS which extends flight range, increases payload as well as reduced fuel consumption [68]. A study investigated the energy savings and CO_2 emission reductions by the year 2050 dependant on the adoption level of AM components in passenger aircrafts in the United States. This study found that the United States can save up to 173GJ of energy/year and reduce CO_2 emissions by 13.3 tons/year in 2050 [69]. This example further justifies the move in industry to further develop solutions around the process and ensure the adoption of the technology.

There are important aspects to discuss that make Ti6Al4V components that are produced using modern additive manufacturing methods different to Ti6Al4V components that are produced conventionally. The first characteristic to discuss are the material properties and how they are affected. Ti6Al4V titanium exists as a bi modal grain microstructure when it is produced through SLS. The properties of Ti6Al4V change significantly depending on the low-temperature α-phase and the high temperature β-phase [70]. The high temperature gradients during the SLS process causes the microstructure of Ti6Al4V produced part to be predominantly martensitic or α-phase. A decrease in the α-phase in a specific component will lead to improved yield stress but lower fracture toughness and quicker crack propagation [71].

During the fabrication process, SLS parameters such as scanning strategy, energy density and scanning velocity affect the component structure [72]. SLS thus does have its challenged as a process. While investigating mechanical properties of SLS Ti6Al4V samples, it was found that the fatigue properties of the specimens is significantly reduced when compared to the same material produced through conventional means. This was attributed to porosity, surface finish and residual stresses - all of which are because of the additive manufacturing process [73]. Another reason for the decrease in fatigue strength can be attributed to material defects due to lack of fusion of the metal powders during the production of Ti6Al4V specimens [74]. Impurities and foreign elements within the powder is also a reason for defects such as oxygen content. Oxygen becomes trapped within the powder in the material during the fusion process which results in micro cracks and thus lower mechanical performance [75]. It has also been reported that additive manufacturing processes increase the yield strength of Ti6Al4V specimens which consequently result in the specimens exhibiting brittle behaviour and as previously mentioned, lower fatigue strength [76]. To combat fatigue strength, it has been reported that chemical etching has shown the best results in improving fatigue strength of SLS produced Ti6Al4V samples [77]. A study investigated the effects of post-process annealing strategies and found that the properties of SLS fabricated Ti6Al4V can have varying microstructures that can cause the component to be more ductile or have a higher Ultimate Tensile Strength (UTS) [78]. Heat treatments can also be used to remove material defects and thus improve fatigue strength but as mentioned, consequently decrease the tensile strength of the component [79]. Laser polishing is another thermal treatment process that affects the microstructure of the specimen which is being widely reported on in literature. A study has reported that laser polishing improves the hardness and wear resistance of Ti6Al4V specimens while also decreasing surface roughness [80]. Although this is also a process involving thermal energy, it appears that this process has the opposite effect on the mechanical properties of the specimen as opposed to what has been previously mentioned. Considering the above, it appears that the final mechanical

properties of the Ti6Al4V part is decided by the SLS Process as well as any processes that proceed its fabrication.

Another characteristic to look at is the surface finish of the Ti6Al4V component. Ideally, these new manufacturing methods also require modern finishing technologies if the application requires. The table below indicates the surface roughness properties of Ti6Al4V titanium after the SLS process:

Table 4: Table indicating surface properties of SLS fabricated Ti6Al4V

Metric	**Value**
Porosity	0.1-0.5 [81] [82]
Profile Surface Roughness, Ra (μm)	5-40 [73] [83] [84]
Residual Stresses, σ (MPa)	100-500 [85]

From the above table, it is seen that the process parameters of SLS will affect the surface roughness of the final component. A study looking into Selective Laser Sintering of Ti6Al4V and pure titanium for dental application reported that the surface roughness of their test specimen was different depending on the direction of the surface relative to the orientation of fabrication. On the Z axis (both XZ and YZ planes), which is the same direction as the layers that are built through the process, the surface roughness (Ra) of the Ti6Al4V specimen was 5.04 μm and 3.4 μm in the XY plane [86]. These differences are significant when considering the scale and operational envelope at which the Aerolap polishing process can operate within. The experiments conducted for the purpose of this study demonstrates how the surface roughness can significantly affect the polishing action.

2.4.3 Review

This literature suggests that two parts fabricated from the same CAD model, the same material and, the same manufacturing technology (Selective Laser Sintering) can still result in two different surface characteristics with specific reference to surface roughness and material microstructure. This is important as part of the development of the technology is to consider the end user and possible issues that may arise. Mitigating these issues would require a thorough understanding on the polishing action and all the factors that can influence the polishing action.

Some of the factors that influence the polishing action are internal parameters of the technology that can be changed such as the material used for the flexible abrasive media and the impinge velocity of the media. Not covered within this research is the inclusion an automated technology upgrade whereby a manipulator arm can rotate and move the component around as per the CAD model to polish complex surfaces efficiently and uniformly. This upgrade would also have its internal parameters such as the feed of the arm and the geometric path the arm uses. The other set of factors that will affect the polishing action are external factors. These external factors are not parameters that the technology can change such as the operating environment (i.e., temperature and humidity) and the incoming component being polished but these factors can affect the polishing action even if the parameters of the technology are kept constant. Later in this report, an argument is made on how the initial surface roughness of the incoming component can contribute significantly to the polishing parameters of the proposed technology. The fabrication of a component that precedes this final finishing process can affect the polishing action that this technology can achieve. Literature has also suggested that there may be a need to perform other finishing methods first to lower the surface roughness into the polishing range the

proposed technology is designed for. Therefore, understanding the SLS process, it's parameters and how it can affect the mechanical properties of the Ti6Al4V alloy are essential when developing this technology.

2.5 Summary

The literature covered in this chapter have highlighted the current published knowledge on polishing technologies and applications, computational methods that have been used to analyse the polishing methods and, Selective Laser Sintering and the Ti6Al4V alloy that are used to fabricate the parts that this technology will polish as the final finishing process. This literature review has also briefly highlighted the various concepts of surface roughness that are used during this study.

The polishing overview chapter highlighted the various studies that have investigated different technologies that are like the proposed finishing process. This section also reported on studies that attempted to change the material composition of abrasive media to achieve desirable polishing characteristics. This section provides an understanding into the various aspects that will need to be considered in designing and analysing the proposed polishing technology.

The computational method chapter discussed three different approaches for investigating the polishing action, namely, Molecular Dynamics, Finite Element Analysis and Computational Fluid Dynamics. The strengths and weaknesses have been discussed for these methods and more importantly, applied within the context of the research being conducted within this report. It was concluded that the use of Finite Element Analysis and more specifically the use of the Explicit Dynamics would be the most appropriate method for this research.

The Selective Laser Sintering and Ti6Al4V chapter developed a deeper understanding into the fabrication process that will precede this polishing process. It concluded that the process parameters of Selective Laser Sintering can change the surface characteristics of the incoming component which can affect the polishing action of the technology being developed. It was also noted that there may be a need for finishing processes to take place before the use of the proposed polishing technology.

The literature review has provided a robust foundation and understanding into current literature regarding this topic. The development and research of the Aerolap technology is conducted with an informed understanding and provides a clear view on the approach that can be used moving during this project.

3 Methodology

The research and development of the polishing process will consist of three main work packages namely: Design and Development, Numerical Calculations and, Computational Experiments.

Design and development summarise the work that has been completed in designing the system and its components in the design processes. The final developed technology is also presented.

There are various theoretical theories that can be applied to understand the polishing process. This will look at contact mechanics, indentation theory and kinetic energy model. The various system parameters will be entered into these calculations with an ideal nanoscale understanding of the surface-surface interaction between the abrasive media and the surface of the component to be polished. A comparison between these models is presented and discussed to understand the various aspects of the model to evaluate which model is more appropriate for the polishing system. The developed models enhance the understanding of flexible media and the components surface interaction. These findings pave the way for a better optimization of the process.

Computational experiments by means of an explicit dynamics model on Ansys to setup parameters that have been informed by work packages that have preceded these experiments. The output of these simulations are analysed and discussed and thus provide a deeper understanding into the interaction at the surface of the flexible abrasive media and the workpiece.

4 System Design

This research project involves the redesign of a polishing technology that incorporates the use of flexible media that improves the efficiency of the current process. There are a few aspects that were required to be designed due to the custom nature of the project which will be reported on. This section will cover the design work that was completed on the system before lockdown restrictions that limited its progress.

4.1 System Overview

The proposed system model is illustrated in Figure 7: Proposed system model for aero-lap polishing machine below including all the major components as well as showing the abrasive cyclic flow through the system.

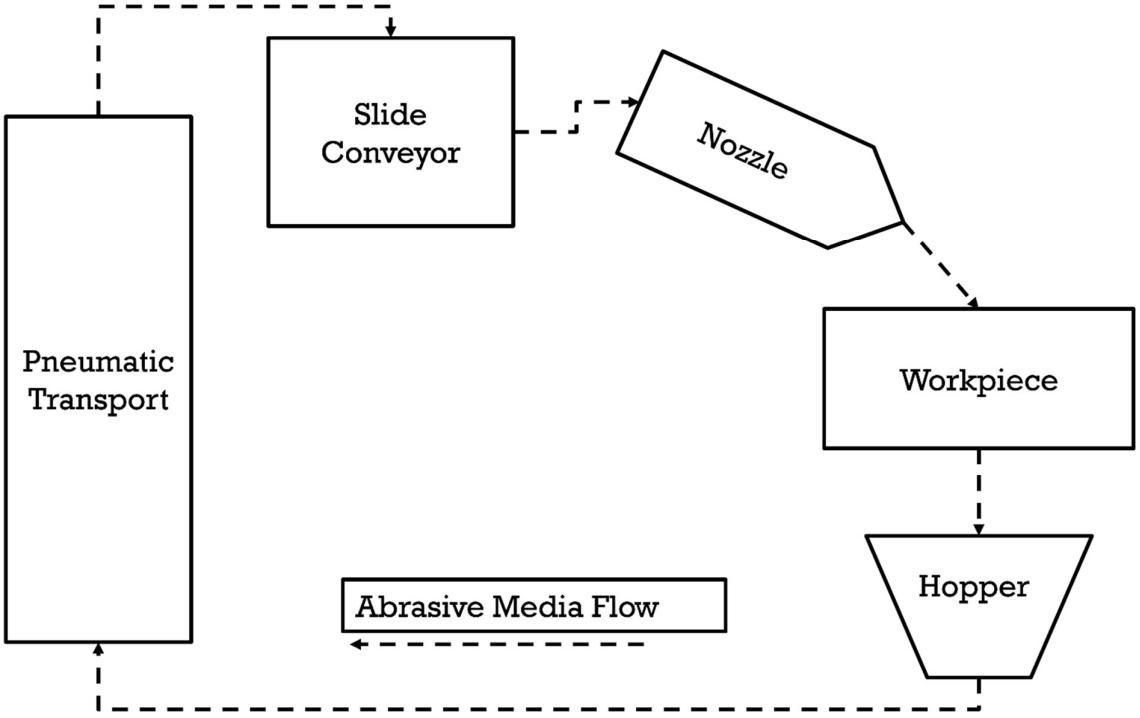

Figure 7: Proposed system model for aero-lap polishing machine

Considering the flexible-abrasive media flow throughout the system shown by the above figure, the system will be explained starting with the hopper. The flexible-abrasives are removed and filled into the system by means of the hopper which collects all the excess abrasive media within the system. The flexible-abrasive media is then transported through the pneumatic transport system which elevates and feeds the abrasive media into the slide conveyor. The slide conveyor then accelerates the flexible-abrasive media to the desired velocity as per requirements of the polishing action into the nozzle. The nozzle directs and controls the flow of the flexible-abrasive media from the slide conveyor. The controlled abrasive media exits the nozzle and impinges onto the workpiece surface causing the required polishing action. The flexible-abrasive media then rebounds off the surface within the workspace area and is collected by the hopper to move through the process until the flexible-abrasive media loses its polishing characteristics and is replaced.

What is not shown on the diagram is the control system that will allow an operator to manage and observe the various process parameters that will be vital to the success of the proposed system. The

control system is also the work horse that will allow for certain automation that can be achieved as well as possible upgrades that will be discussed in the relevant section.

It is also important to note that in when designing this system, the priority will be to include as many off the shelf products as possible to improve the ability to maintain the machine for operators and to also decrease manufacturing costs. Parts that can be found off the shelf will be specified with requirements and parts that require custom design due to its unique function will be designed accordingly. The reason for this decision is that a newer technology will most likely have barriers of entry into a market [87]. Some of these barriers include capital investment required from companies to invest in a new technology and switching expenses that relate to changing a current system that companies may have in place already that may serve a similar function without the benefits of the current system being suggested. Hence keeping costs to a minimum and increasing the ease of maintenance of the system will increase the chances companies adopting the newer technology on their manufacturing and servicing lines. As will be shown during the design process, some subsystems have been designed in greater detail than other elements which may be off the shelf.

4.2 Control System

The control system is part of the design requirements to assist with the managing of various processes in the machine as well as to ensure that safety standards are met. The control system also serves as the interface to where the operator will interact with the various settings required to adjust the properties of the polishing action. This is made possible with the use of a Peripheral Interface Controller (PIC) and various peripherals. The Control system is made up of various sub systems that interact with the PIC which then uses this information from these interactions to perform specified requirements as will be discussed below.

4.2.1 Safety Features

There are required safety features that the machine includes to improve the overall safety of the machine. These features are listed and described below.

Lighting
Lighting refers to the essential requirement that the operator can observe what they are doing due to adequate lighting provided by a workspace light. Other lighting also includes the operation light or tower light which indicates to other operators in the area whether the machine is in use or not.

Door Safety
There are four doors on the machine that provide access to the various sections of the machine to perform maintenance tasks as well as possible upgrades to equipment if necessary. Because this becomes a safety hazard, the doors are fitted with an inexpensive reed switch which is simply a switch that is operated by a magnetic field with the magnet being mounted onto the door and the reed switch being mounted inside the door so that the circuit is closed when the door is closed. By doing so, the PIC can detect whether a door is open or note and can inform an operator of a door that is not closed properly or shut down the machine if a door is opened while it is functioning.

Exhaust fans
The machine contains various equipment and electronics that produce heat while the machine is under operation. Therefore, exhaust fans have been included in the control system to ensure that the build-up of heat due to extended periods of usage is removed by the system by turning on the fans until a safer

operating temperature is reached. The biggest contributor to heat in the system will be the nozzle and the motor.

Emergency Stop Manual Switch
The emergency stop manual switch is essential for the operator to be able to turn off everything during an emergency operation. The emergency switch will be connected to the main power supplies to cut off power to components such as the motor speed controller as well as the PID controller which powers the heat cartridges. The manual stop is also connected to the PID so that it can close the pressure valve initiate any further safety protocols as required under such conditions.

4.2.2 Operational Control Requirements

Aside from the safety requirements for the system, there are also control requirements that assist with the operation of the machine and ensure that the machine can produce a polishing action that is consistent and according to the requirements of the operator. These features are discussed and listed below.

Motor Speed Control
The 3-phase motor used to feed the abrasive mixture into the nozzle is accompanied by a speed controller that can convert the single-phase input of a plug into a three-phase frequency-controlled current that controls the speed of the motor. The motor speed controls the amount of abrasive feed that the nozzle receives which due to the conservation of mass equation, is what the nozzle would be feed onto the workpiece to achieve a polishing action. Therefore, the motor speed is an essential operational requirement for the system as it controls the amount abrasive that is impinged onto the workpiece. The PIC will use a communication protocol (as set by the requirements of the speed controller) which allows the PIC to change and adjust the speed as necessary, either by operator input or by automation and pre-set values.

Operational Sensors
There are further sensors that are required in the machine for the machine to have a full understanding of its own condition. This includes a distance laser sensor to detect the abrasive media in the bin and to check there is still sufficient flexible abrasive media for the machine to run. There will also be pressure sensors across the pressure system to ensure that the required pressure for the venturi exists so that these components are operation. There will also be a speed sensor on the motor to ensure that it is rotating at the required speed. With the motor speed operating lower than expected could mean that the system is blocked between the slide conveyor and the nozzle exit and is struggling to accelerate the flexible-abrasive media through the nozzle. Another way to detect if the motor is working harder than expected is by making use of a thermocouple on the motor and detecting if the heat being emitted is much larger than usual. This redundancy is a suitable way to detect a blockage in the system and to communicate this to the PIC.

Further Upgrades
During this project, there has been a foreseeable requirement for further automation and the inclusion of more features that will not be included for the initial prototype. Such a feature includes a 5D axis manipulator that can automate the polishing action. This would require the PIC to communicate with the motor control boards to achieve the required movement at the required speed. This will also include further sensors that, for example, may check to see that there is no interference (force sensors) with the manipulator arm and that the motors are not overheating (thermocouples) due to this interference. There

will also be required extra processing power to interpret the G code and respond accordingly in real time. Another feature that has been considered is the ability for a camera to be placed into the work area of the system that can use a computer vision algorithm that can map out the surface of the component electronically and allow the algorithm to determine the best method and parameters to polishing. This would be used in conjunction with the 5-axis manipulator arm. The addition of this machine learning feature will require the use of more processing power in real time as well as communication gateways for the camera and other sensors such as lidar that may assist with the algorithm.

4.2.3 Overview

The following diagram shows the high-level overview of the control system and its peripherals.

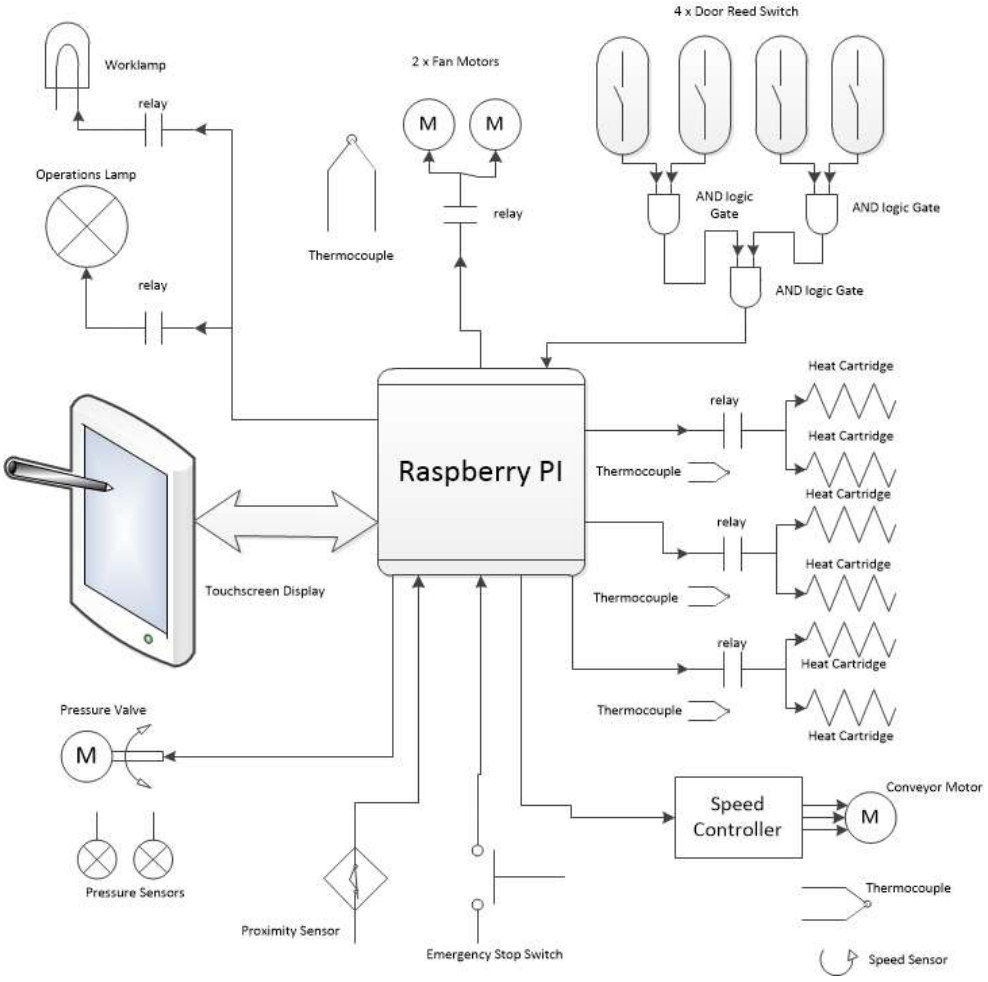

Figure 8: A control system diagram showing the various electronic components will be required to interface with the PIC.

The Raspberry Pi 4B is being used as the PIC as it is inexpensive, well supported and will serve the requirements of the initial system. Regarding future upgrades, the Raspberry Pi 4B is will be able to communicate with additional PIC controllers that will assist with additional required processing where necessary and communicate the outcomes to the Raspberry Pi 4B to make high level decisions and adjust the necessary process parameters as required. The Raspberry Pi 4B will be a crucial component and thus all its processing power should be focused on managing the process parameters. This will keep its load to a minimum and lower the risk of the machine "stuttering" with its processes due to being

overloaded. This becomes a safety concern depending on the consequences that this will cause. Such consequences can include not responding quick enough to an emergency stop switch activation or the touchscreen interface not updating as an operator attempts to make changes to the process parameters.

4.3 Overview of Developed Frame

The following section briefly discusses the designed Aerolap technology that will be used for experimentation. The polishing process is encapsulated within a 1x1m space and is built with the use of aluminium extrusions. The frame is divided into four different quadrants as shown below

Figure 9: The developed prototype of the Aerolap technology.

Each of these quadrant sections contain a door that can be used to access the relevant components within said quadrant. The quadrants house the following components as listed below:

1. The work area where the item being polished is located. This quadrant has a large window that allows a user to observe the work they do.
2. The collecting hopper is on the roof of this quadrant with the bin directly below. Opening the door of this quadrant is how one would replace or add the flexible abrasive media to the system.
3. The biggest quadrant which will contain the interface from the workshop to the machine for both electrical power and to supply the system with air pressure. The power distribution and control boxes are located here which then manages the rest of the process. The air pressure regulator and automated pneumatic valves will also be located here.
4. The final quadrant houses both the slide conveyor (with the motor) and inlet half of the nozzle.

4.3.1 Design Insights

The entire frame that encapsulates the technology is constructed with aluminium extrusions which allow for the system to be flexibly adapted for upgrades and changes for further revisions while also maintaining the sturdy. These extrusions can easily be extended to increase the polishing capacity by incorporating larger components that can accommodate a higher abrasive flow over a larger area which thus increases polishing rate. This therefore allows the system to be flexible and designed according to the specifications of the workshop requirements which can improve the adoption of the technology for both large- and small-scale manufacturing plants. Using aluminium extrusions is also ideal as there are a comprehensive amount of off the shelf accessories that allow for the easy support of the various components (such as electrical cables and pneumatic pipes) that can flexibly be moved as the fixtures are not permanent. Again, this increases the ease of making changes and upgrading if need be.

There is a large clear window that allows the operator to freely see the workspace area and more importantly, be able to see the polishing task at hand. There are also gloves attached just below the window so that an operator can safely hold a component and use the machine without being directly exposed to abrasive media as well as preventing any abrasive media from escaping the system

4.4 Closing Remarks

A significant amount of work has been completed in designing and developing the polishing technology. The finalising of the design and the testing of the final system is currently being undertaken at the University of Cape Town in the advanced manufacturing laboratory as of writing.

One of the aspects of this process where development had not made significant progress is the design of the control system at a lower level than the high level represented here. There was still a considerable amount of work in creating the interfaces on the touchscreen on the side of the frame for the operator as well creating code that runs and manages the machine processes in the background. The hardware for these components still needed to be fully designed and their interfaces to the PIC defined.

Although the scope change is not ideal, being able to focus on the theoretical analysis in more detail and performing simulations allow for a deeper understanding into the process. One of the benefits of performing simulation analysis is that the insights presented by the results can improve the design without the need for creating multiple physical prototypes which can become costly. This understanding can inform further design requirements as well as possible alterations such is the nature of product development [88]. The next two chapters will thus investigate this process and better understand the behaviour of the process due to the addition of the flexible media.

5 Numerical Analysis

As part of developing the polishing mechanism a numerical analysis was done to better understand some characteristics that are involved with this system. This theoretical understanding provides a basis for the design of the simulation experiments and for the design requirements of the machine. Due to the complexity of the design interface, there are a few assumptions that were made and will be elaborated on in their relevant section.

The following clarifications are required for understanding the numerical analysis:

- An abrasive particle refers to a single abrasive particle such as SiC or Diamond powder.
- The flexible media indicates only the flexible media particle such as PET or gelatine.
- When referring to a flexible abrasive media, it refers to the combination of both materials and their arrangement.
- This numerical analysis unveils the study done with abrasives with the mesh sizes #1000, #5000 and #8000 which correspond to abrasive particle diameters of 6.5 µm, 2.5 µm and 1.5 µm respectively. These abrasive sizes are commonly used during various polishing processes and thus have been chosen as the scope of study.

Both the numerical analysis and simulation experiments consider an asperity diameter of around 1.6 µm with some variation in certain analysis. Due to the nature of the surface roughness model, considering a single asperity for simplification of the model can be used as an average estimate of the polishing action because in a real polishing example, there will be variations across the surface. A simplified surface model assumes that a surface has peaks and valleys that on average have a distance of $D_{asperity}$, the corresponding Ra value will thus be the radius length of the asperity and therefore an asperity diameter refers to a surface roughness that is half the diameter of the asperity, i.e., 1.6 µm diameter refers to a surface roughness with Ra= 0.8 µm.

5.1 Contact Mechanics

The fundamental underlying theory of the polishing action is contact mechanics. It is used to describe the behaviour on the surface of an item when two objects physically touch each and push each other according to Newtons Third Law. In general, when two elastic bodies (one spherical surface and another convex surface) exert a load against each other, then a local deformation will occur which will enlarge into line or surface contact and thus causing a polishing action.

5.1.1 Theoretical Approach

The polishing process using the flexible abrasive media applies a controlled amount of impinging force to the workpiece being polished, resulting in reduced surface roughness as the process initiates plastic deformation of surface asperities and displaces the same into the dents and valley of the surface texture. The force acting on the elastic body which is a mixture of flexible media and diamond abrasive particles is computed using the first principles of conservation of momentum and given below:

$$F = \frac{m_1 v_1 - m_1 v_2}{t} \quad \textit{Equation 1}$$

where m_1 is the mass of flexible media, v_1, v_2 are the impinging velocity and final velocity after impact respectively. t is the impact time taken by the flexible media onto the workpiece. The force in the above equation is an average force across the impact time but the force that will contribute to the polishing

action is the maximum force when the asperity has undergone maximum displacement. Therefore, to accommodate this adjustment, the average force is multiplied by 2 to assume a linear loading and unloading force from 0N – F_{max} – 0N. Upon impinging onto the asperity, the flexible media tends to change its shape and hence it is fair to assume that the final velocity v_2 will have a negligible value and therefore the equation can be simplified to:

$$F_{max} = \frac{m_1 v_1}{t} \times 2 \qquad \textit{Equation 2}$$

Shown in the below figure is the impingement of the flexible abrasive media on the surface.

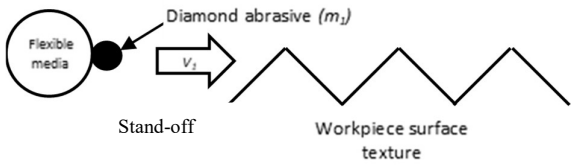

Figure 10: Schematic sketch of flexible media interaction on the workpiece surface.

The local deformation at the contact surface is computed using the principles of contact mechanics described by the following equation.

$$\delta = 1.04\left[(\eta_1 + \eta_2)^2 F^2 \left(\frac{(D_1+D_2)}{D_1 D_2}\right)\right]^{\frac{1}{3}} \qquad \textit{Equation 3}$$

where η_1, η_2 are equated to $\frac{1-\nu_1^2}{E_1}$ and $\frac{1-\nu_2^2}{E_2}$ for the flexible abrasive media and workpiece surface respectively. D_1 and D_2 are the equivalent diameter of the flexible abrasive media and surface finish (R_a) value of the incoming component. The following table shows the properties of flexible media used for computation of local deformation upon impingement of flexible media on the work piece surface texture.

Table 2: Properties of the materials used for this computation

Detail	Value	Detail	Value
Modulus of elasticity of Ti6Al4V alloy (workpiece) (E_2)	110 GPa	Diamond abrasive size (D_1)	1.5 ~ 6.5 µm
Modulus of elasticity of Diamond (E_1)	1 050 GPa	Roughness (R_a) of the incoming Ti6Al4V component (D_2)	0.8 ~ 2 µm
Time taken for the impact of the abrasive particle (t)	20 µs	Mass of each diamond particle (m_1)	6.19E-15 ~ 5.03E-13 kg
Poisson ratio of the Ti6Al4V (workpiece) (ν_2)	0.33	Density of Diamond abrasive (ρ_1)	3500 kg/m^3
Poisson ratio of the Diamond (ν_1)	0.20	Impact velocity of abrasive media (v_1)	0 ~ 80 m/s

Upon impingement of the abrasive media, a local deformation would be imparted and the radius of the local deformation (a) is given as:

$$a = 0.721\left[(\eta_1 + \eta_2) F \left(\frac{(D_1 D_2)}{D_1+D_2}\right)\right]^{\frac{1}{3}} \qquad \textit{Equation 4}$$

Using the contact radius and applied load the stress acting at the at the impinging surface is given as:

$$\sigma = \frac{1.5F}{\pi a^2} \qquad \textit{Equation 5}$$

This load stress will determine whether the polishing action will be due to chipping off asperities or if the asperities will be plastically deformed. This is dependent on the workpiece material properties and its mechanical properties. Ideally, the polishing action should be completed due to plastic deformation as this process will strengthen the surface properties and thus increase the longevity of the components. Chipping off asperities requires stronger polishing forces, with these stronger polishing forces, there is a greater risk of damaging component's surface and that cracks can develop on the surface which thus would weaken the component and decrease the surface life of the component.

5.1.2 Results and Discussion

The following graph shows the force values that correspond with the respective impact velocity using the momentum equation for a single abrasive.

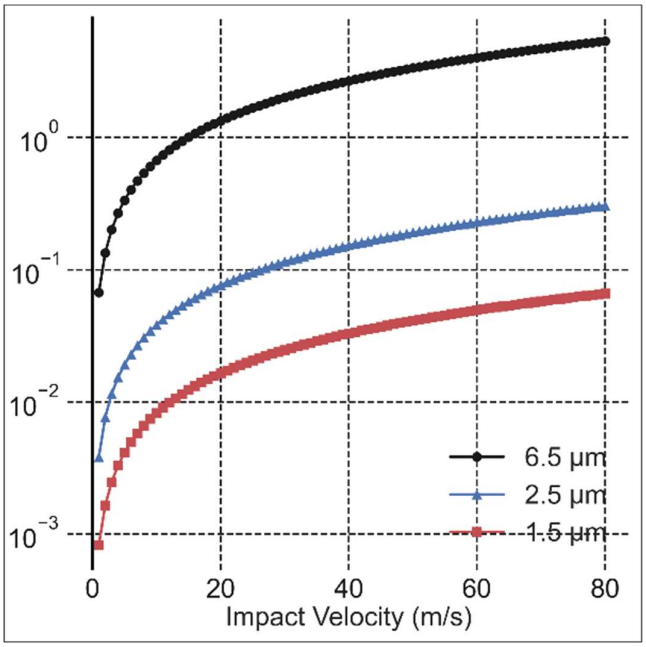

Figure 11: A line graph showing the relationship between impact velocity and impact force that will be used for this computation.

There is a linear relationship between the impact velocity and force. This assumption considers a static impact time of 20 µs whereas in reality, the impact time is expected to be different according to various process parameters. It is expected that higher velocities will result in a quicker impact time than lower velocities which will thus also influence the applied force. This effect is also seen with the #8000 abrasive containing significantly smaller force values for corresponding velocities. However, this simplification is suitable for this analysis as the trends are still observed, the difference in time is established during the simulation experiments which is discussed in the following chapter. For this numerical method, the following graphs are drawn from the perspective of velocity as a linear substitution to force to make the graphs easier to interpret and understand the relationship between velocity, asperity size and the local deformation caused by the impact of a single diamond abrasive particle.

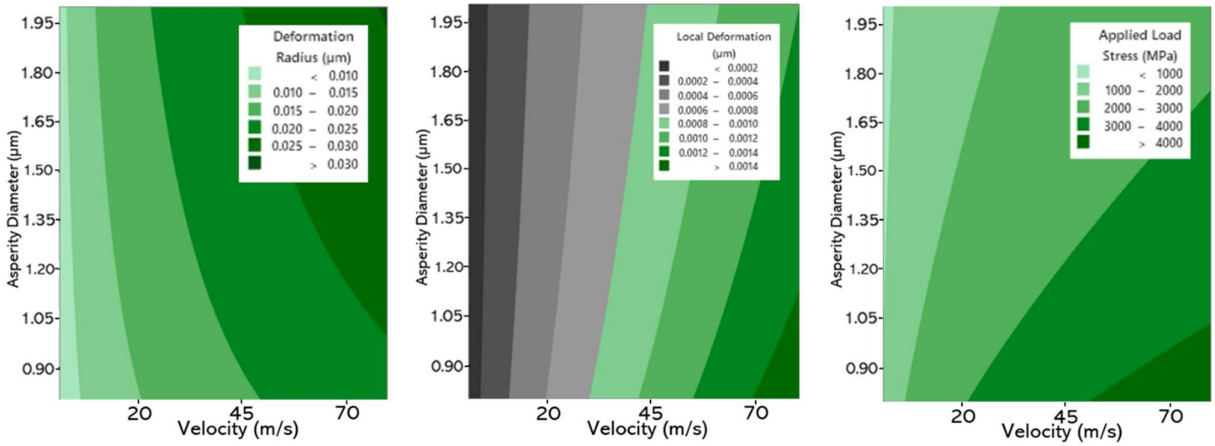

[a] [b] [c]

Figure 12: A contour plot showing the relationship between asperity diameter, abrasive of diameter 6.5 µm impact velocity and a) deformation radius, b) local deformation and c) applied load stress.

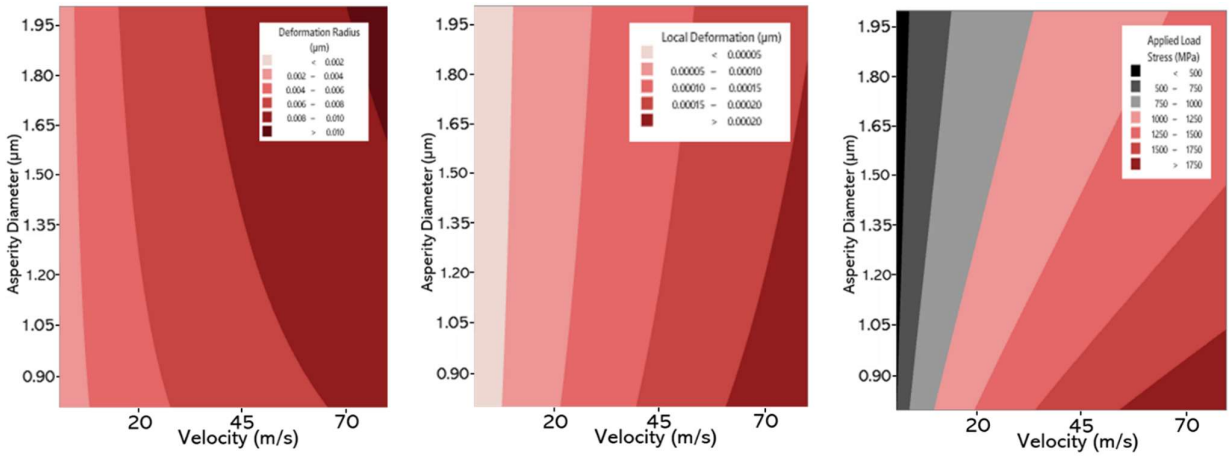

[a] [b] [c]

Figure 13: A contour plot showing the relationship between asperity diameter, abrasive of diameter 2.5 µm impact velocity and a) deformation radius, b) local deformation and c) applied load stress.

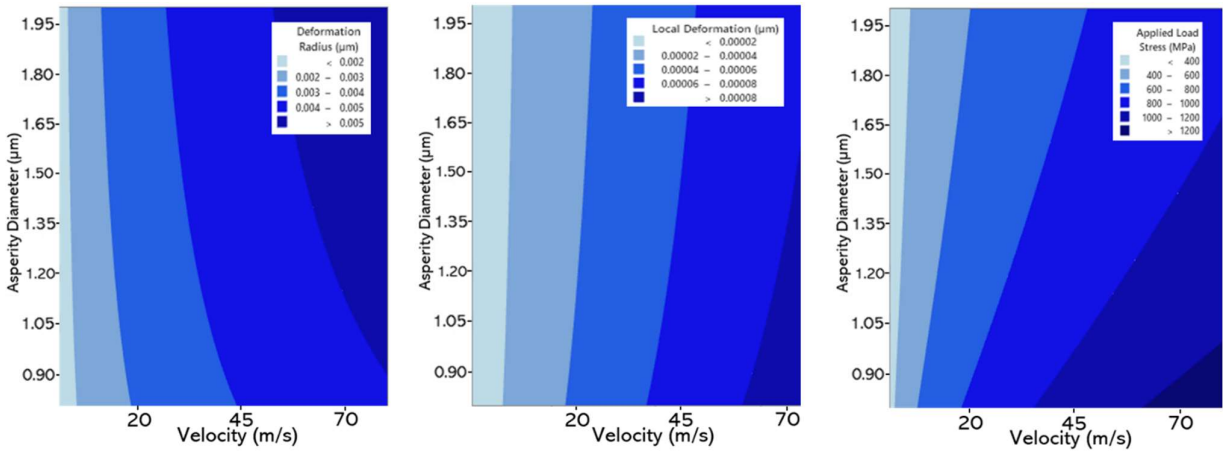

[a] [b] [c]

Figure 14: A contour plot showing the relationship between asperity diameter, abrasive of diameter 1.5 µm impact velocity and a) deformation radius, b) local deformation and c) applied load stress.

The table below summarises the results from the graphs above specifically identifying the maximum values to observe the trends between the graphs for the various parameters.

Table 5: A table summarising the results from the contact mechanics analysis

Abrasive diameter	V_0 (m/s)	Asperity Diameter = 0.8 µm			Asperity Diameter = 2 µm		
		Radius of deformation (µm)	Local deformation (nm)	Load stress (MPa)	Radius of deformation (µm)	Local deformation (nm)	Load stress (MPa)
6.5 µm	10	0.0170	0.387	2 327	0.0151	0.300	1 398
2.5 µm		0.0043	0.060	997	0.0052	0.049	666
1.5 µm		0.0024	0.023	661	0.0029	0.019	475
6.5 µm	25	0.0159	0.712	3 158	0.0205	0.552	1 898
2.5 µm		0.0058	0.111	1 353	0.0071	0.091	903
1.5 µm		0.0033	0.042	897	0.0039	0.036	644
6.5 µm	50	0.0201	1.130	3 980	0.0259	0.876	2 391
2.5 µm		0.0073	0.176	1 705	0.0090	0.144	1 138
1.5 µm		0.0042	0.067	1 130	0.0050	0.057	812
6.5 µm	80	0.0235	1.550	4 654	0.0303	1.200	2 796
2.5 µm		0.0086	0.241	1 994	0.0105	0.197	1 331
1.5 µm		0.0049	0.091	1 322	0.0058	0.077	950

There are a few trends to note from the above results (both the graphs and table) and will each be discussed individually. A relationship introduced by the momentum method is that it equates the polishing action to the size of the abrasive by including the mass of the abrasive in its consideration. The trend that is observed is that the increase in abrasive size increases the loads experienced on the surface of the asperity and thus an increase in MRR. For the abrasive mesh size of #2000 (6.5 µm abrasive diameter), the applied load for a 2 µm diameter asperity resulted in a maximum local deformation of 0.0012 µm whereas the #8000 abrasive (1.5 µm abrasive diameter) resulted in a much lower maximum local deformation of 0.0774 nm. The force exerted by the #8000 abrasive particle for the same data point was unable to reach the yield stress of grade 5 titanium (1 070 MPa) as it only had a maximum stress of 949.53 MPa. This means that the deformation would be 0 µm due to the asperity material only operating within its elastic range and thus will return to its original shape after impact. However, for the case of the 0.8 µm diameter asperity at 80 m/s impact velocity, the #8000 abrasive was able to achieve a maximum stress of 1 322 MPa which means that for surfaces that have a lower Ra value, the smaller abrasives may be more appropriate as the stresses the smaller abrasive applies on the asperity is lower than the larger abrasives. The larger abrasives will apply stresses that exceed the plastic deformation range which can cause the asperity to fracture on its surface which will cause it to be more damaged than when it was initially retrieved. One of the benefits of using this technology is that it strengthens the surface of the workpiece due to plastic deformation at its surface. Therefore, it is important to consider the initial surface roughness of the workpiece and the abrasive size to maximise the polishing benefits rather than damaging more parts.

Another assumption that can be confirmed is that with an increase in initial impact velocity, there will be an increase in deformation and thus the polishing action. As one moves across the velocity axis, for all the graphs the area moves from a lighter to darker colour meaning the MRR rate is thus increasing in value. Therefore, the momentum method is an important aspect of the analysis as it can relate the impact forces over time to the contact mechanics equation which assumes a static force at a specific point in time between two objects. The previous paragraph used the highest data points of velocity at 80 m/s to study the relationship between abrasive size and stress. The following table shows the effect of velocity on the polishing action.

Table 6: A table showing the polishing action of the different abrasive sizes for varying velocities.

Abrasive diameter	Asperity diameter (µm)	V_0 = 5 m/s		V_0 = 40 m/s		V_0 = 80 m/s	
		Local deformation (nm)	Load stress (MPa)	Local deformation (nm)	Load stress (MPa)	Local deformation (nm)	Load stress (MPa)
6.5 µm	0.8	0.244	1 847	0.974	3 694	1.550	4 654
2.5 µm	0.8	0.038	791.3	0.152	1 582	0.241	1 994
1.5 µm	0.8	0.0144	524.7	0.0576	1 049	0.091	1 322

Considering the above table, the slower speeds, for both the #5000 (2.5 µm abrasive diameter) and #8000 abrasive mesh size, have not reached the yield stress of the workpiece material and thus have had no effect on the polishing action. This again verifies that this polishing action is like other polishing methods in that the size of the abrasive particle used is directly proportional to the MRR. However, it can be added to the previous discussion that lowering the impact speed of the larger abrasives can lower the risk of exceeding the plastic deformation range of the asperity surface and thus damaging the component. The following graphs show the crossover line for the three abrasive sizes that can be used to predict when the plastic deformation region of the asperity is reached and the polishing action begins to take place.

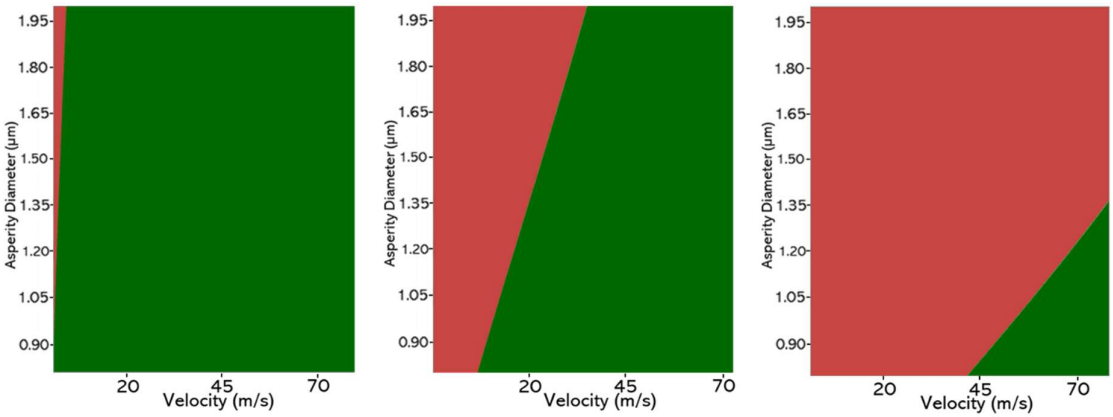

[a] [b] [c]

Figure 15: A contour graph showing the polishing region of the system for abrasive diameter sizes of a) 6.5 µm, b) 2.5 µm and c) 1.5 µm.

From the above graphs, the red zone is an indication that the applied load stress due to; the asperity size, impact velocity and abrasive size will not achieve a polishing action as it is below the yield stress of the component. The #2000 abrasive can polish almost all scenarios within the scope of the study

except for the very low speeds and asperity diameter sizes > 0.9 µm. The #5000 abrasive is unable to perform any polishing action at low impact speeds around 20 m/s dependant on the surface roughness. The #8000 abrasive for most of the scope does not achieve any polishing action except at extremely high speeds (> 45 m/s) and asperity sizes with diameter smaller than 1.35 µm. Therefore, it can be recommended that the #8000 abrasive size be used for surfaces that have an Ra <<< 0.4 µm. This is assuming that the polishing action is not because of fatigue failure - the constant cyclic loading within the elastic limit to cause failure by fatigue. Polishing by this mechanism will result in a significant increase in polishing time as it would require a much higher number of impacts to cause the cyclic loading as opposed to the single impact mechanism which is being studied through this analysis.

The other side of the spectrum that may be more difficult to consider is when the polishing parameters are too harsh such that the surface is damaged due to the excessive forces. The reason this becomes difficult to study is due to the nonlinear behaviour of the material when the yield stress of the material is reached. The surface of the material is expected to strengthen as the asperity plastically deforms and increases the density at the surface which thus increases the surface strength of the material. Upon impact, it is expected that the asperity stress will increase linearly until the yield stress limit is reached. As the load increases passed yield stress, the load stress remains the same as the surplus stress becomes residual stress within the surface. If the load continues increasing passed the maximum residual stress that the material allows, the surface will fracture as a mechanism to release the excess energy at the surface. However, the equations used for this calculation does not accommodate this nonlinear behaviour, therefore it can only be roughly predicted at which point this will take place and then verified through physical experimentation. As a calculated assumption, the ultimate bearing strength of grade 5 titanium is 2 140 MPa [89]. Therefore, the graphs can be updated as shown below.

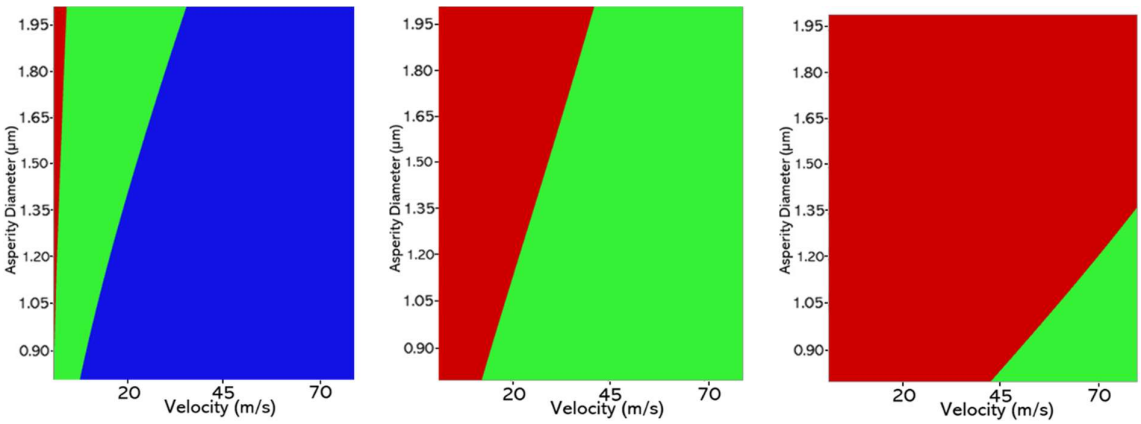

Figure 16: A contour graph showing the polishing region of the system for abrasive diameter sizes of a) 6.5 µm, b) 2.5 µm and c) 1.5 µm.

As before, the red and green regions indicate elastic deformation and plastic deformation respectively. The additional blue region indicates load stresses above the ultimate bearing strength that has been used as a reference point. The #2000 abrasive is most likely going to damage the component surface at any impact speed above 35 m/s for any of the asperity surface roughness levels. For SLS Ti6Al4V components being polished with a surface roughness identical to the scope of these experiments, it would be recommended to make use of the #5000 abrasive as it has the biggest operational area that achieves the polishing action required without damaging the surface.

There are some drawbacks that need to be considered. The first drawback for this method is that it does not allow for the nonlinear material behaviour of the asperity once the yield strength is reached. This method assumes that the workpiece material will continue to operate within the elastic modulus region of the stress curve. The system is purposefully intended to operate within the plastic deformation region of the workpiece to improve the surface properties of the material due to plastic deformation.

Finally, the novelty to the system is the inclusion of a flexible media to be added to the abrasive. A few methods have been attempted to incorporate the flexible media into the equations. The current method of analysis being reported has been identified as the best approach. Considering the understanding that has been developed within this analysis, it is expected that the addition of the abrasive will increase the momentum of the abrasive media and thus increasing the maximum applied force and thus maximum applied stress. To quantify the increase of momentum due to the abrasive is also a challenging task.

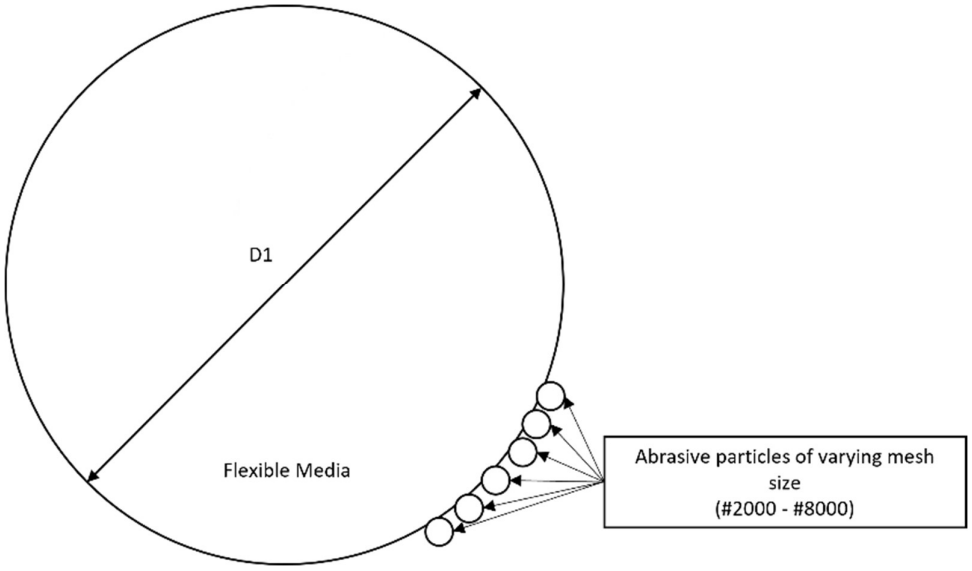

Figure 17: A diagram showing, not to scale, the predicted layout of abrasive particles on the flexible media thus creating a flexible abrasive particle.

As shown in the above diagram, the abrasive particles will surround the flexible media. Upon impact, the flexible abrasive media will impact the surface of the workpiece and thus for each flexible abrasive media impact, there will be many abrasive particle impacts upon many single asperities across a surface. The analysis that is being done considers only the impact of one particle upon one asperity. The statistical expectation is that combination of all the asperity and abrasive particle impacts will have a mean that is like the solutions that have been acquired through this analysis with an error of uncertainty. To quantify the portion of flexible media mass that can be assigned to a single asperity is challenging due to many unknowns that cannot be confidently assumed and therefore any assumption will more likely than not produce unreliable results. This a theme that continues throughout the numerical analysis section. Therefore, it is expected that the addition of the flexible media will increase the apparent mass of the abrasive particle and thus increase the local deformation which means an increase in MRR.

This numerical method has provided a deep understanding into the relationships between the various parameters such as impact velocity, abrasive size, surface roughness and asperity response. It can also be further extrapolated that the governing principles of this method can be applicable to many materials that are fabricated through modern processes which will result in the same trends as identified above except with different values.

5.2 Statical Indentation Theory

Another Numerical approach that can be used in understanding the polishing action is by considering the Statical Indentation theory. This test is used to measure the hardness of a specific material by indenting a tungsten carbide ball onto the surface of a material test-piece. In doing so, an indentation is created and is defined as the Brinell Hardness Number (BHN) (Kgf/mm^2) which is specific to a material.

5.2.1 Theoretical Approach

The BHN for a material is defined by the following equation:

$$BHN = \frac{2*P}{\pi*D(D-\sqrt{D^2-d^2})} \qquad \textit{Equation 6}$$

where P is the applied load (Kgf), D is the diameter of the indenter (mm), and d is the diameter of the indentation. To apply this understanding to the polishing action, P will be varying with impact velocity, D is the diameter of the abrasive particle and BHN is already known for Grade 5 titanium. The equation can be rearranged to solve for d which is the indentation diameter onto the workpiece surface. This equation is then expressed as:

$$d = \sqrt{D^2 - (D - \frac{2*P}{BHN*\pi*D})^2} \qquad \textit{Equation 7}$$

Assuming that the abrasive particle is a perfect sphere, the surface deformation (δ) can be calculated using geometry. Considering the following circle:

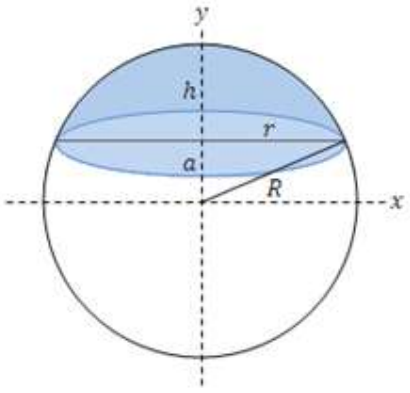

[90]

Figure 18: A circle with naming conventions to study the geometry of a circle

the value h can be equated to surface deformation of the workpiece δ. Using the Pythagoras theorem in conjunction with circle geometry, we can solve for h using the following equation:

$$h = R - a = R - \sqrt{R^2 - r^2} \qquad \textit{Equation 8}$$

where R is the radius of the abrasive particle, and r is half the indentation diameter, therefore writing the above equation in terms of the BHN symbols, we can write:

$$\delta = \frac{D}{2} - \sqrt{\frac{D^2}{2} - (D^2 - \left(D - \frac{2*P}{BHN*\pi*D}\right)^2)} \qquad \textit{Equation 9}$$

Due to the nature of the above equation, it can be predicted that the above equation will be an inverse parabola. The below diagram explains the motion that this equation describes.

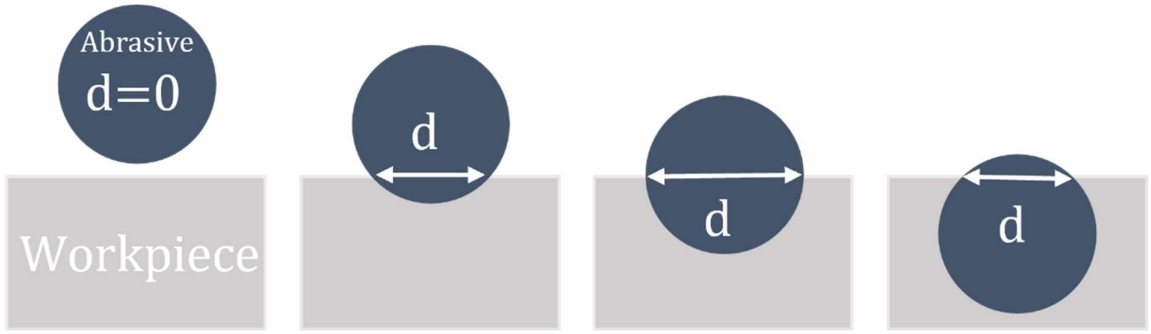

Figure 19: A diagram showing the motion of the abrasive media into the workpiece surface over a period that is represented by the above equations.

Looking at the motion of the abrasive particle, as the abrasive media impinges deeper into the workpiece, the indentation diameter increases. However, this diameter will reach a maximum theoretically which is the size of the abrasive diameter. The above equation also describes the scenario whereby the diameter begins to reduce again to zero as shown in the last example figure. Practically, this is not possible and therefore we can only consider half the graph - when the abrasive particle is half embedded into the workpiece surface. It should be noted that the mathematical equation describes this motion assuming that the material properties remain linear and that the force required to change the momentum of the abrasive particle is high enough to reach this loading on the workpiece. In practice, it is expected that the abrasive media will bounce off for a significantly lower loading force than what the equation describes. It should be noted that both SiC and Diamond powder have much tougher mechanical strength properties than the workpiece material and thus will have the same outcome considering that both abrasive materials will be rigid within this analysis. Therefore, specifying which abrasive is used is not essential as this approach does not consider the respective strengths of the abrasive material but only the result on the workpiece material.

The approach followed to identify the force values that correspond with the three abrasive sizes is by means of an excel spreadsheet and specifically the goal seek function. After setting up the excel spreadsheet using all the relevant equations, there are two indentation data points that we will know, firstly, the indentation of 0 µm with 0N applied force and the second data point knowing that the graph will reach a maximum indentation size to that of the diameter of the abrasive media. Using the goal seek function, we can request excel to find the relevant force that results in the indentation diameter equal to that of the abrasive size. This force was then split into 100 data points from 0N to the maximum force which then plots half the parabola for each corresponding abrasive size value. The table below highlights the properties that were used for this computation.

Table 7: A table showing the properties used for the statical indentation theory.

Detail	Value	Detail	Value
Brinell Hardness Number for Ti6Al4V (*BHN*)	379	Abrasive Diameter (*D*)	1.5~6.5 µm
Applied load (*P*)	0~25.23gf	Abrasive Radius (*R*)	0.75~3.25µm

5.2.2 Results and Discussion

The graphs below show the outcome from these calculations.

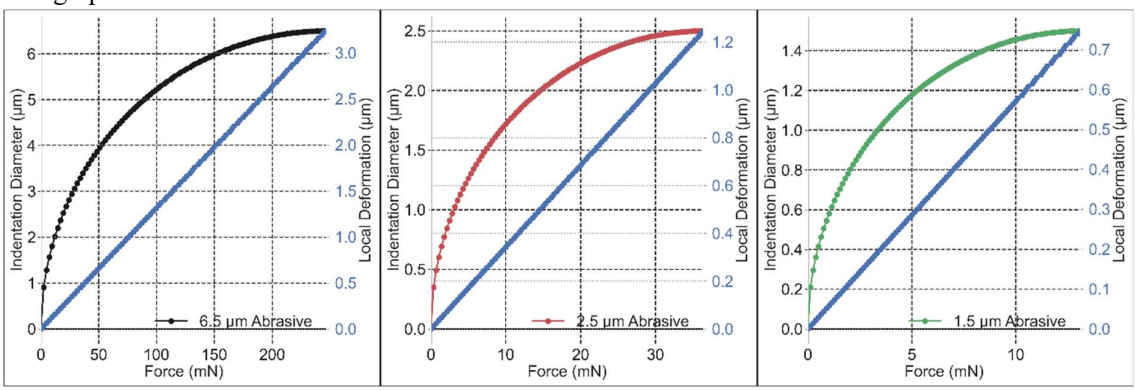

[a] [b] [c]

Figure 20: Line graphs showing the indentation diameter and the local deformation of an asperity for increasing load forces from an abrasive with diameter size a) 6.5µm, b) 2.5 µm and c) 1.5 µm.

From these graphs, the local deformation is linearly proportional to the applied load force and the indentation diameter has an inversely exponential relationship with the applied load force. It can also be noted that as the abrasive size increases, the maximum local deformation that can be achieved is equivalent to half the abrasive size which is due to the geometry of the circle and governing equations. There is an interesting finding by looking closely at all three lines on the same graph.

It appears that a smaller abrasive with the same amount of impact force can result in a higher local deformation of the asperity. This is interesting as it is expected that increasing the abrasive size will result in a higher MRR as most polishing methods. Considering the equation from contact mechanics:

$$\sigma = \frac{1.5F}{\pi a^2} \qquad \textit{Equation 10}$$

Considering that F is kept constant for the above graph for each abrasive size, the applied local stress is inversely proportion to the indentation diameter, meaning that a higher indentation diameter will result in a lower stress. In simple terms, the area over which the force is applied is smaller and thus the local load stress is also lower. Knowing that the stress is the predictor for deformation and load, it can now be seen why the larger abrasive has resulted in a lower local deformation of the asperity for the same force as the other abrasives. Therefore, this investigation preliminary shows that to achieve a finer surface finish, it may be ideal to use larger abrasives to limit the possibility of excessive forces and thus excessive stresses on the surface. But this theory does not accommodate the fact that the force cause by impact will not be as easy to control during the polishing process. An impact is not a consistent force but rather an impulse that is exerted on the workpiece and the impact is dependent on the initial momentum of the abrasive particle. Therefore, it is most likely that the larger abrasives will exert larger forces due to the larger momentum that is required to be changed. Knowing that the change of momentum can be described by the following equation:

$$\Delta P = mv = F\Delta t \qquad \textit{Equation 11}$$

We can attempt to understand the relationship of abrasive size which determines mass *m*, initial velocity (*v*) and applied load(*F*). The difficult aspect to predict without experimentation is the impact time Δt because this value can vary dependant on the elasticity of the two impact materials. With the previous numerical method, time was kept constant to 20 µs. For this analysis, this is not done to prevent the

analysis to have a bias towards a specific time rather than accommodating the variation the variation because of multiple factors such as elasticity and mass.

As per the previous numerical method, this calculation does not include the consideration of the flexible media. To include the flexible media within the constraints of the underlying theory, it is assumed that the flexible media will increase the apparent mass of the abrasive. To define the reasoning in more detail, the mass is apparent is because as the flexible abrasive media impacts the asperity, the asperity surface will exert a force that is required to slow down both the abrasive and flexible media. However, the interaction will only be between the abrasive particle and the asperity. The abrasive particle will feel "heavier" to the asperity surface due to the addition of the flexible media piggybacking on the abrasive particle. This means that for a similar velocity, the MRR of the system can be increased as the applied load would increase along with the stress which results in a larger deformation of the workpiece surface. This aspect is a consideration and will be further developed during the simulation experiments in the following chapter.

This numerical analysis is unable to accommodate the effect of the initial surface roughness as it assumes a surface is flat. The dimensions of the asperity size are not parameters in these calculations and therefore this analysis is unable to show the differences between the various surface finishing types. This method also assumes linear material response which is a theme across all the numerical methods.

5.3 Energy-Work Theorem

The Energy-Work theorem makes use of the principles regarding energy- specifically the energy transferred to a surface to achieve a deformation of an asperity. The energy is in the form of kinetic energy as the flexible abrasive media contains a velocity as it impacts the workpiece surface. The kinetic energy is then transferred to the workpiece surface in the form of distortion energy due to the work done by the flexible abrasive media onto the workpiece. The distortion energy is the energy that is then responsible for causing deformation and thus is the cause of the polishing process.

5.3.1 Theoretical Approach

The kinetic energy of the flexible abrasive media can be quantified by the following equation:

$$KE = \frac{1}{2} * mv^2 \qquad \textit{Equation 12}$$

Where *KE* is the kinetic energy, *m* is the mass of the flexible abrasive media and *v* is the impact velocity. To calculate the mass of the flexible abrasive media:

$$m = \rho * V \qquad \textit{Equation 13}$$

Where ρ is the density of the abrasive media and *V* is the volume. Assuming the abrasive is a perfect sphere, the formula defining the abrasive volume is:

$$V = \frac{4}{3}\pi r^3 \qquad \textit{Equation 14}$$

The work done by the abrasive media is quantified by the equation:

$$WD = \frac{F*\delta}{2} \qquad \textit{Equation 15}$$

Where *WD* is the work done, *F* is the maximum applied load, δ is the local deformation on the workpiece. Note that the above formula is divisible by 2 to accommodate the behaviour upon impact that force gradually increases and decreases and is not a consistent maximum force during the impact motion. Considering that the flow strength of a material is:

$$\sigma_w = \frac{F}{\pi r^2} \qquad \textit{Equation 16}$$

$$\therefore F = \sigma_w * \pi r^2 = \sigma_w * \pi * d * \delta \qquad \textit{Equation 17}$$

It is also assumed that the kinetic energy of the abrasive is fully transferred to the workpiece surface, i.e., the abrasive particle loses all its momentum upon impact. The kinetic energy and the work done can be equated to each other:

$$\frac{1}{2}\left(\rho * \pi \frac{d^3}{6}\right) v^2 = \frac{\sigma_w * \pi * d * \delta^2}{2} \qquad \textit{Equation 18}$$

Which can then be solved for local deformation with:

$$\delta = v * d * \sqrt{\frac{\rho}{6 * \sigma_w}} \qquad \textit{Equation 19}$$

The initial impact velocity to retrieve the corresponding local deformation is from 0 m/s to 80 m/s. The local deformation is then substituted into equation 17$\therefore F = \sigma_w * \pi r^2 = \sigma_w * \pi * d * \delta$

Equation 17 to achieve the maximum force that the abrasive particle will exert onto the asperity surface to cause the deformation. The following table shows the properties and values that were used for this computation.

Table 8: A table showing the properties and values used for the Energy-Work numerical analysis.

Detail	Value	Detail	Value
Diamond Powder Density (ρ)	3500 kg/m^3	Flow strength of Ti6Al4V (σ_w)	1 070 MPa
Impact velocity of abrasive (v)	0~80 m/s	Diameter of abrasive particle (d)	1.5~6.5 µm

5.3.2 Results and Discussion

The following graphs show the relationship between the initial impact velocity, average force for the duration of the impact and the local deformation on the surface of the asperity.

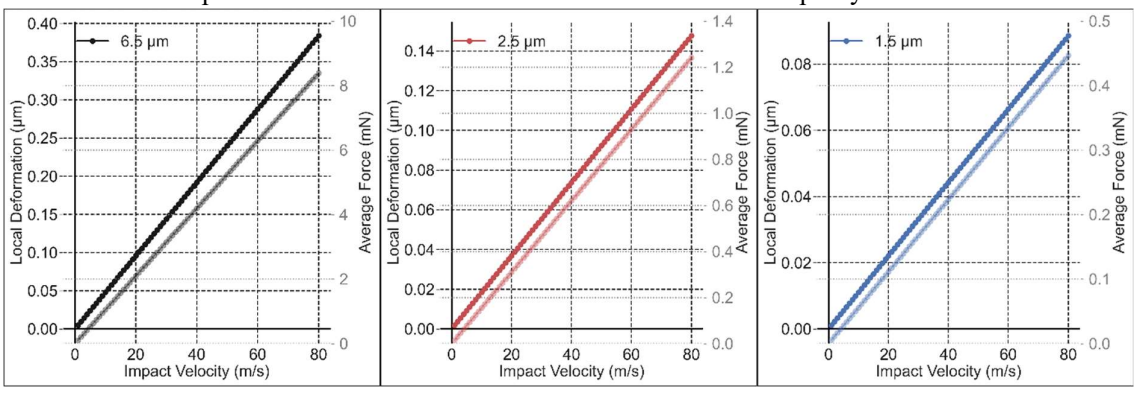

[a] [b] [c]

Figure 21: A line graph showing the local deformation and average force for varying initial impact velocities for abrasive sizes of a) 6.5µm, b) 2.5 µm and c) 1.5 µm.

The impact velocity is a measure of the abrasive media's kinetic energy upon impact. Due to the nature of the equations, the graphs have visually shown:

$$\delta \propto v \propto F \qquad \textit{Equation 20}$$

The relationships between local deformation, initial impact velocity and the maximum force acted upon the asperity is linear in nature and directly proportional. Although the result is simple enough there is behaviour that has been noted with the other theoretical approaches that are similar here. Firstly, the increase of the abrasive size increases the local deformation and thus the polishing action. This is because the kinetic energy is also dependant on the mass of the abrasive material which is increased by the following scale factor over another sized abrasive:

$$K = \frac{r_{bigger}^3}{r_{smaller}^3} \qquad \textit{Equation 21}$$

This relationship has been consistent across all the three abrasive sizes that have been tested with and across all the velocities that have been used. The applied load force is also directly proportional to the local surface deformation and thus can be mentioned that it is still possible for the polishing technology to damage the surface due to excessive forces as seen with most polishing methods.

The benefit of using the energy work theoretical approach is due to its introduction of impact velocity which is a fundamental requirement for the polishing action. The other theoretical methods have not been able to develop a quantifiable relationship between velocity and the local deformation. Through intuition of physics, it is known that the force will be directly proportional and related to the initial impact velocity for the other theoretical approaches, but the relationship has been unable to describe this directly without making assumptions based from an assumed impact time and relating the net average force over the assumed time to initial momentum. This method verifies the assumption of the linear relationship between velocity and local deformation however it does include drawbacks.

Considering the above results and discussion, the addition of the flexible media to the abrasive is again assumed to increase the apparent mass of the abrasive particle except from the perspective of kinetic energy rather than momentum conservation. This will increase the forces that were calculated from the above graphs where the mass of a diamond particle has been considered alone. Due to the relationships that have been described and verified, it can be confidently confirmed that the addition of the flexible media will increase the rate at which the workpiece surface is polished due to the increase in mass and thus momentum of the abrasive particle. The benefit then is that the system does not use as much abrasive media as the case with the current polishing method and that the extra momentum required from the abrasive particle can be increased by a low-cost cheaper alternative (rather than using more abrasives) which thus also improves polishing rate. This can reduce workshop expenses in both the category of labour (due to increased polishing rate) as well as the consumables used for polishing. This is an added note that is applicable is applicable to all the analysis conducted thus far.

5.4 Final Remarks

The theoretical analysis provides a good understanding into the behaviour and relationships that are expected from the polishing system between the various parameters that can be adjusted accordingly. These adjustments allow and operator to flexibly define the polishing action according to the needs of the workpiece being polished. As with other polishing systems, increasing abrasive sizes increases the local deformation and thus polishing rate of the system due to the increased mass of the abrasive. Increasing the impact velocity of the abrasives also assists with increasing the local deformation and thus the polishing rate.

For all the theoretical analysis that have been used in developing the understanding of the process, the first comment is that all the theories applied are related due to the nature of the physics within the system. The physical workings of the system are the same and these theories mathematically define the

polishing action differently as they apply a different approach with emphasis on different physical aspects. Whether it is to consider the asperity and abrasive properties together through contact mechanics, using energy-work theorem or considering a simple strength test as the basis of the analysis, the theories have all produced the same behaviour that should be expected from the polishing action.

Each theory has had their disadvantages that require actual testing to confirm assumptions and quantify these assumptions to be able to predict an outcome more accurately. The theories have also all included linear conditions whereas the impact mechanics is expected to produce nonlinear results. The biggest assumption that will need to be quantified is the inclusion of a flexible media. For all the theories, the challenge has been to quantify the improvement that adding the extra mass of the flexible media to the abrasive particle will have. All the theories have shown that it is expected to improve the polishing action due to the additional mass but quantifying the improvement can only be done by actual testing. This is the challenge that the following chapter will attempt to address.

6 Computational Experiments

Moving onto the simulation experiments, the understanding of the system is further developed by creating various computational experiments investigating various properties. In doing so, we can create a more realistic scenario of the mechanics regarding the system. It is then further investigated how some variables can be adjusted so that a machinist can create a more desirable setup to create a more efficient polishing action.

The chapter is broken down as follows:

- Simulation setup. This section will elaborate on how the ANSYS software is prepared for the various experiments that were completed. We also create a more detailed view of some of the settings used as well as the assumptions that were used throughout the course of these experiments which will thus create a deeper understanding of the researcher throughout these simulations.

- A baseline set of experiments. These experiments consider the simplest polishing action that can be achieved by considering a single abrasive impact on a single asperity. These experiments are used as the baseline so that further experiments completed can be compared to the baseline set of experiments to further verify the various characteristics that are adjusted to improve the polishing action.

- Impinging velocity on polishing action. The most critical variable that can be adjusted to achieve optimum polishing characteristics is the impinging velocity. Velocity is directly proportional to force which creates the polishing action. By understanding the effect of both force and velocity, we can limit micro surface damage caused by excessive forces while optimising polishing time and increasing the efficiency of the system.

- Influence of abrasive size. Considering conventional machining methods, it is widely known that making use of various sized cutting tools can result in various cutting results. In most grinding and polishing tools, the abrasive size of the tool results in differing material removal rates that can either damage a surface if too large an abrasive size is used or increase polishing time significantly if abrasive size is too small. Therefore, investigating abrasive size is an important aspect in developing the polishing action of the machine.

- Varying asperity size. It is common to find that various processes that precede the final finishing process can result in a multitude of surface roughness values. Even for a process such as SLS, dependant on its process parameters, the surface roughness can vary because of this. Considering this this system may be implemented in various workshops, it becomes important to include in the investigation different asperities to account for the different surface roughness figures that can exist.

- Supplementary experiments. Due to the nature of computational experiments, a researcher can never be perfectly sure of the results that are retrieved from the simulation results. There are various reasons for this uncertainty such as experimental setup, software used, simplification as well as assumptions used. To further verify some results and possible ‘blind spots’ relating

to some of the work that is completed, supplementary experimentation is completed to increase the certainty that the explanations of the results and outputs are in fact realistic and true.

- Summary. A brief overview of the experiments that were completed as well as some of the outcomes that were derived from the analysis of the results.

6.1 Simulation Setup

Simulating the impact of the abrasive media and the asperity requires the use of Ansys, more specifically, the use of the explicit dynamics package. The explicit dynamics package is used as it incorporates the physics of short events that are nonlinear in nature and highly transient. Literature confirms that material properties upon impact do not remain the same and therefore assuming linear material conditions will cause the results to be unreliable.

6.1.1 Ansys Explicit Dynamics Background

Explicit dynamics is a numerical method that performs many minuscule time increments. This method makes use of an explicit central-difference time integration rule. [91] The calculation can be expressed as:

$$\dot{u}^{n}_{\left(i+\frac{1}{2}\right)} = \dot{u}^{N}_{\left(i-\frac{1}{2}\right)} + \frac{\Delta t_{(i+1)}+\Delta t_{(i)}}{2} \times \ddot{u}^{N}_{(i)} \qquad \textit{Equation 22}$$

$$u^{N}_{(i+1)} = u^{N}_{(i)} + \Delta t_{(i+1)} \dot{u}^{N}_{\left(i+\frac{1}{2}\right)} \qquad \textit{Equation 23}$$

Where u^N is a degree of Freedom (such as displacement or rotation) and the subscript *i* refers to the time step. Knowing that u^N can be replaced by displacement x, the equations can be redefined as:

$$v^{n}_{\left(i+\frac{1}{2}\right)} = v^{N}_{\left(i-\frac{1}{2}\right)} + \frac{\Delta t_{(i+1)}+\Delta t_{(i)}}{2} \times \alpha^{N}_{(i)} \; 24 \qquad \textit{Equation 25}$$

$$\chi^{N}_{(i+1)} = \chi^{N}_{(i)} + \Delta t_{(i+1)} v^{N}_{\left(i+\frac{1}{2}\right)} \qquad \textit{Equation 26}$$

Where υ is velocity and α is acceleration. Using this calculation (which can define change over a period with Finite Element Analysis) Ansys is able to provide simulations that are able to characterise geometry, material properties, forces and dynamics over a period of time.

6.1.2 Setup

Ansys contains an intuitive workflow for setting up explicit dynamics' simulations. The following section will discuss the workflow that has been incorporated as well as the specific settings that were used in formulating the simulations for the experiments that follow. The figure below shows a typical workflow that Ansys requires when setting up the experiments.

6.1.2.1 Engineering Data

Engineering data consists of several material libraries where the user selects the various materials that will be used in the simulation process. These library material files contain the important mechanical properties that are required for the simulation process which the software will use in its calculations.

6.1.2.2 Model

Geometry

There are 3 geometries that are predominantly used for these simulations, namely:

- Workpiece surface
- Abrasive particle
- Flexible particle

The material properties are applied uniformly to the varying geometries dependant on the requirements of the simulation. These differences will be explained while discussing the various experiments.

Coordinate Systems

The coordinate system used the X-Z plane as the floor of the experiments with the -y direction indicating the initial velocity that is applied to the abrasive media as shown in the picture below.

Connections

There were only two connections that were applied to these simulations. The first connection is the interface of the abrasive particle and the workpiece asperity. The connection was created to limit unnecessary computational power used to calculate the abrasive travelling through air before finally contacting the asperity. Therefore, this connection allowed the simulations to start from the exact point where these two geometries meet.

The second connection is the interface of the abrasive particle to the flexible particle. It is assumed that the abrasive particle attaches itself to the flexible particle and therefore at the point of contact, they are connected.

Mesh

The meshes were initially autogenerated according to the program, however there were some issues that were which needed to be addressed. Firstly, there is a limit on the number of nodes and elements that can be used with the student version of Ansys. Therefore, it was important to lower the mesh quality where it was not necessary and improve mesh quality at areas that are being investigated. The two areas that where the mesh was refined were both connections that existed in the geometry. The most crucial aspect of this research was to account for the force transfer between the geometries and therefore refining these contact areas is essential. The second area of refinement was the asperity. The polishing process being investigated is characterised by the deformation of the asperity and hence it is important to ensure that the mesh quality is sufficient to mimic a realistic scenario. To accommodate these refinements the mesh quality at the upper part of the flexible particle and the walls of the workpiece were minimised. The ‘body’ of the workpiece containing the asperity was also reduced in height to lower the number of elements and nodes on the simulation. This reduction in the body of the workpiece was verified by performing simulations and verifying that there is still a net zero stress on the bottom and side walls of the workpiece.

6.1.2.3 Setup

Initial Conditions

The initial condition for the experiment was assigning the respective velocities to the moving bodies that were being investigated. These velocities were assigned to the entire bodies and not regions as that would assume an initial strain. For all the experiments, this only included the abrasive particle and the flexible media, and they were assigned the same velocity towards the asperity as they are assumed to be moving at the same speed upon impact. The velocity was varied according to the requirements of the experiment.

Another initial condition is to assume that there is no initial pre-stress between the abrasive particle and the asperity. This is included so that the contact area between the surfaces exert no forces upon initial impact due to the way the simulation is setup.

Fixed Supports

The body of the asperity was fixed in the z, x and y axis as it is assumed the material is continuous through these points and that there is a net zero velocity at these points. This also simplified the assumption that the net velocity is only a result of the impinging media and the velocities of the asperity due to an operator holding the component is miniscule in comparison to the impingement velocity.

Analysis Settings

The settings within Ansys are extremely comprehensive. Most analysis settings have been used on their default settings as recommended by Ansys and this section will only elaborate on the settings that have been purposefully adjusted for the requirements of the experiments.

Step Control	
Number Of Steps	1
Current Step Number	1
Load Step Type	Explicit Time Integration
End Time	6.e-005 s
Resume From Cycle	0
Maximum Number of Cycles	20000
Maximum Energy Error	0.1
Reference Energy Cycle	0
Initial Time Step	Program Controlled
Minimum Time Step	Program Controlled
Maximum Time Step	Program Controlled
Time Step Safety Factor	0.9
Characteristic Dimension	Diagonals
Automatic Mass Scaling	No

The “End time” for each experiment was adjusted according to the results that were retrieved. This limited the computational power required by shortening the time of the simulation to just after the required observation has been computed so that the computer would refrain from computing unnecessary results. The “Maximum number of Cycles” is limited again to 20 000 to save computational time. This number is chosen so that the data points are sufficient to observe the trend but not too minimal where these trends cannot be observed due to too big a time step with regards to the integration step size.

Erosion Controls	
On Geometric Strain Limit	No
On Material Failure	Yes
On Minimum Element Time Step	No
Retain Inertia of Eroded Material	Yes

Due to the nature of the simulations, the erosion controls were tested with the material failure being toggled between yes and no. It was found that this was required at "yes" as the material would deform unrealistically rather than just breaking off from the simulation on material failure. The inertia of the eroded material was also retained. This setting has affected some results by showing extremely high velocities with some results due to the eroded materials.

Output Controls	
Step-aware Output Controls	Yes
Save Results on	Cycles
Result Cycles	100
Save Restart Files on	Equally Spaced Points
Restart Number of Points	5
Save Result Tracker Data on	Cycles
Tracker Cycles	1
Output Contact Forces	Time
Time	1. s

The results are saved as 100 equally spaced cycles. This ensures that the various experiments contain results of the same format so that the comparisons and analysis of the simulations are consistent. The results are also required to be step aware which was found to produce the best and most consistent results due to ensuring the process considering the output throughout the calculation.

6.1.2.4 Solution

The programme then computes all the necessary characteristics of the simulation. The solution then uses the various values at the various nodes over time and can compute various parameters as defined by the user to make the solution more readable for a researcher. The parameters that have been used include:

- Deformation
- Velocity
- Acceleration
- Elastic Strain and,
- Von-Mises Equivalent Stress

These solutions contain the data that is analysed to assist with the investigation into this polishing process.

6.2 Baseline Experiments

The baseline experiments are performed to verify the mechanics of the software and to use these experiments as the control. The control is critical to ensure that each set of experiments are only changing a single factor and that the differences between the results are due to the single variable that is being investigated and nothing further. This ensures that there are no further elements that can influence the change in result except for the specific characteristic being tested.

6.2.1 Experiment Explanation

The Baseline experiment simulates the impact of a single SiC abrasive onto a 1.6-micron asperity. The simulation does not introduce a flexible particle yet as we are interested in only the impact of the abrasive particle onto the asperity. This is the simplest form of the polishing action.

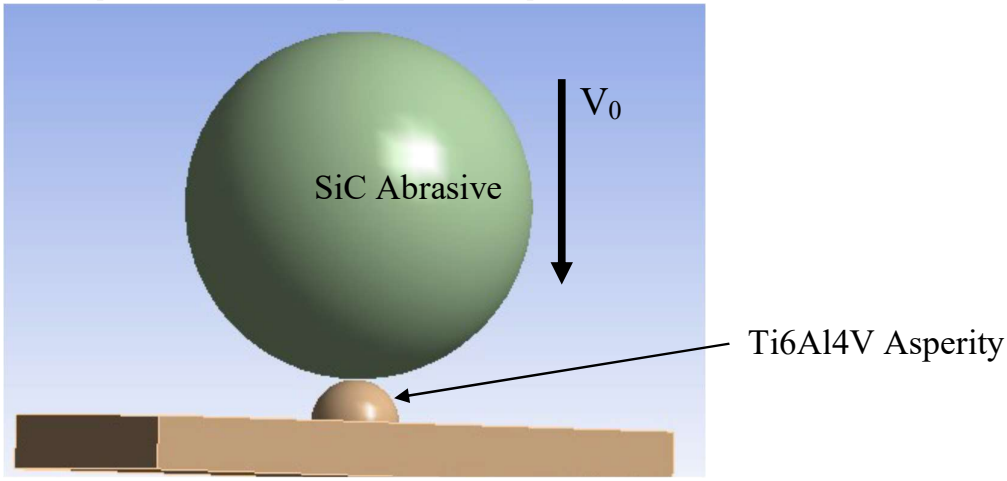

Figure 22: Baseline experiment setup showing a single 6.5 micron SiC abrasive impinging onto a 1.6-micron asperity on a Ti6Al4V surface

For this set of experiments, the only variable being changed is the velocity of the SiC abrasive. The initial velocity of the Abrasive is in the -y direction (the bottom of the figure) as shown in Figure 22. The height of the titanium material below the asperity is significantly reduced to lower the computational time it takes to complete these experiments. It is also noted that the height of the material selected does not affect the results due to the stresses from the polishing action not being significant enough to transfer through the surface. This is verified by noting that the stresses on the bottom plane of the titanium sample surface being null. The below table are the experiments that were conducted for the baseline tests.

Table 9: Baseline Experiments indicating initial velocities.

Test #	V_0 (m/s)	Asperity Size (µm)	Abrasive Size (µm)
1	1	1.6	6.5
2	5	1.6	6.5
3	15	1.6	6.5
4	25	1.6	6.5
5	35	1.6	6.5

6.2.2 Results

The graph below shows the velocity of the entire SiC abrasive particle over a period. Each line indicates an initial velocity towards the abrasive has responded over a period.

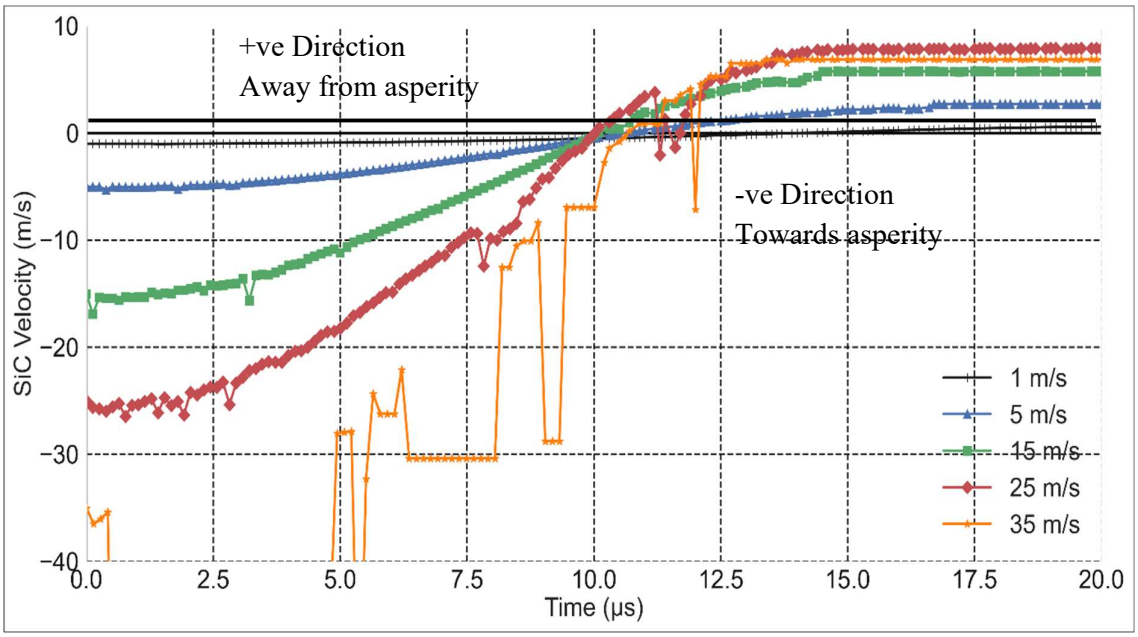

Table 10: A line graph showing the SiC abrasive velocity over a period for varying initial input velocities.

Considering the above figure, the abrasive particle bounces off the asperity at a velocity much lower velocity than the original impact velocity. This means that energy is transferred from the abrasive particle into the surface of the workpiece. The change in velocity is due to the change in acceleration which is due to the force exerted onto the asperity. This impact force onto the asperity is what will create the deformation and cause the polishing action. The Von Mises Equivalent stress is used in this analysis as it is a metric based on distortion energy. Upon impact of the abrasive particle onto the surface of the workpiece, in elastic impact conditions, energy is simply transferred back into the abrasive in the form of kinetic energy. However, in a real-life scenario, it is expected that the mechanical forces from impact causes work onto the body which then converts the kinetic energy of the abrasive into strain energy in the body of the workpiece. Some of this strain energy is distortion energy which is the basis of the Von Mises criterion. This criterion is essential as it is a good predictor of when a material will undergo failure-whether in the form of plastic deformation or a fracture. With regards to the polishing action, it is expected that the material should fail in one of these two ways for polishing to take place. The test with initial velocity 35 m/s produced an inconsistent result even though the trend can still be identified and seen. This inconsistency is due to the excessive forces caused by the impact on the asperity which causes some nodes and elements to accelerate and chip away from the main body in the simulation. This failure occurs because the abrasive reaches its theoretical failure limit which causes a fracture. These fractures of the SiC abrasive then accelerate to extreme velocities as shown in the diagrams which is not an accurate representation of the abrasive particle and hence why this is cropped in the above graph.

The graphs below show both the deformation and Von Mises Equivalent stress on the asperity for varying impact velocities.

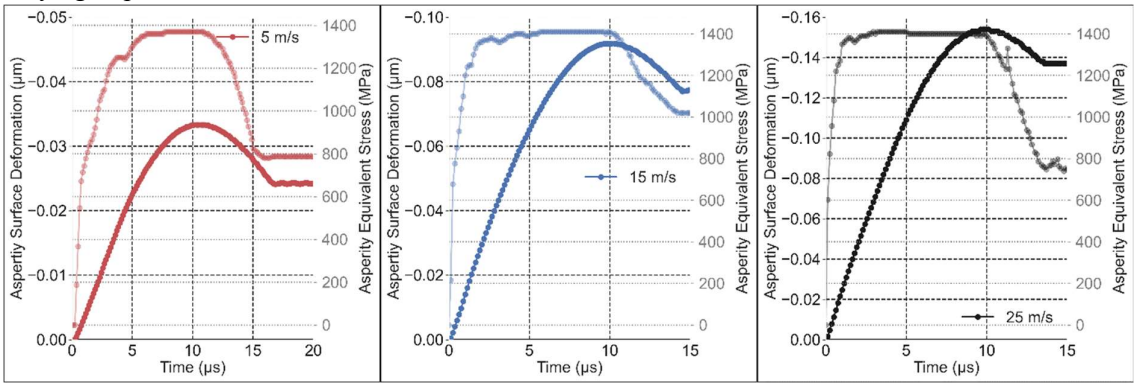

[a] [b] [c]

Figure 23: The surface stress and deformation over time for the asperity at an initial impact velocity of a) 5 m/s, b) 15 m/s and c) 25 m/s.

From the above graphs, the asperity's deformation on its surface is negative due to the negative y direction being towards the body of the surface. The loading and unloading pattern can clearly be seen by the increase in stress and deformation and then the release as the abrasive particle moves away. The other assumption that is verified is that with an increase in velocity, the momentum of the abrasive is increased and thus the impact forces are greater which results in a higher Von Mises stresses and thus higher deformation. The observation that is crucial for the success of the polishing process is that after impact, the asperity has undergone plastic deformation and maintains a permanent deformation on its surface which means that the polishing action has been achieved. This permanent deformation is also directly proportional to the initial impingement velocity. Another expectation that has been verified is that after unloading, there remains residual stress within the asperity surface. This is the result of the strain hardening and thus the surface strength of the material has been improved.

It is also shown on the graphs that the stress of the asperity increases during elastic deformation until it reaches 1400 MPa whereby the stress remains constant as the asperity undergoes plastic deformation during the rest of its loading cycle before being unloaded. Looking at the material data used by Ansys, the initial yield stress of the asperity material is 1 330 MPa and the maximum yield stress is 2 120 MPa. These two different yield stress values are used during explicit dynamics to account for the material changes as it undergoes an impact. As with most materials, during plastic deformation the material undergoes strain hardening which strengthens the material during this phase of loading Therefore the yield strength on the surface of the material will improve under plastic deformation until the maximum limit. Once the stress increases passed the maximum limit, the material surface will fracture and thus damage the surface.

As an addition to these experiments, the same simulations were conducted for velocities 5, 15 and 25 m/s except with an annealed Ti6Al4V workpiece. The annealing process for titanium can result in a more ductile material and thus different properties of the surface. The annealed yield stress is 845 MPa which causes the material to be more ductile. This supplementary experiment is considered as it has been noted in literature that the various characteristics of the SLS process as well as any further fabrication processes can affect the mechanical properties of titanium. Meaning that an operator is required to understand the mechanical properties of the workpiece dependant on its fabrication process because the system setup would need to be changed to achieve desired polishing characteristics. This also indicates that the system-through extrapolation-would also be able to polish various materials that

may not necessarily be Grade 5 Titanium which improves the flexibility of the system. The graphs below show the asperity deformation and stress of an annealed Ti6Al4V workpiece.

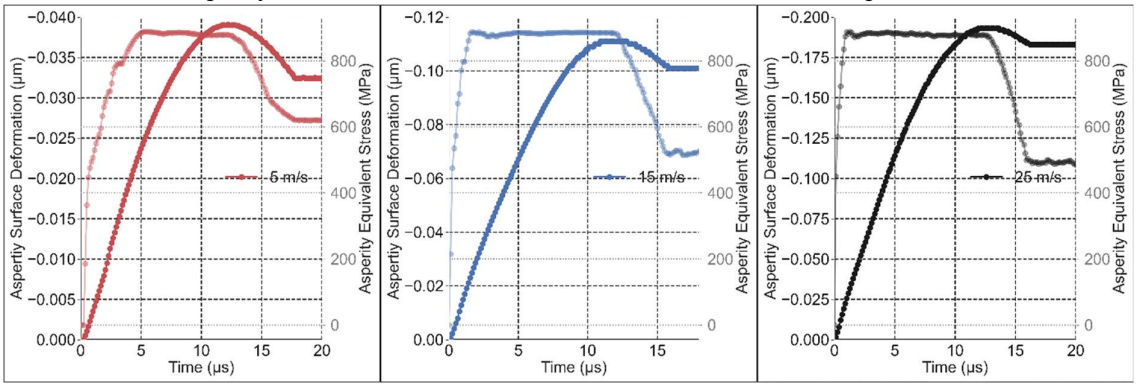

[a] [b] [c]

Figure 24: The surface deformation and equivalent stress over an impact time for the asperity at a) 5 m/s, b) 15 m/s and c) 25 m/s.

With the increase in the materials ductility due to annealing, it is seen that the asperity stress will settle rise until 845 MPa (the annealed titanium yield stress) and undergo plastic deformation. This is similar to the results of the initial Ti6Al4V material however the values are different due to different mechanical properties. It is also noted that due to the increase in ductility, the period of the impact is slightly longer. The table below represents shows the final polishing action as well as the residual stresses for the three different velocities.

Table 11: A table showing the final polishing action and respective residual stresses.

V_0 (m/s)	Plastic Deformation (μm)		Residual Stress (MPa)	
	Ti6Al4V	Annealed Ti6Al4V	Ti6Al4V	Annealed Ti6Al4V
5	0.024	0.032	787	620
15	0.077	0.101	1020	525
25	0.137	0.183	770	490

Looking at these results, the weaker of the two materials results in higher plastic deformation and lower residual stress than the stronger titanium under the same initial impingement velocities. As expected, the higher the impact velocity, the higher the permanent deformation and thus polishing action. We can also observe the loading and unloading behaviour of these tests and demonstrate the same behaviour in a different way with a traditional stress vs strain graph.

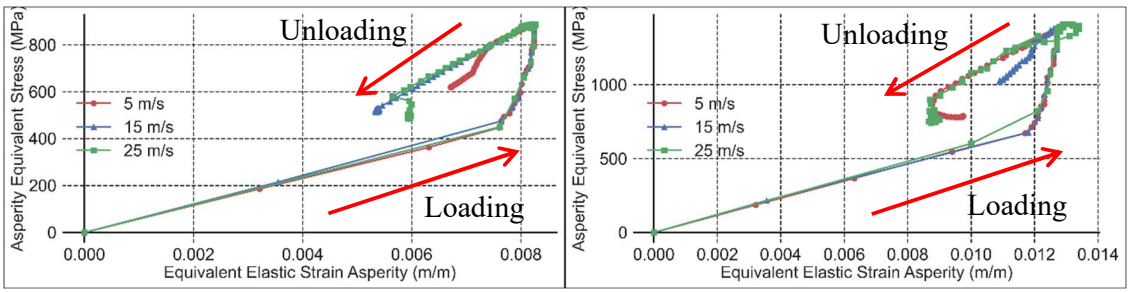

[a] [b]

Figure 25: Stress vs strain graphs of the asperity made of a) Ti6Al4V and b) annealed Ti6Al4V.

The two different materials show similar response patterns regarding the loading and unloading behaviour respective to its own mechanical properties.

In summary, after investigating the baseline tests we therefore have a better understanding of the basics regarding the impact of the SiC abrasive onto a workpiece surface and specifically, an asperity. The relationship between impact velocity, deformation and stress is well defined. We have also briefly explored the analysis of a different-more ductile material and the results are promising in suggesting that the proposed system can be used for multiple workpiece materials and not only the titanium that is being studied for the purpose of this research. Another outcome from these experiments is that we have also been able to successfully replicate the polishing process in its simplest form. This forms a good foundation for the further insight into the feasibility of the system being proposed.

6.3 Impinging Velocity

The following set of tests will also consider the impact of the abrasive onto an asperity as with the baseline tests. The difference with this technology is involving flexible media to bring about desirable characteristics such as reducing polishing time. Therefore, these tests will be the exact same as the baseline tests except the flexible media will be included with these simulations.

6.3.1 Experiment Explanation

Considering the mixing process of the abrasives and the flexible media to create the "flexible abrasives", it is therefore assumed that for every flexible particle that is found within the mixture will contain many abrasive particles around it on the outside. To simplify this arrangement, we zoom in on a single abrasive and flexible media interface as shown in the picture below.

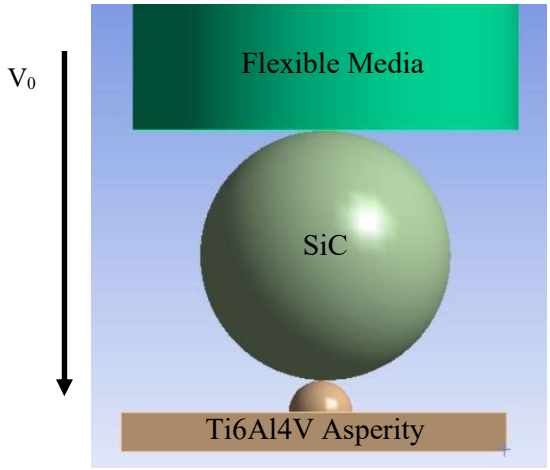

Figure 26: An image showing the simulation setup including the addition of the flexible media.

This simplification is an accurate representation of a single asperity interface and can be assumed that the surfaces (of both the flexible abrasives and workpiece) is continuous and repetitive which allows the results of the single impact to be mimicked across the surface of the material. The SiC abrasive and flexible media are assumed to be moving at the same speed at the point just before impact onto the asperity. Therefore, in setting up these experiments, the abrasive particle and flexible particle both take on the same initial velocity upon impact of the asperity. However, the differences in materials and that the items are not chemically or mechanically bonded does not mean during impact they maintain similar velocities which is demonstrated further in this chapter. The table below lists the details of the experiments that are undertaken within this section:

Table 12: A table showing the experiment parameters of investigating impinging velocity.

Test #	V_0 (m/s)	Asperity Size (µm)	Abrasive Size (µm)	Flexible Size (µm)
6	5	1.6	6.5	5 Radius 10 Height
7	15	1.6	6.5	
8	25	1.6	6.5	
9	35	1.6	6.5	

Again, a very similar format from the baseline tests except the effect of adding flexible media is the area of study within this section.

6.3.2 Results

We first inspect the behaviour of the SiC abrasive with respect to its velocity as we have previously determined the asperity deformation and stress is dependent on the initial impact velocity. In doing so, we can more clearly see the effect the flexible media has on the polishing action. The following graph shows the abrasive velocity over time for initial impingement velocities of 5, 15, 25 and 35m/s.

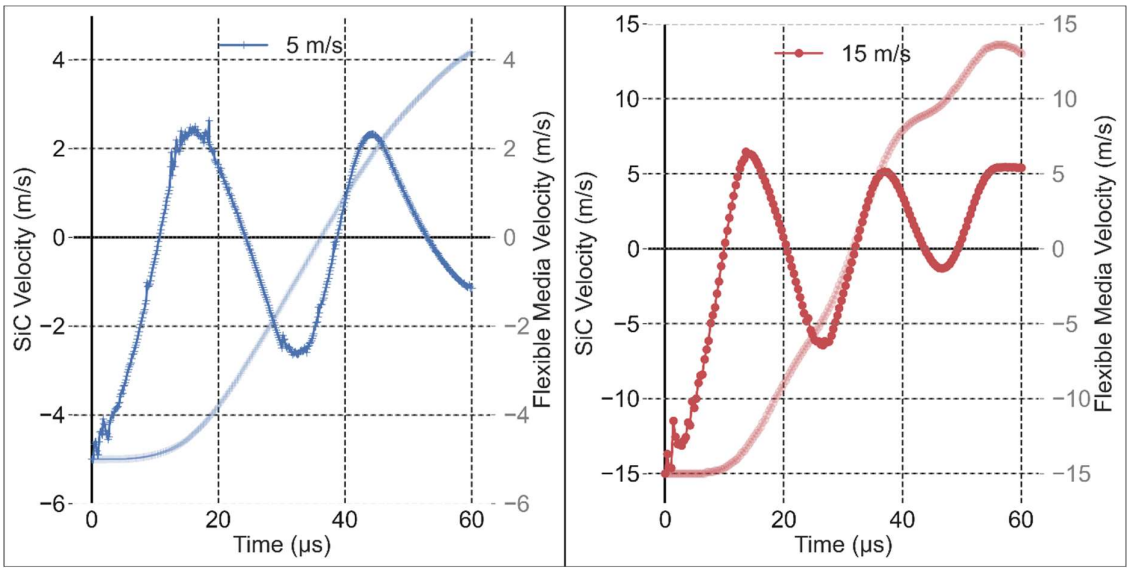

[a] [b]

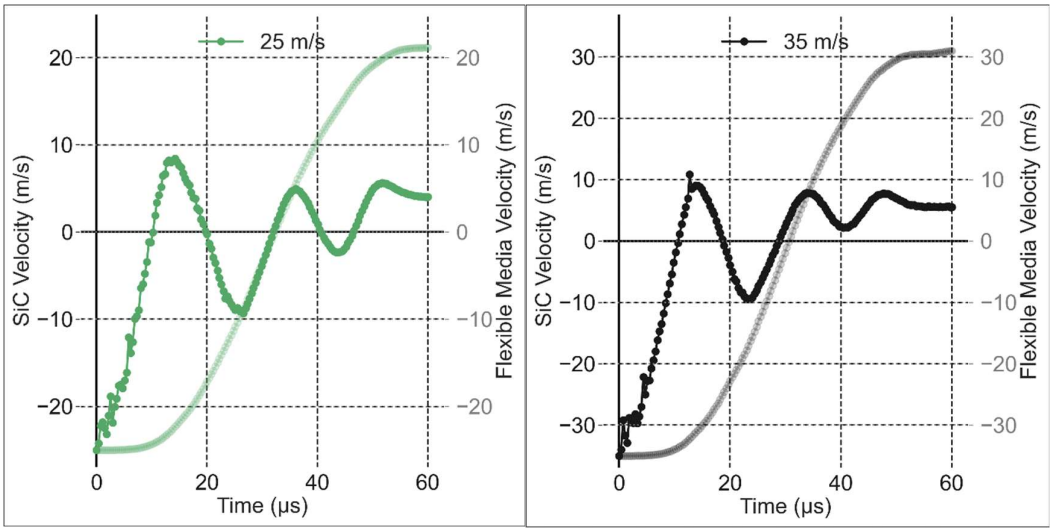

Figure 27: A velocity vs time graph for the SiC abrasive and HDPE flexible media for initial velocities of a)5 m/s, b) 15 m/s, c) 25 m/s and d) 35 m/s.

From the graphs above, the first observation that can be noted is that the flexible particle acts as a spring that allows the SiC abrasive to oscillate. Considering only the flexible media, it simply changes direction of motion from negative and towards the asperity to positive and away from the experiment at a velocity just below its initial impact velocity. This follows a similar trend that the abrasive particle alone has shown in the first set of experiments. The SiC molecule impacts the asperity and starts moving towards the flexible media, however, the flexible media is still moving in the negative direction which forces the asperity to impact the asperity again at a speed that is similar to the speed of the flexible media at that specific point in time. The oscillatory motion slows down towards the experiment (due to the flexible media completing its impact process) which therefore implies that the oscillatory motion is due to the addition of the flexible media. Because of this, it can be stated that the SiC abrasive will continue to oscillate and repeatedly impinge onto the asperity while the flexible media still carries momentum towards the asperity. To assess the effect of the additional flexible media on the polishing process, the same set of graphs inspecting the deformation and stress on the asperity is show below.

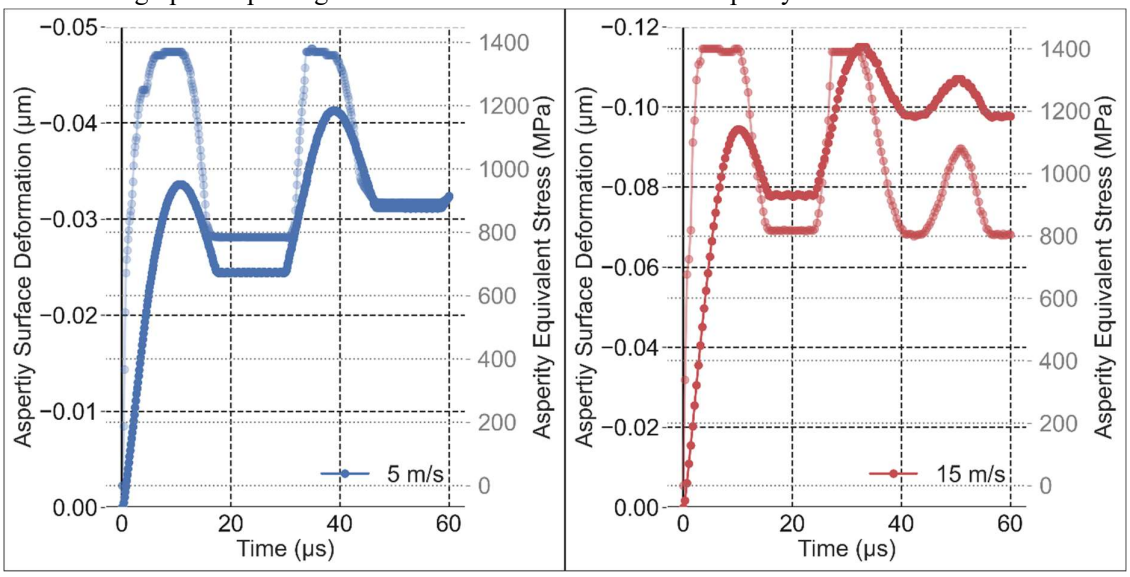

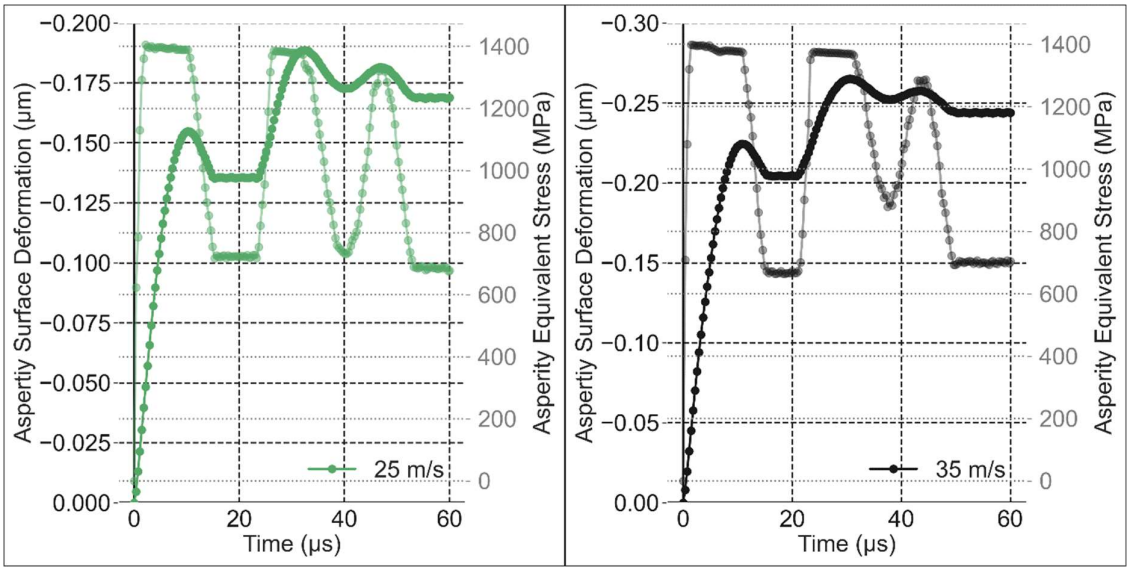

Figure 28: The deformation and stress of the asperity over time for initial velocities of a)5 m/s, b) 15 m/s, c) 25 m/s and d) 35 m/s.

The stress and deformation graphs confirm the oscillatory motion of the SiC abrasive particle. Upon initial impact, the plastic deformation is achieved after the first deformation peak and that the polishing action has taken place. Upon subsequent SiC abrasive impacts, the deformation increases passed the first peak towards a second peak and settles at a higher permanent plastic deformation than the first impact. The table below summarises the results from these experiments

Table 13: A table highlighting the effect of the flexible media on the polishing process.

Asperity Deformation (µm)				
Velocities (m/s)	Baseline	1st impact	2nd impact	Diff (%)
5	0.024	0.024	0.031	29.2
15	0.077	0.078	0.098	27.3
25	0.137	0.136	0.169	23.4
35	0.211	0.205	0.244	15.6

The initial impact of the abrasive media onto the asperity shows that the results are the same as was the case with the baseline tests that were completed. However, due to the addition of the flexible media, using HDPE as a flexible material result in an increase in polishing deformation by as much as 29.2 % for 5m/s impingement. As the initial velocity increases, the increase in polishing efficiency decreases down to 15.6 % for 35 m/s. The reason for the decrease so drastically at 35 m/s is because some of the energy that would normally be transferred to the surface of the asperity but instead is stored in the SiC abrasive as the abrasive fails and fractures at this initial velocity. This discovery implies that the addition of the flexible media does not decrease polishing time due to controlling polishing forces but rather due to the repeated impact that the flexible media causes. For every single abrasive particle that impacts an asperity, the updated technology can replicate a few more impacts dependant on the characteristics of the flexible media and its momentum. This means that the polishing time can be decreased due to the increase in efficiency due to the flexible media.

Another comment is that the system will still require the operator to have the necessary skills to not damage the component due to excessive polishing forces. This improvement in overall efficiency allows an operator to run at a lower impingement velocity which lowers the risk of damaging a part while still polishing at a quicker rate. The interacting dependencies for this system will be further investigated and mathematically discussed during later experimentation.

6.4 Asperity Size

When defining surface roughness, the values retrieved are usually averages over the specimen area. This is because in nature the surface will never have the same peak heights and valley depths. To add, due to various SLS fabrication parameters, the surface roughness from this process can vary and will not always be 1.6 microns. Therefore, these experiments investigate the behaviour of the polishing method across different surface roughness levels. The images below show the initial setup with the varying asperity sizes. These experiments also assist with defining the manufacturing flexibility of the system and the abrasive finishing category the technology may fit under.

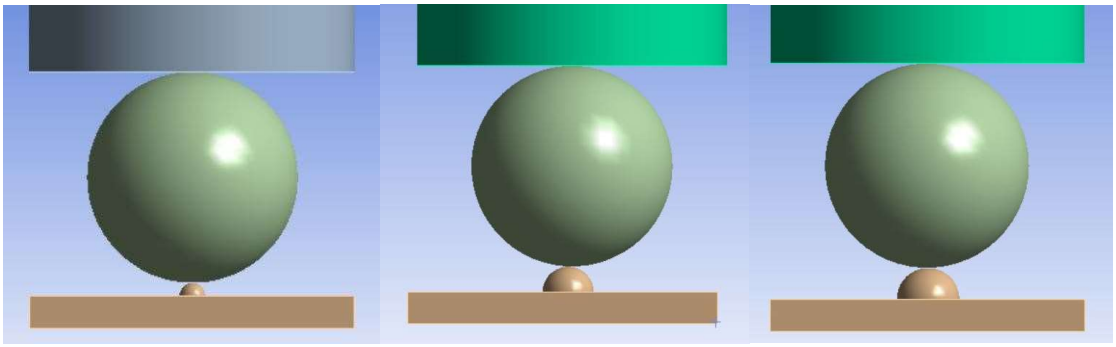

[a] [b] [c]

Figure 29: Images showing the varying sizes of the asperity of a) 0.8µm, b) 1.6 µm and c) 2.5 µm.

6.4.1 Experiment Explanation

To investigate the polishing process on surface roughness, we vary the size of the asperity to 0.8 µm, 1.6 µm and 2.5 µm. The initial velocities are also varied between the usual 5, 15 and 25 m/s. The flexible media size remains constant as well as the SiC abrasive at 6.5 µm. The table below is a summary of the experiments that were conducted:

Table 14: A table showing the experiment parameters investigating asperity size.

Test #	V_0 (m/s)	Abrasive Size (µm)	Asperity Size (µm)	Flexible Size (µm)
10	5	6.5	0.8	5 Radius 10 Height
11			1.6	
12			2.5	
13	15		0.8	
14			1.6	
15			2.5	
16	25		0.8	
17			1.6	
18			2.5	

6.4.2 Results

The graphs below show the stress and strain of the asperity over the impact period for varying velocities.

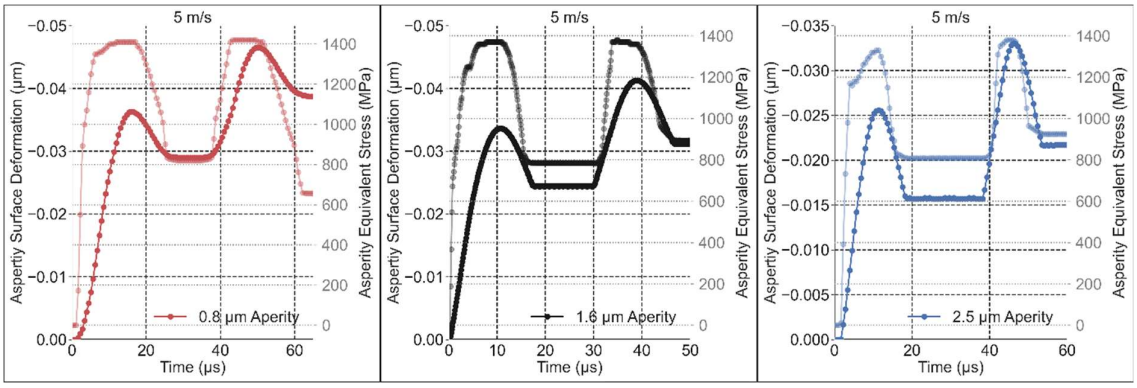

[a] [b] [c]

Figure 30: The following graphs shown the deformation and stress curves of the asperity over time with an initial impact velocity of 5 m/s and an asperity size of a) 0.8 µm, b) 1.6 µm and c) 2.5 µm.

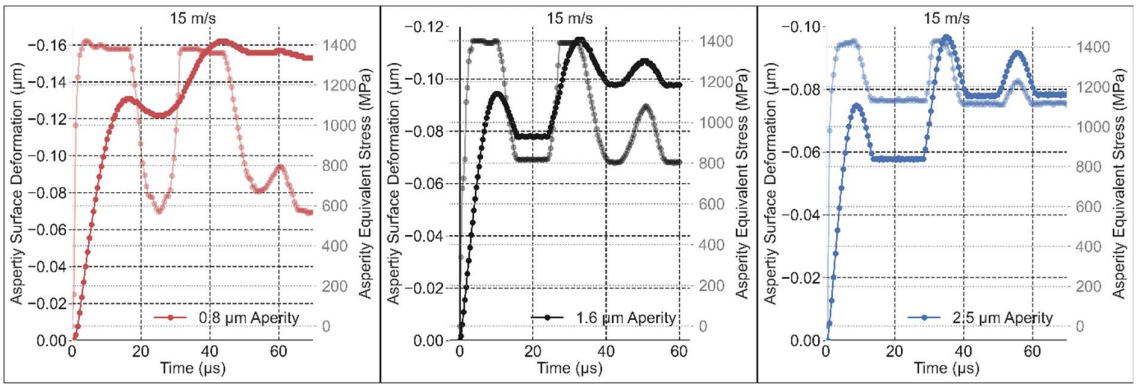

[a] [b] [c]

Figure 31:The following graphs shown the deformation and stress curves of the asperity over time with an initial impact velocity of 15 m/s and an asperity size of a) 0.8 µm, b) 1.6 µm and c) 2.5 µm.

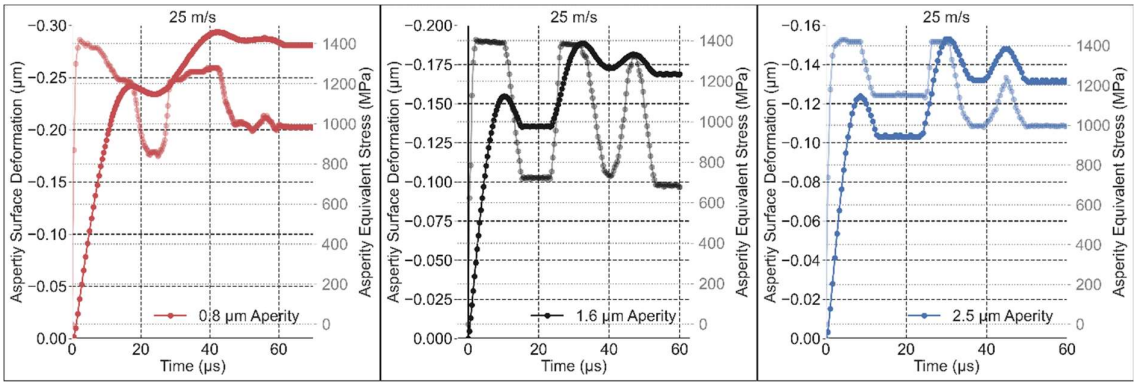

[a] [b] [c]

Figure 32:The following graphs shown the deformation and stress curves of the asperity over time with an initial impact velocity of 25 m/s and an asperity size of a) 0.8 µm, b) 1.6 µm and c) 2.5 µm.

Table 15: A table summarising the final asperity deformation for varying velocities and varying asperity sizes.

Asperity Deformation (µm)			
Velocity	0.8 µm Asperity	1.6 µm Asperity	2.5 µm Asperity
5 m/s	0.039	0.031	0.022
15 m/s	0.156	0.098	0.078
25 m/s	0.281	0.169	0.131

The pattern which is consistent throughout these experiments is that the higher the velocity, the higher the impact forces and these set of results are no different thus the initial velocity will not be discussed within this section as this has been elaborated on before. Analysing these results, the original surface finish of a material, due to previous fabrication processes, can determine the polishing action that takes place. Finer surface finishes result in higher surface deformation and rougher surface finishes result in lower surface deformation. To explain this behaviour, we can revise the contact mechanics equations that were used as part of the theoretical studies. Consider the equation:

$$a = 0.721\left[(\eta_1 + \eta_2)F\left(\frac{(D_1D_2)}{D_1+D_2}\right)\right]^{\frac{1}{3}} \qquad \textit{Equation 27}$$

Knowing that all the variables from this equation remain the same and the only variables that change are D_2 (the size of the asperity) and a (radius of local deformation) dependant on the asperity size change. Focusing on only the expression:

$$\left(\frac{(D_1D_2)}{D_1+D_2}\right) \qquad \textit{Equation 28}$$

As the size of the asperity increases, this expression will also increase which increases the value of a considering that all the other variables remain constant. At first glimpse this appears contradictory because the results suggest that an increase in asperity size decreases the deformation (and thus radius of local deformation). However, consider the following equation for the impact load's stress at the impingement surface:

$$\sigma = \frac{1.5F}{\pi a^2} \qquad \textit{Equation 29}$$

As a increases, the surface stress exponentially decreases which means that the local deformation will also decrease exponentially. This is because the increase in the radius of local deformation results in a higher stress due to a larger surface area where the force is transferred. Because the load stress is lower as the asperity size increases, it can be concluded that the local deformation will also thus decrease. Another equation within the contact mechanics equations that would have resulted to the same conclusion is:

$$\delta = 1.04\left[(\eta_1 + \eta_2)^2F^2\left(\frac{(D_1+D_2)}{D_1D_2}\right)\right]^{\frac{1}{3}} \qquad \textit{Equation 30}$$

The above equation is the method used to calculate the *actual* local deformation imparted onto a surface under load. Within this equation, there is an expression that is the inverse of equation 27 and thus increasing the asperity diameter will result in a decrease in deformation.

Considering the practicality of this result and its effect on the use of the new technology, this emphasises again the skills required by an operator to achieve a polishing action that is desirable. This is because the surface texture of the component in question can also influence the polishing characteristics. Therefore, to achieve similar polishing characteristics for a similar part that may have been finished

through a pre finishing process, it would be recommended to change the abrasive mesh size or to adjust the slide conveyor motor speed to change the impact velocity if replacing the abrasive media constantly may make the process more inefficient timewise.

6.5 Abrasive Size

Another element to investigate while defining the system is the effect of the abrasive size. With most polishing methods, a larger abrasive size results in a larger material removal rate. Fine polishing usually requires the use of very small abrasives. This set experiments investigate the effect of the abrasive size on the polishing characteristics for this system

6.5.1 Experiment Explanation

To investigate the effect of abrasive size, the mesh sizes of #2000, #5000 and #8000 SiC was investigated. This results in the SiC abrasive being 6.5, 2.5 and 1.5 microns in diameter respectively. This is also studied at the three different velocities of 5, 15 and 25m/s. The table below is a summary of the experiments that were conducted.

Table 16: A table showing the experimental parameters used to investigate the effect of abrasive size.

Test #	V_0 (m/s)	Asperity Size (µm)	Abrasive Size (µm)	Flexible Size (µm)
19	5	1.6	6.5	5 Radius 10 Height
20			2.5	
21			1.5	
22	15		6.5	
23			2.5	
24			1.5	
25	25		6.5	
26			2.5	
27			1.5	

6.5.2 Results

The following graphs show the stress and deformation graphs for the experiments conducted in this section.

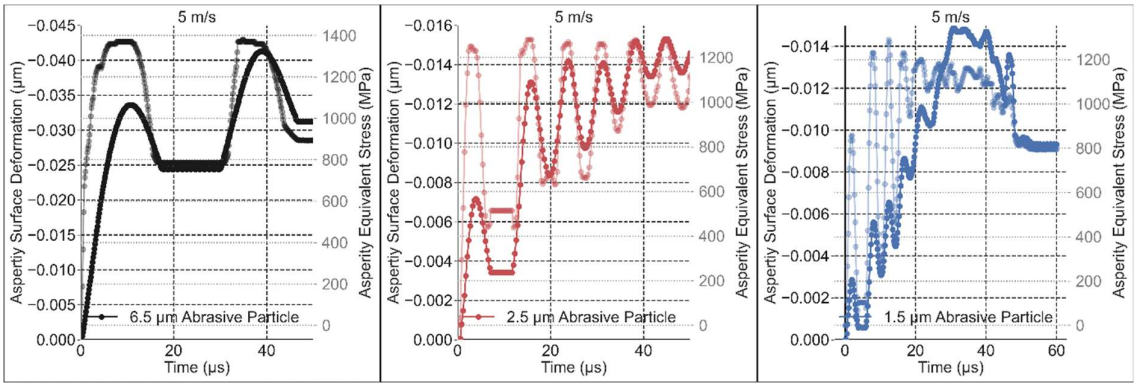

[a] [b] [c]

Figure 33: The following graphs shown the deformation and stress curves of the asperity over time with an initial impact velocity of 5 m/s and an abrasive particle size of a) 6.5µm, b) 2.5 µm and c) 1.5 µm.

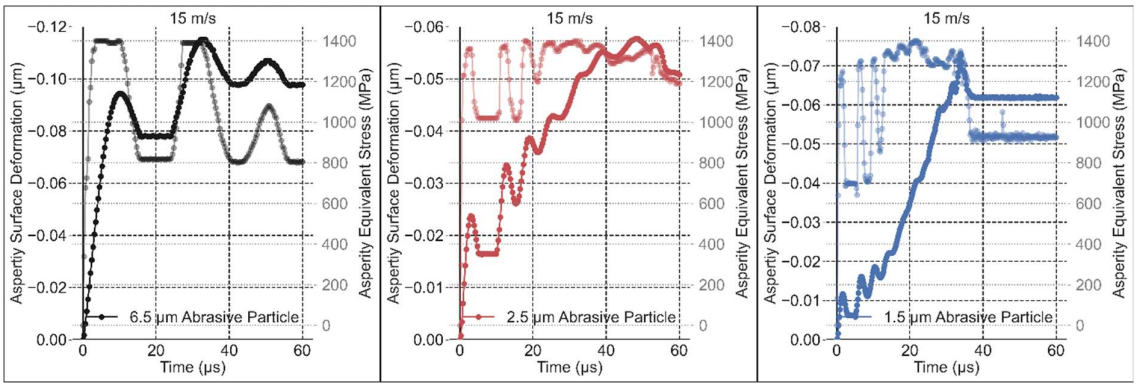

[a] [b] [c]

Figure 34: The following graphs shown the deformation and stress curves of the asperity over time with an initial impact velocity of 15 m/s and an abrasive particle size of a) 6.5µm, b) 2.5 µm and c) 1.5 µm.

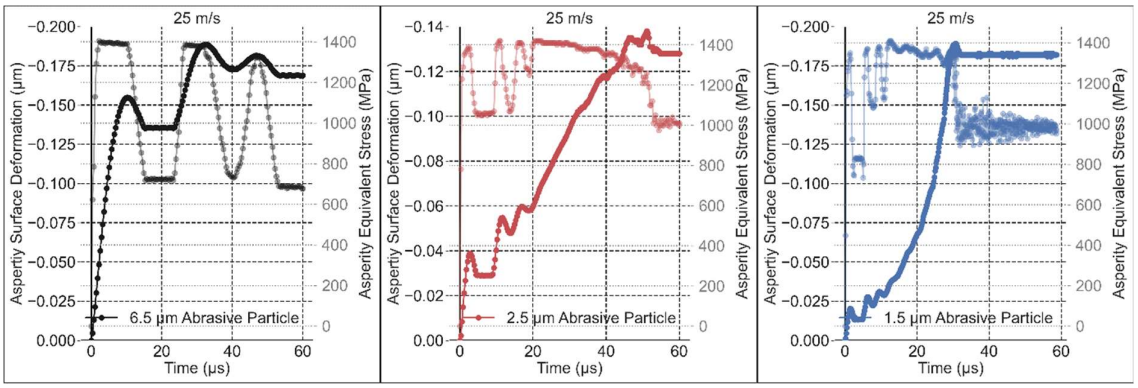

[a] [b] [c]

Figure 35:The following graphs shown the deformation and stress curves of the asperity over time with an initial impact velocity of 25 m/s and an abrasive particle size of a) 6.5µm, b) 2.5 µm and c) 1.5 µm.

Without the use of the velocity graphs, it can already be seen that the oscillation period increases as the abrasive size becomes smaller. This is expected as the total momentum of the abrasive is smaller due to the decrease in its mass. An expectation from these results due to similarities with other polishing methods is that with a decrease in abrasive size (and thus an increase in abrasive mesh size), the deformation on the asperity should be lower as the abrasive size becomes smaller. When trying to achieve finer surface finishes, finer abrasives are usually used, and these results verify that a similar trend exists for this polishing technology. The tables below highlight the results from these experiments.

Table 17: The table below summarises the asperity deformation for varying abrasive sizes and impact velocities.

Asperity Deformation (µm)			
Impact Velocity	6.5 µm abrasive	2.5 µm abrasive	1.5 µm abrasive
5 m/s	0.031	0.014	0.009
15 m/s	0.098	0.051	0.062
25 m/s	0.169	0.128	0.182

Considering the expression from equation 30$\delta = 1.04\left[(\eta_1+\eta_2)^2F^2\left(\frac{(D_1+D_2)}{D_1D_2}\right)\right]^{\frac{1}{3}}$ Equation 30 except where D_1 (the abrasive size) is being adjusted rather than D_2. The same conclusion can be

mathematically explained with the same theory and equations. However, looking at the 1.5 µm abrasive at an initial impact velocity of 15 and 25 m/s, the trend seems to be overruled by other system dependencies as it contains the highest asperity deformation for 25 m/s initial velocity and has higher deformation than the larger 2.5 µm abrasive size. However, the trend that was noted expects it to be the lowest deformation. The brief explanation for this phenomenon is that the ratio of flexible media to the abrasive particle's respective masses allow the smaller abrasive to simulate the weight of the bigger flexible media but still maintain the strength characteristics of SiC. This data point and discrepancy will be further elaborated on and discussed in the next set of experiments.

6.6 Supplementary Experimentation

There is reasonable evidence that suggests the momentum equation and the masses of the various components come into effect. The effect on the size of the abrasive has been investigated which is directly proportional to its mass and thus its momentum when undergoing a velocity. For this reason, we also needed to investigate the role that the flexible particle has in these simulations. In practice, the particle will not be as small as is demonstrated in the simulations but will rather be a continuous flexible particle since the flexible media in practice will be about 1 mm in size. The flexible media will contain many abrasives attached across its surface because the abrasive is within the low micron scale which is significantly lower than the flexible media. Therefore, one impact of the flexible particle will result in a multitude of impacts of abrasive particles and asperities across the workpiece surface such as the ones being studied through these experiments.

6.6.1 Experiment Explanation

The dimensions of the flexible media have been changed to increase its momentum by changing its volume and thus mass. The current shape of the flexible particle is a cylinder with a height *H* and a Diameter *D* as shown in the following image.

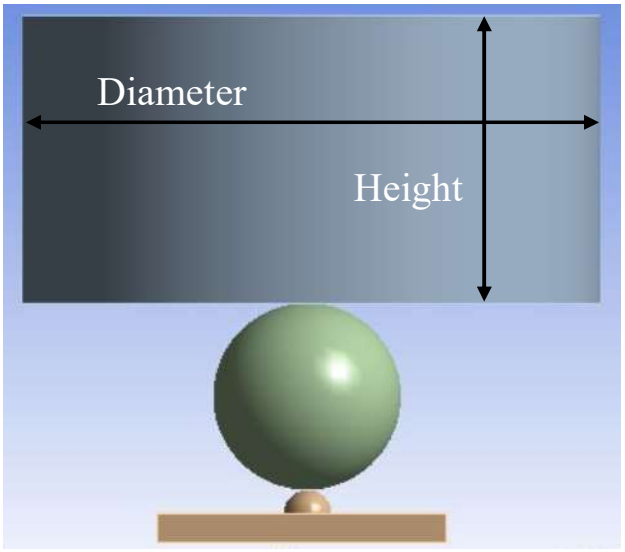

Figure 36: A figure showing the experimental set up for testing varying flexible media volumes.

For these experiments, the height and diameter have been changed to 10 and 20 microns which accommodates the three volumes that were used. The table below summarises the experiments that were conducted to achieve this which is a table followed by the relative volume and mass of the flexible media.

Table 18: A table showing the experimental parameters during the supplementary experimentation.

Test #	V_0 (m/s)	Asperity Size (µm)	Flexible Size (DxH µm)	Abrasive Size (µm)
28	5	1.6	10 x 10	6.5
29			10 x 20	
30			20 x 10	
31	15		10 x 10	
32			10 x 20	
33			20 x 10	
34	25		10 x 10	
35			10 x 20	
36			20 x 10	

Table 19: A table showing the Volumes and masses for the flexible media volumes that were used.

Volume #	D (µm)	H (µm)	Volume ($µm^3$)	Mass (µg)
1	10	10	785.4	0.00075
2	10	20	1570.8	0.00151
3	20	10	3141.6	0.00302

6.6.2 Results

The graphs below show the abrasive particles velocity over time for the four different flexible particle volumes that have been used.

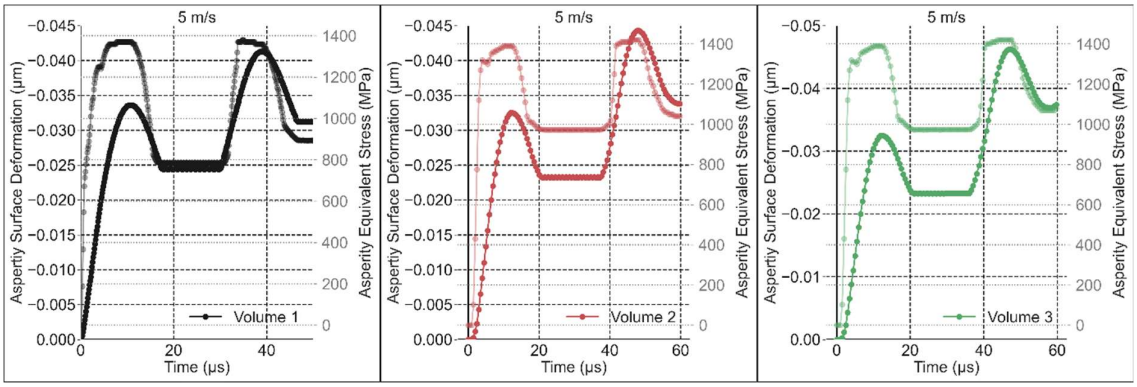

[a] [b] [c]

Figure 37: The following graphs show the deformation and stress curves of the asperity over time with an initial impact velocity of 5 m/s and a flexible media particle of volume of a) #1, b) #2 and c) #3.

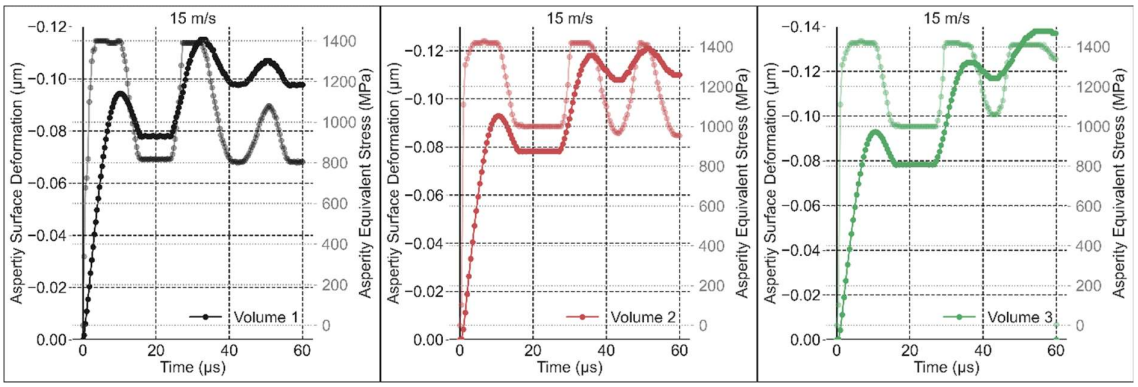

[a] [b] [c]

Figure 38: The following graphs show the deformation and stress curves of the asperity over time with an initial impact velocity of 15 m/s and a flexible media particle of volume of a) #1, b) #2 and c) #3.

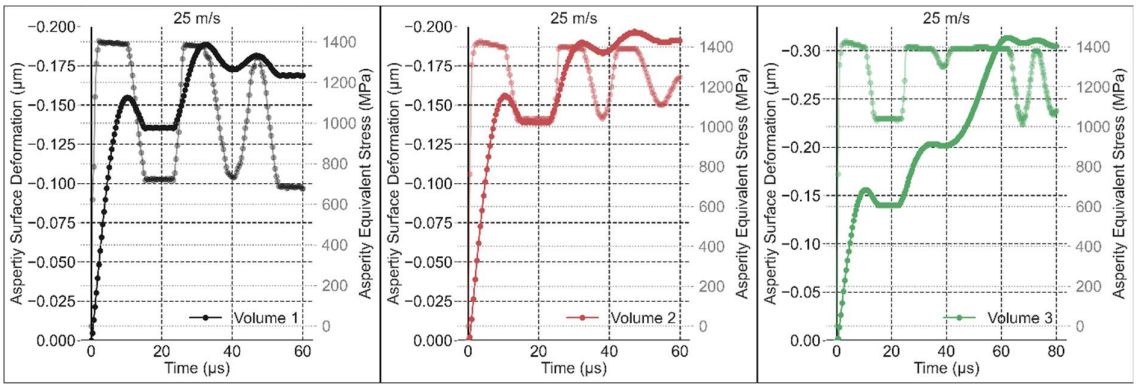

[a] [b] [c]

Figure 39: The following graphs show the deformation and stress curves of the asperity over time with an initial impact velocity of 25 m/s and a flexible media particle of volume of a) #1, b) #2 and c) #3.

The table below summarises the results from these simulations.

Table 20: A table showing the asperity deformation at varying flexible media masses and impact velocities.

Asperity Deformation (µm)			
Velocity	Volume #1	Volume #2	Volume #3
5 m/s	0.031	0.034	0.037
15 m/s	0.098	0.110	0.138
25 m/s	0.169	0.191	0.305

These results show that increasing the volume and the mass of the flexible media have shown an increase in the deformation of the asperity. The graphs that have been drawn show that by increasing the mass of the flexible media, the abrasive material oscillates three times rather than the two times that has been seen with the simulations that have been conducted this far using Volume #1. This is expected due to a higher initial momentum of the flexible media that requires a higher force and/or length of time to change its direction away from the asperity. To understand this phenomenon, we can refer to the first principles of physics. The following diagram shows the various forces and reaction forces that exist within the system.

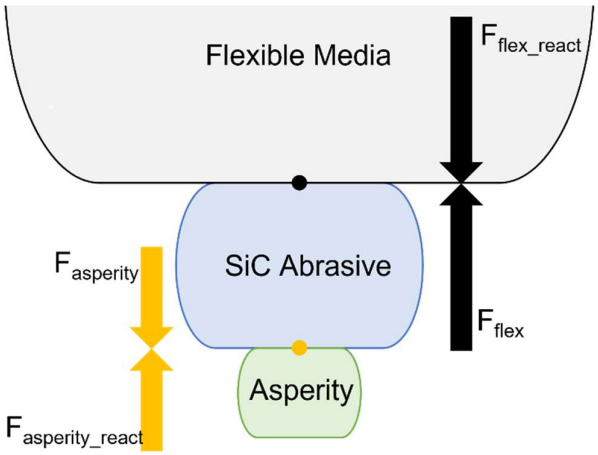

Figure 40: A diagram showing the interaction forces of the Flexible Media, SiC abrasive and the Asperity.

The above diagram considers the forces from the perspective of the SiC abrasive particle. Due to Newtons third law, we know that the reaction forces have the same value as their respective counterpart. We know that the abrasive particle has a higher mechanical strength than both the asperity and the flexible media, if this was not the case, we would not be able to polish the asperity. Therefore, we assume that the SiC is a rigid body within this system of interacting bodies. Considering this system as a simple spring mass damper, we know through the experimentation that the addition of the flexible media causes the spring effect during impact for the abrasive. The damper is a component that reduces velocity over a period due to converting the kinetic energy into another form such as heat due to friction. In this idealised system, the loss in kinetic energy of the abrasive and flexible media is transferred to the asperity surface in the form of strain hardening. Then the asperity in this system becomes the damper.

During the initial impact, it was shown in the velocity experiments that the resulting plastic deformation is very similar as to not having a flexible abrasive-that is until- the following impacts that are caused due to the flexible media. Consider the momentum of the abrasive media with the following equation:

$$P_{abrasive\ media} = P_{SiC} + P_{HDPE} \qquad \textit{Equation 31}$$

Which can be further expanded to:

$$P_{abrasive\ media} = m_{SiC} * v_{SiC} + m_{HDPE} * v_{HDPE} \qquad \textit{Equation 32}$$

Whereby P is the momentum of the abrasive media, v is the respective velocity and m is the respective mass. The equation defining the change of momentum can be expressed as:

$$\Delta P_{abrasive\ media} = F_{asperity\_react} * \Delta t \qquad \textit{Equation 33}$$

The force onto the asperity has been studied thus far to understand the deformation, however the equal and opposite reaction force is now being analysed. Initially, the $F_{asperity}$ is used to change the momentum of the SiC abrasive material and push it away at a velocity after considering the necessary loses. This is because the F_{flex} is negligeable as they are moving at similar speeds. However, as the interaction continues, the abrasive media begins to oscillate around 0 m/s essentially being stationary and thus P_{SiC} can equate to zero. As a simplification of these force interactions, the SiC abrasive becomes a vehicle to "transport" the $F_{asperity}$ to the flexible media to change the momentum of the flexible media P_{HDPE}. Therefore, towards the end of the interaction, the $F_{asperity}$ is a reaction force to F_{flex} and therefore the system can be simplified to a simple impact by the flexible media that is defined by the change of momentum equation:

$$\Delta P_{HDPE} = F_{asperity} * \Delta t \qquad \textit{Equation 34}$$

Even with this simplification, the polishing strength required for polishing the Ti6Al4V workpiece remains as the SiC abrasive is still physically between the two bodies. Knowing that the mass of the flexible media is significantly higher than the SiC abrasive, we know that the momentum of the flexible media is thus greater than the SiC abrasive. Therefore, the asperity will be required to transmit a higher force over a longer period to slow down the flexible media as defined by equation 33 $\Delta P_{abrasive\ media} = F_{asperity\_react} * \Delta t$ Equation 33. Therefore, the larger mass of flexible media within these simulations has contributed to a higher deformation on the asperity. The relationship of asperity deformation and flexible media mass is not linear because during impact, the asperity undergoes strain hardening and thus becomes tougher and requires more force to achieve local deformation.

Remembering that the flexible media will be much larger in comparison to the SiC abrasives and that there will be multiple SiC abrasives along its surface, it is difficult to predict the actual mass ratio of the SiC abrasive and flexible media portion that can be used under the conditions of studying a single asperity impact. However, it can be assumed that these asperity deformation results may be achieved in reality and possibly higher than what Ansys has produced. Unfortunately, the only conclusion that can be made is within the limitations of the simulation and its setup. The following table revises the possible improvement in process efficiency.

Table 21: A table revising the possible efficiency improvement due to the addition of the flexible abrasive

Asperity Deformation (µm)					
V_0	Baseline	Initial Result	Initial Diff (%)	Updated Result	Updated Diff (%)
5 m/s	0.024	0.031	29.2	0.037	54.2
15 m/s	0.077	0.098	27.3	0.138	79.2
25 m/s	0.137	0.169	23.4	0.305	122.6

Through these simulations, the initial understanding that higher velocities reduce the efficiency of the new technology is inaccurate. These results show that the increase in velocity can improve efficiency by as much as double. The Von Mises failure criteria is based off distortion energy and therefore to explain this behaviour we will consider the energy of the system before and after impact. The initial energy (E) of the system can be defined by:

$$E_{t=0} = E_{SiC,t=0} + E_{HDPE,t=0} \qquad \textit{Equation 35}$$

Which can be further defined by the kinetic energy equation:

$$E_{t=0} = \frac{1}{2} m_{SiC} {v_{SiC,t=0}}^2 + \frac{1}{2} m_{HDPE} {v_{HDPE,t=0}}^2 \qquad \textit{Equation 36}$$

Due to the conservation of energy theorem, we know that:

$$E_{t=0} = E_{t=end} \qquad \textit{Equation 37}$$

The energy at the end of the impact can be defined by:

$$E_{t=end} = E_{SiC,t=end} + E_{HDPE,t=end} + E_{Distortion} + E_{losses} \qquad \textit{Equation 38}$$

Where $E_{distortion}$ is the energy stored in the asperity surface that increases its surface strength and E_{losses} is the energy that has been lost. This lost energy included can be due to sound energy, distortion of the abrasive and the flexible media, and friction which may cause both thermal energy and electrical static energy dependant on the electrical properties. Rearranging the above equations:

$$E_{Distortion} = E_{t=0} - E_{losses} - (E_{SiC,t=end} + E_{HDPE,t=end}) \qquad \textit{Equation 39}$$

Assuming that a certain percentage of the original energy within this system is converted to these various forms, we can introduce constants into the equation:

$$E_{t=0} = \eta_{distortion} E_{Distortion} + \eta_{losses} E_{losses} + \eta_{final\_velocity} (E_{SiC,t=end} + E_{HDPE,t=end}) \quad \textit{Equation 40}$$

The constants η are ratios that show mathematically the distribution of the energy after impact. The following equation links the energy equations to momentum equations:

$$E_{t=0} = P_{t=0} * \frac{1}{2} * v_{t=0} \quad \textit{Equation 41}$$

Considering Equation 39 and Equation 40, it can be stated that:

$$P_{t=0} \propto E_{Distortion} \propto \delta_{Asperity} \quad \textit{Equation 42}$$

Therefore, the initial result that an increase velocity reduces the efficiency of the system and the updated results are accepted. Even though the efficiency increases with impact velocity, it should be noted that negative effect of this trait is that the risk of damaging the surface of the component due to excessive forces also increases with impact velocity.

In the previous set of experiments there was a discrepancy for test #27. After discussing and explaining the energy theorem, the intricate mathematical relationship between the abrasive size and the influence of the flexible media size has caused the discrepancy it did within the explanation that was given for the pervious set of experiments. However, after concluding that the deformation of the asperity is dependent on the energy theorem, and more specifically the total momentum of the system, it can also be concluded that the ratio between P_{SiC} and P_{HDPE} can influence which of the two energies contributes the most to the final asperity deformation. In the case of that specific experiment, it appears that the flexible media had an overpowering momentum in comparison to the SiC abrasive. For the other tests whereby the SiC abrasive contributed significantly to the asperity deformation, the $P_{HDPE\ \text{relative}}$ to the P_{SiC} was not the stronger dependency. With this being mentioned, there is most likely a cross over ratio whereby the momentum of the SiC abrasive will stop becoming a significant contributor to deformation and the momentum of the flexible media will become the stronger predictor for the polishing characteristics.

6.7 Preliminary Experiment

Although not included within the scope of this research, a preliminary experiment has been completed on the developed and manufactured polishing process. These results are included to demonstrate that a polishing action is achieved using the suggested method and that there is merit to the numerical and computational analysis that has been reported on in this report. The experiment involved the polishing of a sample Selective Laser Sintered Ti6Al4V 10 x 10 x 10 mm block. The table below shows the parameters of the experiment.

Table 22: A table showing the parameters of the preliminary experiment.

Parameter	Value
Impact Velocity	31.4 m/s
Water Content	10 %
Flexible Media Content (Gelatine)	89.9 %
Diamond Content	0.1 %
Diamond Powder Mesh Size	#5000

The results for this experiment are shown in the graph below.

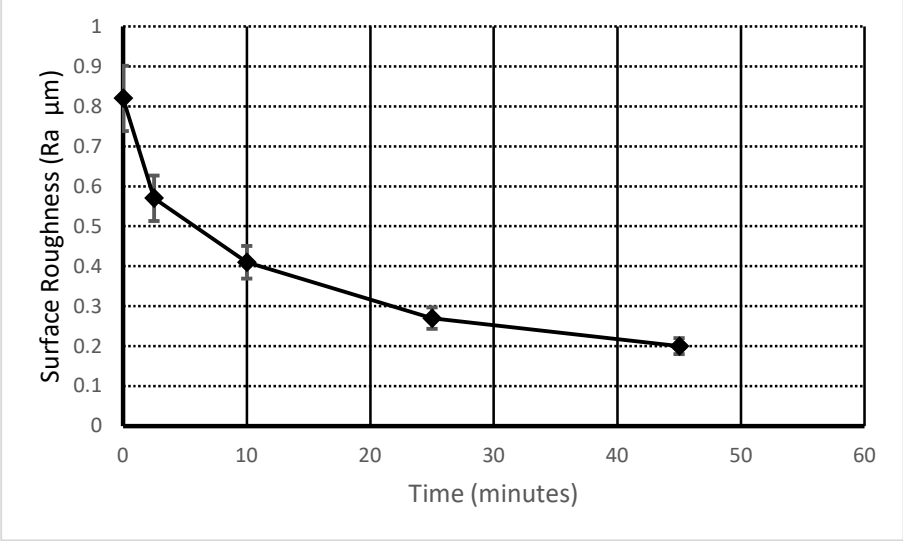

Figure 41: A line graph showing the surface roughness change over time.

The curve of the experiment mimics an exponential decay curve which indicates that over time the Material Removal Rate decreases as the surface strength of the workpiece improves. The initial roughness of the sample block has an Ra of 0.82 µm before polishing. At the end of the experiment, the roughness decreases to 0.2 µm after 45 minutes of polishing. It should also be noted that after only 25 minutes of polishing, the surface roughness Ra reduced to 0.27 µm. The remaining 15 minutes reduced the Ra to 0.2 µm. This can be attributed to the surface residual stresses due to the polishing impact forces which increases the surface strength and therefore lowers the polishing rate. Another possible cause for the drop in polishing action is due to the wear of the abrasive media as it is recycled through the system and over time its polishing effect is lowered. This behaviour is quite frequently observed during similar polishing processes and thus these results show a step in the right direction with the suggested polishing mechanism.

According to a study by Kuppuswamy et al. [8], a polycrystalline diamond (PCD) inserts with an initial Ra of 0.55 µm was polished down to an Ra of 0.29 µm in 25 minutes using a similar process except for the use of rubber granules and diamond particles (ø 0.02 mm) as the flexible abrasive media. Comparing the two experiments, the most significant parameter differences are the impact velocities, the abrasive size and the material of the component being polished. The impact velocity of the abrasive media was 0.4 m/s – significantly slower than the 5 m/s used during this research. However, the size difference in diamond powder particles used in the study translates to a mass that is 512 times higher than the 2.5 µm diameter diamond particle used for the experiment above. The increased size (and therefore mass) of the diamond abrasive particles in the abrasive media required the use of a lower impact velocity according to the momentum equation which observes a linear relationship between velocity and mass. This is a relationship that has also been observed during the stimulatory analysis and therefore the lower velocity used during the study still corresponds with the analysis reported on during this research. Considering momentum of only the diamond particles, the study has a 6.5 times higher momentum than with the above experiment.

PCD has an elastic modulus of 1090 GPa compared to the 110 GPa of SLS manufactured Ti6Al4V. It is thus expected that polishing PCD inserts should take significantly longer than Ti6Al4V samples. If a linear relationship is assumed for the effect of component material, the PCD insert should take 9.9 times longer to polish under similar polishing conditions. In this experiment, it has taken roughly 20 minutes to polish the Ti6Al4V sample from and Ra of 0.55 µm to an Ra of 0.29 µm whereas the study has taken 25 minutes for the PCD insert. This is a 0.8 times difference between the two experiments. Considering these three effects, we can use the following metric to quantify the difference between the results from the two experiments:

$$Performance\ Ratio = \frac{1}{6.5} \times \frac{1090}{110} \times \frac{20}{25} = 1.22 \qquad \textit{Equation 43}$$

A performance ratio of 1.22 indicates that the two experiments, considering only the above three factors, have a performance gap of 22% between each other. In simpler terms, the polishing performance of the above experiment is 22% lower than the experiment reported on by Kuppuswamy et al [8]. It is noted that this is a simplification of the many variables that affect the polishing action that were note considered. These variables include the material's surface response due to differing chemical composition, different surface fatigue behaviour, different composition of the flexible abrasives (the study does not reveal the composition of the flexible abrasives), differing nozzle design (which affects the abrasive flow and impingement onto the surface) and differing experimental conditions. The above simplification also excludes the various errors that are to be expected between the two experiments due to various causes. However, achieving a preliminary result that performs within a 22% range of the results retrieved by another study proves that the system being developed is on the correct trajectory. Various performance gains can still be achieved as this is an experiment from the initial prototype and many changes will still be made.

This shows that the proposed polishing process has merit and that only as much as 0.1% composition of abrasive material to surround a flexible media is required to achieve the desired polishing action that has been investigated during this report. The use of gelatine for this experiment and the use of rubber by the similar study also confirms the ability to source and experiment with other materials that are more sustainable and environmentally friendly than the HDPE polymer that was used for the purposes of the simulations. The comparison to existing literature that polishes PCD rather than Ti6Al4V also confirms that the suggested polishing mechanism may be able to polish other materials other than SLS Ti6Al4V components.

6.8 Final Remarks

The addition of flexible media to the abrasives used for the polishing action manages to improve the overall polishing process. The polishing process is improved in terms of polishing time as well as process costs. The results from this research have shown that the system efficiency can increase by a scale factor of 2.2 which means that the polishing time can be reduced by as much as half the time if the process parameters are correct and translate into the physical machine. By adding the flexible media, it was shown that due to the addition of the elasticity and momentum of the flexible media, it allows for multiple abrasive particle impacts for each flexible media impact onto the workpiece surface. In comparison, having more impacts onto a workpiece surface for the same mass flowrate increases the MRR of the polishing system which thus increases polishing speed and thus reduces polishing time. Normally with an increase in MRR, the risk involved in increasing polishing forces can cause unwanted effects and essentially damage the component in some cases but with this method of increasing MRR,

the risk is not increased and the risk of damaging a component is the same as is the case with only making use of abrasive particles alone. The risk remains and will depend on the abilities of the operator on its success specifically in managing the polishing characteristics such as the composition of the abrasive media and the impact velocity (by setting the slide conveyor motor speed).

The flexible media used is also fundamental in the characteristics of the polishing process. The benefit of this addition is that having the choice of using other materials make the system more versatile for various scenarios and materials that may not have been studied within the bounds of this research. The choice of flexible media in large scale operations is a feature that can be used in optimising material cost and manpower hours to improve the business case and the financial efficiency of the system and thus save on costs.

The size of the abrasive is another characteristic that can be used in defining the polishing characteristics of the system. The increase in abrasive size and thus its mass and momentum, increases the MRR of the polishing process due to increased forces changing the momentum of the abrasive particle. Increasing abrasive size is a fact that has been applicable with most polishing methods and this polishing system is not any different in this regard. During the manufacturing process, there are various levels of MRRs which can be found throughout the manufacturing pipeline. The abrasive size and slide conveyor motor speed can be adjusted to replicate the MRR of a grinding process or polishing process dependant on the specific requirements of the part being fabricated which again improves the versatility and application of this system within workshops. These parameters can change the category of surface finishing methods that this technology may find itself in. This is essential where flexible manufacturing technologies are increasing in their popularity due to the demands of the market with constant changes to components due to the increase in design turnaround times with credit to the 4^{th} Industrial Revolution.

The research that has been done has shown promising results for the feasibility of the proposed technology. However, the simulation findings suggest that the initial assumption that the addition of a flexible media will assist with the managing of excessive polishing forces (due to the increase of the flexibility in the media) will lower the polishing forces on a workpiece is inaccurate. The abrasive particles within the flexible abrasive media still respond as their own entity and will follow a polishing process that is like that of the Aerolap system initially developed [8].

7 Conclusion and Recommendations

This dissertation has reported on the extensive research that has been completed in developing a modern polishing solution for Grade 5 titanium workpieces that are manufactured by making use of the Selective Laser Sintering process. This was achieved through analytical and numerical simulations.

7.1 Conclusion

The following conclusions can be made from the findings of this report:

1. The polishing process with flexible abrasives is a novel technology that can be flexibly applied to factories that make use of modern additive manufacturing technologies to fabricate components. The technology can be applied to a variety of component materials. The polishing technology can also be used to refurbish components that contain complex geometry that was historically discarded or recycled.
2. Polishing time can be significantly reduced by incorporating this technology in workshops. With a reduction in polishing time, companies can save labour costs and improve the efficiency of their fabrication/refurbishment processes and therefore produce more output which can also result in higher profits.
3. The addition of the flexible media has shown that less abrasives can be used in exchanged for a cheaper alternative which is another cost saving due to the addition of the flexible media.
4. This improvement can bring down operational costs for workshops due to time savings as well as costs on abrasives as this system allows for the use of less abrasives and more natural materials which are cheaper to procure.
5. The polishing process can be optimised according to the requirements of the machinist and task at hand as with other polishing methods. Properties such as impact velocity and abrasive size can help the machinist achieve desirable polishing characteristics.
6. The technology is unable to prevent certain polishing discrepancies that take place due to excessive polishing forces such as edge-chipping, cracks, micro grooving, and gouge marks. There is still an elevated level of skill that is required by the machinist to prevent damage to components while using this technology.

The conclusions presented above are findings from the simulation results which will require physical experimentation of the technology to validate the above conclusions to the technology prototype.

7.2 Recommendations

The following recommendations have been identified as a result from the work done during this dissertation:

1. One of the important elements that contribute to the success of this technology is the abrasive media. It is therefore important to further research how flexible abrasives contribute to the polishing action and how various characteristics of the flexible abrasive media (including material) can be used to optimise characteristics for polishing as well as moving towards a less wasteful and more “green’ technology. The vibratory analysis is an interesting avenue to investigate further, however, there are still too many unknowns at the time of writing to develop

the vibration model of the system. The unknowns can be defined through physical experimentation.

2. Ideally this system will be fully developed and ready for market. However, further development and research outside the scope of this dissertation needs to be completed to achieve an industry product. This includes improving on the current initial prototype, scaling the system to handle larger workpieces, and finalising the finer details that can improve the technology to be safe and user friendly for operators in industry.
3. Due to the scope of this dissertation, it has been noted that in an industry that uses a variety of metals and not just necessarily Grade 5 titanium, it may be important to test and optimise this system on a variety of metals that have been manufactured differently for different use cases to increase the flexibility of the technology outside the scope of just the aeronautical industry. Increasing the scope of use for technology will enable it to bring more value to the world when adopted into a variety of industries. Even though this can be extrapolated, the verification tests still need to be concluded.
4. The need for automation is still an existing challenge. Due to the nature of the SLS fabricated components, the various geometries that can be achieved may require an extremely skilled worker to complete the polishing process effectively and not to damage the component. Being able to automate the polishing process (by means of a 5-axis manipulator arm that can read electronic drawings, understand workpiece geometry, and manoeuvre itself appropriately to achieve the required polishing) will reduce waste, save costs, improve efficiency which then improves the profitability of the process.

These recommendations are not exhaustive, but they do however provide an overview of further development which can improve the technology as well as improving the wealth of knowledge in the scientific community.

8 References

[1] G. Awari, C. Thorat, V. Ambade and D. Kothari, Advanced Materials & Processes, Advanced Materials & Processes: CRC Press, 2021.

[2] M. Kearns, "Titanium: alive, well, and booming!," *Advanced Materials & Processes,* vol. 163, no. 9, p. 63+, 2005.

[3] D. Banerjee and J. C. Williams, "Perspectives on Titanium Science and Technology," *Acta Materialia,* vol. 61, pp. 844-879, 2013.

[4] G. Lütjering and J. C. Williams, Titanium (2nd Edition), Springer, 2007.

[5] Z. Liu, B. He, T. Lyu and Y. Zou, "A Review on Additive Manufacturing of Titanium Alloys for Aerospace Applications: Directed Energy Deposition and Beyond Ti-6Al-4V," *JOM,* vol. 73, no. 6, pp. 1804-1818, 2021.

[6] I. Gibson, D. Rosen, B. Stucker and M. Khorasani, "Powder Bed Fusion," in *Additive Manufacturing Technologies*, Springer, Cham, 2021, pp. 125-170.

[7] E. Olakanmi, R. Cochrane and K. Dalgarno, "A review on selective laser sintering/melting (SLS/SLM) of aluminium alloy powders: Processing, microstructure, and properties," *Progress in Materials Science,* vol. 74, pp. 401-477, 2015.

[8] R. Kuppuswamy, S. Ozbayraktar and H. Saridikmen, "Aero-lap polishing of poly crystalline diamond inserts using Multicon media," *Journal of manufacturing Processes,* vol. 14, pp. 167-173, 2012.

[9] J. T. Black and R. A. Kohser, "DeGarmo's Materials and Processes in Manufacturing: Tenth Edition," in *DeGarmo's Materials and Processes in Manufacturing: Tenth Edition*, John Wiley & Sons, 2008, pp. 756 - 789.

[10] M. J. Neale, "Basic Information," in *The Tribology Handbook*, Oxford, Butterworth-Heinemann, 1995, pp. E1.1 - E8.3.

[11] A. Ebrahimi and S. Akbarzadeh, "Mixed-elastohydrodynamic analysis of helical gears using load-sharing," *Journal of Engineering Tribology,* vol. 228, no. 3, pp. 320-331, 2014.

[12] D. A. H. Hanaor, Y. Gan and I. Einav, "Static friction at fractal interfaces," *Tribology International,* vol. 93, pp. 229-238, 2016.

[13] Q. Xin, "10 - Friction and lubrication in diesel engine system design," in *Diesel Engine System Design*, Woodhead Publishing, 2013, pp. 651-758.

[14] International Organisation for Standardization, Geometrical Product Specifications (GPS) — Surface texture: Profile method — Terms, definitions and surface texture parameters, Geneva: International Organisation for Standardization, 1997.

[15] D. Whitehouse, Surfaces and Their Measurement, London: Elsevier Science & Technology, 2004.

[16] Harrison Electropolishing L.P., "Calculating surface finishes," Harrison Electropolishing, [Online]. Available: http://www.harrisonep.com/electropolishing-ra.html. [Accessed 15 October 2021].

[17] B. Bhushan, "2 Surface roughness analysis and measurement techniques," in *Modern Tribology Handbook*, Boca Raton, CRC Press LLC, 2001.

[18] International Organization for Standardization, ISO 1302:2002 Geometrical Product Specifications (GPS) — Indication of surface texture in technical product documentation, Geneva: International Organization for Standardization, 2012.

[19] ISO Finishing, "Surface Roughness in Manufacturing," ISO Finishing, June 2018. [Online]. Available: https://isofinishing.com/surface-roughness-in-manufacturing/. [Accessed 20 October 2021].

[20] CNC Cookbook, "Complete Guide to Surface Finish Symbols, Charts, RA, RZ, Measurements, and Callouts," CNC Cookbook, 2020. [Online]. Available: https://www.cnccookbook.com/surface-finish-chart-symbols-measure-calculators/. [Accessed 2021 October 20].

[21] F. Hashimoto, H. Yamaguchi, P. Krajnik, K. Wegener, R. Chaudhari, H.-W. Hoffmeister and F. Kuster, "Abrasive fine-finishing technology," *CIRP Annals - Manufacturing Technology,* vol. 65, no. 2, pp. 597-620, 2016.

[22] P. Zhang, D. Z. Zhang, D. Peng, Z. Li and Z. Mao, "Rolling contact fatigue performance evaluation of Ti–6Al–4V parts processed by selective laser melting," *The International Journal of Advanced Manufacturing Technology,* vol. 96, no. 9-12, pp. 3533-3543, 2018.

[23] T. Bremerstein, A. Potthoff, A. Michaelis, C. Schmiedel, E. Uhlmann, B. Blug and T. Amann, "Wear of abrasive media and its effect on abrasive flow machining results," *Wear,* vol. 343, pp. 44-51, 2015.

[24] E. S. Leonard and L. E. Samuels, Metallographic Polishing by Mechanical Methods, A S M International, 2003.

[25] A. S. Iquebal, D. Sagapuram and S. T. S. Bukkapatnam, "Surface plastic flow in polishing of rough surfaces," *Scientific Reports,* vol. 9, no. 1, pp. 10617-11, 2019.

[26] B. Hoyle, "Abrasives," in *The Gale Encyclopedia of Science, 6th ed., vol. 1*, Gale, 2021, pp. 3-5.

[27] M. P. Groover, in *Fundamentals of Modern manufacturing MAterials, Processes, and Systems*, John Wiley & Sons, Inc, 2010, pp. 621-629.

[28] A. Azami and A. Azizi, "Rotational abrasive finishing (RAF); novel design for micro/nanofinishing," *The International Journal of Advanced Manufacturing Technology 91,* pp. 3159-3167, 2017.

[29] T. T. W.F. Gale, "10 - Metallography," in *Smithells Metals Reference Book*, Butterworth-Heinemann, 2004, pp. 10-1 - 10-87.

[30] H. Y. K. H. D. J. E. S. L. Y. J. S. J. J Kim, "Friction and thermal phenomena in chemical mechanical polishing," *Journal of Materials Processing Technology,* Vols. 130-131, pp. 334-338, 2002.

[31] L. Wang, P. Zhou, Y. Yan and D. Guo, "Investigation on nanoscale material removal process of BK7 and fused silica glass during chemical-mechanical polishing," *International Journal of Applied Glass Science,* vol. 12, no. 2, pp. 198-207, 2020.

[32] A. V. Balyakin, A. N. Shvetcov and E. I. Zhuchenko, "Chemical polishing of samples obtained by selective laser melting from titanium alloy Ti6Al4V," *MATEC Web Conf. 224 01031,* vol. 224, p. 01031, 2018.

[33] A. Balyakin, E. Zhuchenko and E. Nosova, "Study of heat treatment impact on the surface defects appearance on samples obtained by selective laser melting of Ti-6Al-4V during chemical polishing," *Materials Today: Proceedings,* vol. 19, no. 5, pp. 2307-2311, 2019.

[34] I. D. Marinescu, E. Uhlmann and T. K. Doi, Handbook of Lapping and Polishing, CRC Press, 2007.

[35] V. Rana, A. C. Petare and N. K. Jain, "Advances in Abrasive Flow Finishing," in *Advances in Abrasive Based Machining and Finishing Processes*, Springer, Cham, 2020, pp. 147-181.

[36] T. Wang, D. Chen, W. Zhang and L. An, "Study on key parameters of a new abrasive flow machining (AFM)," *The International Journal of Advanced Manufacturing Technology,* vol. 101, pp. 39-54, 2019.

[37] R. Butola, R. Jain, P. Bhangadia, A. Bandhu, R. Walia and Q. Murtaza, "Optimization to the parameters of abrasive flow machining by," *Materials Today: Proceedings,* vol. 5, pp. 4720-4729, 2018.

[38] P. Ali, S. Dhull, R. Walia, Q. Murtaza and M. Tyagi, "Hybrid Abrasive Flow Machining for Nano Finishing - A Review," *Materials Today: Proceedings,* vol. 4, pp. 7208-7218, 2017.

[39] J.-W. Lee, S.-j. Ha, Y.-K. Cho, K.-B. Kim and M.-W. Cho, "Investigation of the Polishing Characteristics of Metal Materials and Development of Micro MR Fluid Jet Polishing System for the Ultra Precision Polishing of Micro Mold Pattern.," *Journal of Mechanical Science and Technology,* vol. 29, no. 5, pp. 2205-2211, 2015.

[40] A. Wang and S. Weng, "Developing the polymer abrasive gels in AFM processs," *Journal of Materials Processing Technology,* Vols. 192-193, pp. 486-490, 2007.

[41] T. Bremerstein, A. Potthoff, A. Michaelis, C. Schmiedel, E. Uhlmann, B. Blug and T. Amann, "Wear of abrasive media and its effect on abrasive flow machining results," *Wear,* Vols. 342-343, pp. 44-51, 2015.

[42] K. Kowsari, D. James, M. Papini and J. Spelt, "The effects of dilute polymer solution elasticity and viscosity on abrasive slurry jet micro-machining of glass," *Wear,* vol. 309, no. 1-2, pp. 112-119, 2014.

[43] J. Polanski, "4.14 - Chemoinformatics," in *Comprehensive Chemometrics*, Elsevier, 2009, pp. 459-506.

[44] H. Dai, H. Yue, Y. Hu and P. Li, "The Removal Mechanism of Monocrystalline Si in the Process," *Tribology Letters,* vol. 69, no. 2, p. 66, 2021.

[45] R. Chen, S. Li, Z. Wang and X. Lu, "Mechanical model of single abrasive during chemical mechanical polishing:," *Tribology International,* vol. 133, pp. 40-46, 2019.

[46] C. Sheng, M. Zhong and W. Xu, "A study on mechanism of sapphire polishing using the diamond abrasive by molecular dynamics," *Mechanics of advanced materials and structures,* pp. 1-13, 2021.

[47] Z. Bi, "Chapter 8 - Applications—Solid Mechanics Problems," in *Finite Element Analysis Applications*, Academic Press, 2018, pp. 281-339.

[48] H. Li and J. Chen, "Determination of elastic moduli of elastic–plastic microspherical materials using nanoindentation simulation without mechanical polishing," *Beilstein Journal of Nanotechnology,* vol. 12, pp. 213-221, 2021.

[49] D. A. H. Hanaor, Y. Gan, and I. Einav, "Static friction at fractal interfaces," *Tribology International,* vol. 93, pp. 229-238, 2016.

[50] N. Kumar and M. Shukla, "Finite element analysis of multi-particle impact on erosion in abrasive water jet machining of titanium alloy," *Journal of Computational and Applied Mathematics,* vol. 236, no. 18, pp. 4600-4610, 2012.

[51] J. Reiner, J. P. Torres, M. Veidt and M. Heitzmann, "Experimental and numerical analysis of drop-weight low-velocity impact tests on hybrid titanium composite laminates," *Journal of Composite Materials,* vol. 50, no. 26, pp. 3605-3617, 2016.

[52] J. Tu, G.-H. Yeoh and C. Liu, "Computational Fluid Dynamics - A Practical Approach (3rd Edition)," in *1.1 What is Computational Fluid Dynamics.*, Oxford, Elsevier, 2018, pp. 1-3.

[53] C. C. L. H. M. L. W. L. C.J. Wang, "A novel multi-jet polishing process and tool for high-efficiency polishing," *International Journal of Machine Tools & Manufacture,* vol. 115, pp. 60-73, 2017.

[54] W.-B. Kim, E. Nam, B.-K. Min, D.-S. Choi, T.-J. Je and E.-C. Jeon, "Material removal of glass by magnetorheological fluid jet," *International Journal of Precision Engineering and Manufacturing,* vol. 16, pp. 629-637, 2015.

[55] K. Hai, L. Li, H. Hu, Z. Zhang, Y. Bai, X. Luo, L. Yi, X. Yang, D. Xue and X. Zhang, "Distribution model of the surface roughness in," *Applied Optics,* vol. 59, no. 28, pp. 8740-8750, 2020.

[56] C. Cheung, C. Wang, Z. Cao, L. Ho and M. Liu, "Development of a multi-jet polishing process for inner surface finishing," *Precision Engineering,* vol. 52, pp. 112-121, 2018.

[57] J. Lister, "Uses of Computers in Scientific Research," Techwalla, [Online]. Available: https://www.techwalla.com/articles/uses-of-computers-in-scientific-research. [Accessed 12 November 2021].

[58] Y.Tsuji, T. Tanaka and T.Ishida, "Lagrangian numerical simulation of plug flow of cohesionless particles in a horizontal pipe," *Powder Technology,* vol. 71, no. 3, pp. 239-250, 1992.

[59] P. Kieckhefen, S. Pietsch, M. Dosta and S. Heinrich, "Kieckhefen, Paul ; Pietsch, Swantje ; Dosta, Maksym ; Heinrich, Stefan," *Annual review of chemical and biomolecular engineering,* vol. 11, no. 1, pp. 397-422, 2020.

[60] H. Norouzi, R. Zarghami and N. Mostouf, "New hybrid CPU-GPU solver for CFD-DEM simulation of fluidized beds," *Powder Technology,* vol. 316, pp. 233-244, 2017.

[61] W. E. Frazier, "Metal Additive Manufacturing: A Review," *Journal of Materials Engineering and Performance,* vol. 23, pp. 1917-1928, 2014.

[62] I. Gibson, D. Rosen, B. Stucker and M. Khorasani, Additive Manufacturing Technologies, Third Edition, Enschede: Springer, 2021.

[63] T. Pasang, B. Tavlovich, O. Yannay, B. Jackson, M. Fry, Y. Tao, C. Turangi, J.-C. Wang, C.-P. Jiang, Y. Sato, M. Tsukamoto and W. Z. Misiolek, "Directionally-Dependent Mechanical Properties of Ti6Al4V Manufactured by Electron Beam Melting (EBM) and Selective Laser Melting (SLM).," *Materials,* vol. 14, no. 13, p. 3603, 2021.

[64] J. Liu, "Method for apparatus for three-dimensional additive manufacturing with a high energy high power ultrafast laser". United States of America Patent US 9 , 770 , 760 B2, 26 September 2017.

[65] O. M. Ivasyshyn and A. V. Aleksandrov, "Status of the titanium production, research, and applications in the CIS," *Materials Science,* vol. 44, no. 3, pp. 311-327, 2008.

[66] P. Krakhmalev, I. Yadroitsev, I. Yadroitsava and O. de Smidt, "Functionalization of Biomedical Ti6Al4V via In Situ Alloying by Cu during Laser Powder Bed Fusion Manufacturing," *Materials (Basel),* vol. 10, no. 10, p. 1154, 2017.

[67] C. Cui, B. Hu, L. Zhao and S. Liu, "Titanium alloy production technology, market prospects and industry development," *Materials and Design,* vol. 32, no. 3, pp. 1684-1691, 2011.

[68] M. Kahlin, "Fatigue Performance of Additive Manufactured Ti6Al4V in Aerospace Applications," Linköping University Electronic Press, Linköping, 2017.

[69] R. Huang, M. Riddle, D. Graziano, J. Warren, S. Das, S. Nimbalkar, J. Cresko and E. Masanet, "Energy and emissions saving potential of additive manufacturing: the case of lightweight aircraft components," *Journal of Cleaner Production,* vol. 135, pp. 1559-1570, 2016.

[70] L.-L. Xing, W.-J. Zhang, C.-C. Zhao, W.-Q. Gao, S.-J. Shen and W. Liu, "Influence of Powder Bed Temperature on the Microstructure and Mechanical Properties of Ti-6Al-4V Alloy Fabricated via Laser Powder Bed Fusion," *Materials,* vol. 14, no. 9, p. 2278, 2021.

[71] B. Van Hooreweder, D. Moens, R. Boonen, J.-P. Kruth and P. Sas, "Analysis of Fracture Toughness and Crack Propagation of Ti6Al4V Produced by Selective Laser Melting," *Advanced Engineering Materials,* vol. 14, no. 1-2, pp. 92-97, 2012.

[72] L. Thijs, F. Verhaeghe, T. Craeghs, J. Van Humbeeck and J.-P. Kruth, "A study of the microstructural evolution during selective laser melting of Ti–6Al–4V," *Acta Materialia,* vol. 58, no. 9, pp. 3303-3312, 2010.

[73] P. Edwards and M. Ramulu, "Fatigue performance evaluation of selective laser melted Ti–6Al–4V," *Materials Science and Engineering: A,* vol. 598, pp. 327-337, 2014.

[74] S. Leuders, M. Thöne, A. Riemer, T. Niendorf, T. Tröster, H. A. Richard and H. J. Maier, "On the mechanical behaviour of titanium alloy TiAl6V4 manufactured by selective laser melting: Fatigue resistance and crack growth performance," *International Journal of Fatigue,* vol. 48, pp. 300-307, 2013.

[75] M. Koike, P. Greer, K. Owen, G. Lilly, L. E. Murr, S. M. Gaytan, E. Martinez and T. Okabe, "Evaluation of Titanium Alloys Fabricated Using Rapid Prototyping Technologies—Electron Beam Melting and Laser Beam Melting," *Materials,* vol. 4, pp. 1776-1792, 2011.

[76] T. M. Mower and M. J. Long, "Mechanical behavior of additive manufactured, powder-bed laser-fused materials," *Materials Science and Engineering A,* vol. 651, pp. 198-213, 2016.

[77] P. Jamshidi, M. Aristizabal, W. Kong, V. Villapun, S. C. Cox, L. M. Grover and M. M. Attallah, "Selective Laser Melting of Ti-6Al-4V: The Impact of Post-Processing on the Tensile, Fatigue and Biological Properties for Medical Implant Applications.," *Materials,* vol. 13, no. 12, p. 2813, 2020.

[78] G. M. Ter Haar and T. H. Becker, "Selective Laser Melting Produced Ti-6Al-4V: Post-Process Heat Treatments to Achieve Superior Tensile Properties," *Materials (Basel),* vol. 11, no. 1, p. 146, 2018.

[79] S. Tammas-Williams, H. Zhao, F. Léonard, F. Derguti, I. Todd and P. Pragnell, "XCT analysis of the influence of melt strategies on defect population in Ti–6Al–4V components manufactured by Selective Electron Beam Melting," *Materials Characterization,* vol. Materials Characterization, pp. 47-61, 2015.

[80] y.-H. Li, B. Wang, C.-P. Ma, Z.-H. Fang, L.-F. Chen, Y.-C. Guan and S.-F. Yang, "Material Characterization, Thermal Analysis, and Mechanical Performance of a Laser-Polished Ti Alloy Prepared by Selective Laser Melting," *Metals,* vol. 9, no. 2, p. 112, 2019.

[81] H. Gong, K. Rafi, H. Gu, G. D. Janaki Ram, T. Starr and B. Stucker, "Influence of defects on mechanical properties of Ti–6Al–4V components produced by selective laser melting and electron beam melting," *Materials & Design,* vol. 86, pp. 545-554, 2015.

[82] X. Zhao, S. Li, M. Zhang, Y. Liu, T. B. Sercombe, S. Wang, Y. Hao, R. Yang and L. E. Murr, "Comparison of the microstructures and mechanical properties of Ti–6Al–4V fabricated by selective laser melting and electron beam melting," *Materials & Design,* vol. 95, pp. 21-31, 2016.

[83] K. S. Chan, M. Koike, R. L. Mason and M. Okabe, "Fatigue Life of Titanium Alloys Fabricated by Additive Layer Manufacturing Techniques for Dental Implants," *Metallurgical and Materials Transactions A,* vol. 44, no. 2, pp. 1010-1022, 2016.

[84] B. Vayssette, N. Saintier, C. Brugger and M. El May, "Surface roughness effect of SLM and EBM Ti-6Al-4V on multiaxial high cycle fatigue," *Theoretical and Applied Fracture Mechanics,* vol. 108, p. 102581, 2020.

[85] B. Vayssette, N. Saintier, C. Brugger, M. Elmay and E. Pessard, "Surface roughness of Ti-6Al-4V parts obtained by SLM and EBM: Effect on the High Cycle Fatigue life," *Procedia Engineering,* vol. 213, pp. 89-97, 2018.

[86] Y. Harada, Y. Ishida, D. Miura, S. Watanabe, . H. Aoki, T. Miyasaka and A. Shinya, "Mechanical Properties of Selective Laser Sintering Pure Titanium and Ti-6Al-4V, and Its Anisotropy," *Materials (Basel, Switzerland),* vol. 13, no. 22, p. 5081, 2020.

[87] MaRS, "Barriers to entry: Factors preventing startups from entering a market," 2021. [Online]. Available: https://learn.marsdd.com/article/barriers-to-entry-factors-preventing-startups-from-entering-a-market/. [Accessed 7 April 2021].

[88] ACI USA Inc., "6 Benefits of F.E.A. in Designing Structural Engineering Materials," ACI USA Inc., 2018. [Online]. Available: https://acicorporation.com/blog/2019/10/11/6-benefits-of-f-e-a-in-designing-structural-engineering-materials/. [Accessed 5 November 2021].

[89] MatWeb, "Titanium Ti-6Al-4V (Grade 5), STA," MatWeb, November 2021. [Online]. Available: http://www.matweb.com/search/datasheet.aspx?MatGUID=b350a789eda946c6b86a3e4d3c577b39.

[90] AmBrSoft, "Sphere Cap," AmBrSoft, 20 April 2015. [Online]. Available: http://www.ambrsoft.com/TrigoCalc/Sphere/Cap/SphereCap.htm. [Accessed October 2021].

[91] M. I. o. Technology, "Explicit Dynamic Analysis," [Online]. Available: https://abaqus-docs.mit.edu/2017/English/SIMACAEANLRefMap/simaanl-c-expdynamic.htm#simaanl-c-expdynamic-t-ExplicitDynamicAnalysis-sma-topic1. [Accessed 1 September 2021].

[92] P. Machinery, "PK Machinery," 2019. [Online]. Available: https://www.pkmachinery.com/faq/insufficient-lifting-capacity-of-bucket-elevator.html. [Accessed 10 April 2019].

[93] Jiangsu Yunxing Machinery Technology Co., Ltd., "Alibaba: plastic screw auger conveyor," 2019. [Online]. Available: https://www.alibaba.com/product-detail/plastic-screw-auger-conveyor-with-a_60572127979.html. [Accessed 11 April 2019].

[94] Schmalz, "SEC-400 A2," Schmalz, [Online]. Available: https://www.schmalz.com/en/vacuum-technology-for-automation/vacuum-components/special-grippers/feed-ejectors/feed-ejectors-sec-306349/10.02.01.01620/.

[95] W. B. du Preez and G. Booysen, "ADVANCES IN Ti6Al4V ADDITIVE MANUFACTURING IN SOUTH AFRICA," in *Proceedings of the 13th World Conference on Titanium*, 2016.